Master Thesis

"A statistical analysis on the system performance of a Bluetooth Low Energy indoor positioning system in a 3D environment"

By G.G. Haagmans
Geoscience and Remote Sensing, TU Delft

Assessment Committee:
Dr.ir. A.A. Verhagen (Chair) - Geoscience and Remote Sensing, Civil Engineering and Geosciences Faculty, TU Delft, the Netherlands

Ir. R. Voûte - Vice President Consulting Geo-ICT, CGI Nederland, the Netherlands & Department Urbanism, Faculty of Architecture and the Built Environment, TU Delft, the Netherlands

Ir. E. Verbree - OTB, Research for the Built Environment, Faculty of Architecture and the Built Environment, TU Delft, the Netherlands

Prof.dr.ir. R.F. Hanssen - Geoscience and Remote Sensing, Civil Engineering and Geosciences Faculty, TU Delft, the Netherlands

TU Delft

Master Thesis

"A statistical analysis on the system performance of a Bluetooth Low Energy indoor positioning system in a 3D environment"

by

G.G. Haagmans

to obtain the degree of Master of Science

at the Delft University of Technology,

to be defended publicly on Thursday 22 June 2017 at 14:00.

Student number:	4420543	
Project duration:	September, 2016 – June, 2017	
Assessment committee:	Dr. ir. A.A. Verhagen,	Geoscience and Remote Sensing, TU Delft
	Ir. R. Voûte,	CGI Nederland & Department Urbanism, TU Delft
	Ir. E. Verbree,	OTB - Research for the Built Environment, TU Delft
	Prof. dr. ir. R.F. Hanssen,	Geoscience and Remote Sensing, TU Delft

This thesis is confidential and cannot be made public until publication

Abstract

Since GPS tends to fail for indoor positioning purposes, alternative methods like indoor positioning systems (IPS) based on Bluetooth low energy (BLE) are developing rapidly. Generally, IPS are deployed in environments covered with obstacles such as furniture, (partition-) walls, people and electronics influencing the signal propagation. The major factor influencing the system performance and to acquire optimal positioning results is the geometry of the beacons. The geometry of the beacons is limited to the available infrastructure that can be deployed (number of beacons, basestations and tags), which is dependent on the budget and deployment effort of the customer. This leads to the following challenge: Given a limited number of beacons, where should they be placed in a specified indoor environment, such that the geometry contributes to optimal positioning results?

This challenge is approached by using theoretical design computations. The design computations require the definition of a chosen 3D space, the number of beacons, possible user tag locations and a performance threshold (e.g. required precision). For any given set of beacon and receiver locations, the precision, internal- and external reliability can be determined on forehand. The results of a given geometry have been validated by deploying an IPS of BlooLoc and comparing the observed precision with the modeled precision for a chosen set of user tag locations. The theoretical model showed a precision pattern with several equivalent precision patterns of the measured data, however, some significant differences could not be explained physically and the model has to be adapted further. Besides determining the precision based on a set of beacon and receiver locations, the model is able to select the optimal geometric configuration based on a performance threshold (e.g. required precision). Depending on the performance threshold, the optimal configurations can either be a single solution or consist of multiple solutions that satisfy the performance threshold of the customer. The performance threshold varies depending on the use case and the user requirements. Therefore, the amount of possible combinations in terms of 3D space, amount of available beacons, possible beacon locations, user tag locations and performance thresholds are limitless and the model can thus be used for all kind of applications.

All in all, the initial model (design computations) can be used by IPS customers for all kind of applications. The model is able to select the optimal geometric configuration in terms of precision based on a performance threshold specified by the user. Furthermore, the model requires user specified input parameters and the amount of possible combinations are therefore unlimited. Although the initial model has to be adapted further to account for the differences in modeled and measured data as a consequence of environmental factors, the initial model is a good initiative for the rising indoor positioning market and its customers. Therefore, the model can be adapted further such that it can explain significant differences between the modeled and the measured data by including factors that influence the system performance in real life, such as materialistic properties, signal attenuation, interference, multipath, NLOS etc.

Acknowledgments

I would like to thank my supervisors at the TU Delft, Sandra and Edward, for their extensive feedback and support throughout the whole project. Not only the support and feedback regarding my thesis, but also with respect to the proposed paper we wrote. Furthermore, the feedback challenged me to explore and extend my knowledge about the subject. A special thanks to my daily supervisor at the TU Delft, Sandra, for the opportunity to carry out this project, the many brainstorm sessions and discussions we had. Another special thanks to my daily supervisor at CGI, Robert, for his support and the fact that he was so closely involved in my project. Thanks for the many brainstorm sessions, the opportunity to explore a company like CGI, the many motivational speeches and many additional projects like conferences, GEO-ICT practice meeting, the Indoor Lab, recruitment events etc. were I had the opportunity to help.

Preface

This report represents the MSc thesis for the graduation project of the master track Geoscience and Remote Sensing at the faculty of Civil Engineering and Geosciences for the Delft University of Technology. The graduation project has been carried out in collaboration with CGI, a Canadian global information technology (IT) company with their Dutch headquarters located in Rotterdam. The aim of the research is to enhance the system performance of Bluetooth Low Energy (BLE) systems used for indoor positioning in large 3D spaces by testing and evaluating both theoretical design computations and practical experiments. What exactly is meant by terms as BLE systems, system performance, indoor positioning, and large 3D spaces will be elaborated further in this report. The practical experiments will be carried out with the indoor positioning technology of BlooLoc, a Belgium tech company that lies within the focus of CGI.

By way of example, during one of many conferences, CGI wanted to deploy an indoor positioning system using Bluetooth in order to create an easy way to find, locate and guide visitors through the conference. However, the conference building consisted of large open spaces exceeding the range of several beacons which caused serious issues for accurate positioning of the visitors. Since it is preferred to track and guide every individual on the conference, it is important that the system performance of the indoor positioning system is optimal. Therefore, to assess the system performance in terms of accuracy and precision of an indoor positioning system, a model predicting the precision within a 3D space as a consequence of a geometric configuration would be useful. The organization of the conference would be able to assess the system performance on forehand and find the optimal geometric configuration.

Since, indoor positioning is becoming a more and more important topic in our society, several use cases and their corresponding requirements in terms of system performance will be described. The theoretical design computations and the practical experiments will be based on related use cases and their requirements. Furthermore, the theoretical design computations will try to select the optimal geometric configuration based on a specified performance threshold (e.g. required precision).

By G.G. Haagmans
Delft, June 2017

List of Abbreviations

AOA	*Angle of Arrival*
AP	*Access Points*
BLE	*Bluetooth Low Energy*
BLUE	*Best Linear Unbiased Estimation*
CiTG	*Civil Engineering and Geosciences*
DOP	*Dilution of Precision*
FHSS	*Frequency Hopping Spread-Spectrum system*
FP	*Fingerprinting*
GDOP	*Geometric Dilution of Precision*
GNSS	*Global Navigation Satellite System*
GPS	*Global Positioning System*
HCI	*Host Controller Interface*
HDOP	*Horizontal Dilution of Precision*
IOS	*IPhone Operating System*
IPS	*Indoor Positioning System*
IR	*Infrared*
ISM	*Industrial, Scientific and Medical band*
K-NN	*K-Nearest Neighbor algorithm*
LBS	*Location Based Services*
LOS	*Line-of-Sight*
MDB	*Minimal Detectable Bias*
MDE	*Minimal Detectable Effect*
NLOS	*Non-Line-of-Sight*
OMT	*Overall Model Test*
PDOP	*Position Dilution of Precision*
PPZ	*Possible Position Zone*
RF	*Radio Frequencies*
RMS	*Root Mean Square*
RSS	*Received Signal Strength*
RSSI	*Received Signal Strength Indicator*
SIG	*Special Interest Group*
TOA	*Time of Arrival*
TDOA	*Time Difference of Arrival*
VDOP	*Vertical Dilution of Precision*
Wi-Fi	*Wireless Fidelity*
WLAN	*Wireless Local Area Networks*
WLSE	*Weighted Least Squares Estimation*

Contents

List of Figures

1 Introduction

1.1. Problem statement

Almost everyone uses the Global Positioning System (GPS) to navigate from a certain location on Earth to another specific destination. Originally, GPS was developed as a Global Navigation Satellite System (GNSS) for the US military services but is currently also used for civil and commercial purposes. The current GNSS consists of a minimum of 24 active satellites distributed over six circular orbits with four or more satellites each [12]. In theory, it is possible to receive the signals of three or more GPS satellites from almost every position on the Earth's surface and a minimum of four GPS satellites is required to determine any position on the earth's surface [12]. Furthermore, GPS is a well-known navigation system for outdoor applications, however the accuracy of GPS for civil users is limited and varies in a range of meters to tens of meters depending on absolute or relative positioning. However, the connection with GPS satellites tends to fail when the receiver is located within an indoor environment, causing an increase in the positioning uncertainty or even an inability to localize at all. The signal strength of a transmitted GPS signal weakens and gets distorted while penetrating trough buildings to the receiver. The amount of distortion or weakening is depending on the type of construction of the building, for instance, a GPS signal travels much easier trough glass than through concrete walls. Another GPS error is caused by the reflection of the initial transmitted signal on objects in the vicinity of the receiver, known as multipath [12]. The multipath problem causes one or more secondary propagation paths which can distort the amplitude and phase of the initial signal [12]. As a consequence, the reflected signals cause a significant error and an inaccurate positioning.

In case of driving from A to B using a GPS navigation device, it is most likely that you are not bothered by a vertical positioning uncertainty of several meters, however, an accurate horizontal positioning is desired. In contrast to the positioning of a car, your vertical positioning uncertainty becomes of much greater importance when entering a building with several floors or a warehouse with multiple shelves on top of each other. In this case, a person needs to know exactly on which floor he or she is located for guidance through the building or on what shelf a product is located in a distribution center. In general, indoor environments are more complex in both vertical and horizontal directions than outdoor environments.

Since GPS is not available for indoor positioning purposes, another market emerged with alternative methods to overcome this problem. One of the alternative methods comprises indoor positioning systems (IPS), replacing the loss of GPS signals in indoor environments. First of all, an IPS is defined by Depsey [6] as *"a system that continuously determines the real-time position of something or someone in a physical space such as in a hospital, a gymnasium, a school, etc."*. The real-time positions of the users of the IPS are often derived via the location of their tags or mobile devices. Subsequently, the rising market of IPS is widespread and contains many technologies that can be used for indoor positioning. In order to delineate the scope of the thesis, the research emphasizes the Bluetooth technology and a comparison between Bluetooth and several alternative methods will be made. Bluetooth is a wireless technology that can be used for short-range communication between different Bluetooth enabled devices [8]. From the original Bluetooth systems emerged an enhanced Bluetooth Low Energy (BLE) system. BLE was developed as a low-power solution for control and application monitoring [11]. BLE is due to its power-efficiency suited for devices that run for long periods on power

sources [26], such as mobile phones. The IPS that has been used in this research is an BLE positioning system of BlooLoc [2].

1.1.1. Clarification of terminology

Before proceeding to the research questions, it is necessary to make a distinction between the terms positioning and localization. Positioning refers to a position in x and y coordinates for 2D and x, y and z coordinates for 3D of a person or an object. If the object moves to another position, the positioning system will automatically update the coordinates of the object with respect to the new position. However, without knowledge of the surrounding environment or infrastructure of the building, the position becomes useless and uninterpretable for systems and humans [33]. Mautz [23] defines the term localization as follows

> *'The term 'localization' underlines that the application requires topological correctness of the sensor locations, whereas the absolute coordinate position is of minor importance'.*

The localization of an object or person puts an absolute coordinate position into perspective regarding their environment and can exclude areas where it is not likely for a person to be, for example on a table, or the other way around, it can include areas where persons are expected to be walking. The terms positioning and localization are closely correlated with each other within the field of indoor positioning, but there is a clear distinction in the definitions of both terms. Since this research includes a model that uses the x, y, and z coordinates within a 3D space of an imaginary person or object, the main focus throughout this thesis lies on positioning.

1.1.2. Indoor positioning applications

In our modern way of life indoor positioning has become a trending topic and is applicable in almost every branch. Moreover, considering the continuous improvement in technology and knowledge, future indoor positioning systems will find even more applications, which makes it promising to enhance- and contribute to -indoor positioning systems. In this section, several example applications are elaborated to get a better understanding of the wide-spread field, wherein indoor positioning/localization is applicable.

One of the most common applications that people are able to identify with, is indoor localization using smartphones and tags to do smart grocery shopping. By giving a shopping list as input, the system provides you a smart and efficient way to walk through the supermarket. Furthermore, buying behavior of the clients can be analyzed and the supermarket can adapt or make changes based on this analysis.

Another important indoor localization application is for example in hospitals and care centers. A hospital environment offers countless possibilities for both tags (for tracking patients, finding equipment, etc.) and smartphones or tablets (for locating medical staff or visitor navigation) [33]. Furthermore, it is possible to track elderly people in care centers, for example the system triggers an alarm when a patient with dementia would exit a designated area (geo-fencing) [2].

Other examples of indoor localization applications are applied to airports, train/subway stations and shopping malls. Airports are often complex buildings with many facilities and many travelers need to find their way under time pressure. An IPS could guide people in a smart and quick way to the right place, gives information about queue time at the security and can tell you to avoid crowded places if you are in a hurry. On the other side, if you have some time left before departure and the system can find the nearest shops and facilities for you. The same principle applies for large train stations, subway stations and (underground) shopping malls.

Final example, indoor localization can also be used to locate a free desk within the office building or finding free seats in the train during rush hour. Indoor positioning/localization is an important and innovative technology and is applicable on a whole lot more applications than described so far.

1.2. Challenge

An IPS should be able to achieve accurate positions of the user devices where GPS is failing. However, to cover for instance a convention center existing of large open spaces and high ceilings, the signal propagation

range of the available number of beacons is often exceeded, leading to serious issues for accurate positioning of the visitors. In such a case, the geometric constellation of the beacons is in direct relation with the precision and accuracy of the positioning results. To solve this problem, the customer wants to know in what geometry the beacons should be deployed on forehand to retrieve optimal positioning results for a given 3D space and with minimal costs. The first factor to take into account when deploying an IPS is that indoor environments are covered with obstacles such as furniture, (partition-) walls, human beings and electronics in Line-of-Sight (LOS) influencing signal propagation in different ways. The second factor is depending on the physical aspects such as signal strength, range and signal attenuation. Finally, the third factor, the geometric configuration of the beacons, plays a major role in acquiring optimal positioning results. The geometry of the beacons is limited by the available infrastructure that can be deployed (number of beacons, basestations and tags), which on its turn is dependent on the budget and deployment effort of the customer [5]. Therefore, knowledge about the geometric deployment of an IPS is required in order to obtain optimal positioning results. This leads to the following question: "Given a limited number of beacons, where should they be placed in a specified indoor environment, such that the geometric configuration of the beacons provide optimal positioning results?"

1.3. Research questions

1.3.1. Main research question

Several positioning techniques will be elaborated in this thesis. However, the main focus of the thesis lies on BLE positioning systems. The differences between other positioning techniques and the BLE IPS of BlooLoc will be described. Furthermore, several experimental settings will be tested using the Bluetooth Low Energy system of BlooLoc to answer the main research question:

> ***"What kind of geometric configuration of a BLE indoor positioning system is needed to enable the required system performance for given use cases in a 3D environment?"***

To understand the main research question, the main question can be subdivided into two parts. The first part *'kind of geometric configuration of a BLE indoor positioning system ... in a 3D environment'* is referring to the geometric configuration of the beacons of an BLE indoor positioning system. Given a number of beacons, millions of geometric configurations can be made for deployment in an indoor 3D environment. The second part of the main research question is stated as *'to enable the required system performance ... for given use cases'* and is referring to two key elements in this research, the system performance and the use cases. The geometric configuration is related to the system performances and will be expressed in terms of statistical quantities, such as accuracy, precision and reliability. The required system performance defines the performance threshold (e.g. required precision) which on its turn is dependent on the defined use case. Different use cases will be described in consultation with CGI, eventually a selected use case will provide the requirements for the system performance.

Finally, the third important part of the main research question describes the setting, namely *'in a 3D environment.* The large spaces are defined as spaces or rooms with a ceiling higher than 3 meters and smaller than 20 meters. The boundary condition defining the large spaces as rooms with ceilings between 3 and 20 meter height is chosen because indoor positioning systems tend to become less accurate in such environments. Buildings with large open spaces and high ceiling have often multiple subfloors within the open space. For clarification of this boundary condition the train station of Utrecht Central (Netherlands) will be used as a reference. The station hall of Utrecht Central consists of a very large open space with a high curvy ceiling (Figure 1.1) including several restaurants as subfloors above the station hall and the train platforms below the station hall. Furthermore, the aim of the research is to obtain an accurate 3D IPS in these large spaces, meaning that all kinds of structures like multiple floors, levels within a floor, large staircases etc. should be taken into account.

Figure 1.1: The station hall of Utrecht Central (Netherlands) containing high ceilings a large open space, subfloors and platforms.

1.3.2. Sub-questions

To answer the main research question, several sub-questions have been defined. The sub-questions act as a foundation to create a well-structured answer on the main research question. To find out what kind of geometric configuration of a BLE indoor positioning system is needed, it is important to understand the technology and the physical parameters. The sub-questions will be answered with the help of literature, experiments and data analysis.

1. “What is the current state of the system performances and what improvements are possible?”

   Before the start of the research it is good to know the state-of-the-art of the current Bluetooth systems. What are the accuracies and precisions at the moment, what are the bottlenecks/challenges and what improvements to the systems are possible? This sub question is mainly answered in Chapter 1 and 2.

2. “What are the pros and cons in terms of performance of the Bluetooth Low Energy system of BlooLoc?”

   It is necessary to look at the advantages and disadvantages of the BlooLoc system and a comparison will be made with Essensium. Similar to BlooLoc, Essensium is a Belgium company based in Leuven with an expertise in positioning technology. However, Essensium uses TOA instead of RSSI measurements for positioning and the comparison between BlooLoc and Essensium is within the interest for CGI. Furthermore, it is of importance to describe the different wireless technologies, for example cameras, infra-red, WLAN/Wi-Fi, and ZigBee, which can be used for indoor positioning and compare them with Bluetooth Low Energy systems. The different positioning techniques are described and compared in Chapter 2.

3. “What are the most important factors that influence the system performance?”

   In order to develop good theoretical design computations and put good experiments into practice, it is very important to figure out the factors that can influence the system in both positive and negative ways. The most important factors, such as system characteristics, obstructions (people/objects and infrastructure), reflections, and construction of the building that influence the system performance will be investigated and described in Chapter 4.

4. "What is the optimal (minimal) configuration to get the required precision?”

   The minimal configuration of the BLE systems of BlooLoc to get the required precision should be investigated, so that requirements can be setup that can be used as input data for the theoretical design computations and the experiments. The design computations are fully explained in Chapter 5, together with the derivation of the total precision by the model. Eventually, the search for the optimal configuration is described in Chapter 7.

5. “What are different use cases and how should the system be adapted to fulfill these?”

   The requirements in terms of accuracy and precision are highly dependent on the use cases. Based on these requirements, the theoretical designs computations can be set up which can be used to compute how the system should be adapted to fulfill the requirements. The use cases and user requirements are elaborated in Chapter 4. Furthermore, three different geometric scenarios are tested by the design computations. The set-up is explained in Chapter 5 and the results are discussed in Chapter 6.

6. “What are the maximum number of moving objects that can be seen for the use cases and monitored accurately by the system?"

   Another important factor in this research is to investigate how many objects can be monitored accurately by the system. It is important to say that the maximum number of moving objects is highly influenced by many factors such as infrastructure of the building, the geometric configuration of the beacons, etc. (Chapter 4 and 8).

1.4. Available material and boundary conditions

CGI provided a BLE starter kit of BlooLoc that can be used for experimental purposes. BlooLoc is a tech company headquartered in Leuven (Belgium) and offers “yooBee”, which is the hardware and software for accurate indoor positioning [2]. The BlooLoc starter kit costs 2750€ and consists of 15 yooBee beacons, a basestation and three tags. The practical experiments during this research will be performed with the BlooLoc starter

kit of CGI. The basestation covers an area of approximately $500m^2$, which is called a Cell. Since all devices serviced by a Cell should be within the range of the basestation, the range of wireless indoor connections is limited to a recommended $450m^2$ [2]. Besides the three tags, the beacons also provide location references for smartphones updating the position data every second [2]. The large spaces described in the main research question are defined as spaces or rooms with a ceiling higher than 3 meter and smaller than 20 meter and have been illustrated on basis of the station hall of Utrecht Central in Figure 1.1.

1.5. Organization of the thesis

After the introduction, including the problem statement, the research questions and several examples of indoor positioning applications, this thesis will be built up in 8 parts including the introduction (Chapter 1). Chapter 2, called Fundamentals of Bluetooth, will elaborate the Bluetooth technology and starts with a short history of Bluetooth. The principles of Bluetooth will be explained and the protocol stack will be elaborated. Before the experimental setup can be made, it is necessary to examine the state-of-the-art Bluetooth systems and their system performances. Furthermore, chapter 2 provides an comparison with several indoor position techniques and their differences/similarities in terms of system performances with respect to Bluetooth technology. Finally, the functionality of the BLooLoc IPS will be examined and the advantages and disadvantages defined.

The third chapter (3) (Positioning methods and measuring principles of BLE) comprises the different positioning techniques and the measuring principles that can be used for indoor positioning using BLE systems. Subsequently, the fourth chapter (4) (Use Cases, requirements and system performance) will provide an overview of several use cases that are of interest for this research. The overview contains requirements for the system performance for each use case and forms the basis for the experimental setups. Furthermore, the factors influencing the system performance of indoor positioning systems will be discussed.

Continuing to the fifth chapter (5)(Methodology), explains the statistical methods and models that are used for the theoretical design computations. Terms as functional model, linearization, data quality control, accuracy, precision, reliability etc. are covered in this chapter. Proceeding into chapter 6 (Theoretical and experimental results), the setup of the practical experiments will be discussed which are partly depending on the results derived by the theoretical design computations. Subsequently, the results from both the design computations and the practical experiments will be discussed. Furthermore, the obtained data from the experiments will be processed, analyzed and examined. After the analysis, the obtained results from the practical experiments will be discussed and compared with results from the theoretical design computations in chapter 7 (Interpretation and Discussion). Chapter 7 comprises the discussion and validation of the model by making a comparison with the results of the practical experiments. Furthermore, selecting the optimal configuration out of millions of possible configurations based on a performance threshold will be discussed along with several improvements regarding the model. Eventually, in chapter 8 (Conclusions and Recommendations) the sub-questions are answered in order to formulate an answer on the main research question. The answers to the sub-question, the main research question and the preceding discussion are used to draw conclusions. Finally, a section reflecting on some recommendations for future research will close up this thesis.

2

Fundamentals of Bluetooth

This chapter starts with a introduction (section 2.1) to the Bluetooth technology by going back in time. Subsequently, the physical principles and architecture of Bluetooth are elaborated in section 2.2. Section 2.3 shows an overview of several wireless technologies that are applicable for indoor positioning. Furthermore, it is of importance to describe the different wireless technologies, for example cameras, infra-red, WLAN/Wi-Fi, and ZigBee, which can be used for indoor positioning and compare them with Bluetooth Low Energy systems. Eventually, the functionality of the BLE indoor positioning of BlooLoc is discussed and an explanation about the BLE positioning with BlooLoc is given (section 2.4).

2.1. History of the Bluetooth technology

The name Bluetooth originates from a Danish king called Harald Blåtland (Bluetooth), who reigned from 940 to 985 AD and was able to unite his country under Christianity [9]. In 1994, the Swedish telecommunications equipment and services company Ericsson started researching on a short-range wireless solution that could be used to connect devices wireless [8]. In 1998, a Special Interest Group (SIG) including Ericsson, IBM, Nokia, Toshiba, and Intel arouse to promote the Bluetooth technology and expanded rapidly to almost 1500 member companies in four years [9]. Gupta [14] defines Bluetooth as follows

> *"Bluetooth is a global standard for short-range, low-power, low-cost wireless technology that allows devices to communicate with each other over radio links".*

Bluetooth's initial role was to replace the networks of cables between devices with a wireless connection. Many computers had cables connecting with for instance a keyboard, mouse, headsets, printers, and monitors. Bluetooth made it possible to connect these devices wireless with the computer. The developers soon realized that this technology could bring much more than connecting devices. Currently, almost all mobile phones and laptops/computers have built in Bluetooth technology and Bluetooth has become a globally prominent technology.

Since the public release of the Bluetooth technology, the Special Interest Group (SIG) kept developing and improving the technology. As part of the Bluetooth 4.0 specification introduced by the SIG [3], the Bluetooth Low Energy (BLE) emerged as an enhancement to the Bluetooth technology [14]. In contrast to the previous Bluetooth systems, the Bluetooth Low Energy was developed as a low-power solution for control and monitoring applications [11], for instance monitoring the Bluetooth activity around you. Due to coin cell batteries, the low-power solution extends much further and the BLE technology becomes applicable for use cases where it is hard to frequently recharge devices appended with BLE. Therefore, Bluetooth Low Energy is more suited for devices that run for long periods on power sources [26], such as mobile phones.

2.2. The principles of Bluetooth technology

By using Bluetooth for indoor positioning purposes, this technique can be considered as a 'Remote sensing' technique. Rees and Rees [28] define remote sensing as

> *"The collection of information about an object without making physical contact with it".*

Since Bluetooth can be used as a tool for locating and gathering information about objects, it becomes part of the subject 'Remote sensing'. The gathered information about objects is mostly carried by electromagnetic radiation enabling wireless communication. Therefore, it is important to get a better understanding of the characteristics of this radiation before proceeding to the principles of the Bluetooth technology itself. Remote sensing can be subdivided into passive systems, detecting naturally occurring radiation, and active systems, which are emitting radiation and receiving, measuring, and analyzing the radiation that reflects from the target [28].

The correlation between frequency and wavelength has been derived by James Clerk Maxwell, who integrated the laws of magnetism and electricity in the 1860s and suggested that propagating light was part of electromagnetic radiation [28]. The relation between the speed of light $c = 299792458$ *m/s*, cyclic frequency f and the wavelength λ can be expressed as

$$c = f \times \lambda \rightarrow \lambda = \frac{c}{f} \tag{2.1}$$

For the full derivation of equation 2.1, study read chapter 2 *"Electromagnetic waves in free space"* of the book *'Physical Principles of Remote Sensing'* by Rees and Rees [28]. From equation 2.1 can be concluded that in case the frequency increases, the wavelength decreases and vice versa. In theory, the frequencies of electromagnetic waves can approach any value and the wide spectrum of different frequencies and wavelength is known as the electromagnetic spectrum (Fig. 2.1). The electromagnetic spectrum can be subdivided into smaller parts with names such as UV-radiation, infrared radiation, microwaves, radio waves, visible light etc., mostly referring to the origin of where the radiation is generated or detected [28].

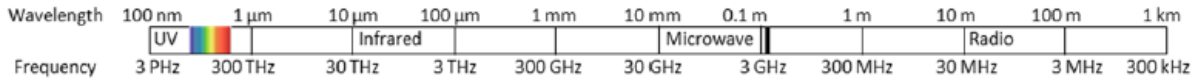

Figure 2.1: The electromagnetic spectrum showing both frequency (Hz) and wavelength (m). The visible light is indicated by the rainbow colored pattern and the black bar indicates the operating frequency of Bluetooth systems. Source: Mautz [23].

2.2.1. Architecture of Bluetooth

The architecture of BLE consists a layered network structure and the BLE protocol stack can be divided in two major parts, the lower layers, referred to as 'controller' and the upper layers, often referred to as 'host' (Fig. 2.2). The different layers of the protocol stack will be discussed and the properties of the controller (lower layers) will be elaborated further, in contrast to the implementations within the host (upper layers) since this is outside the scope of this thesis.

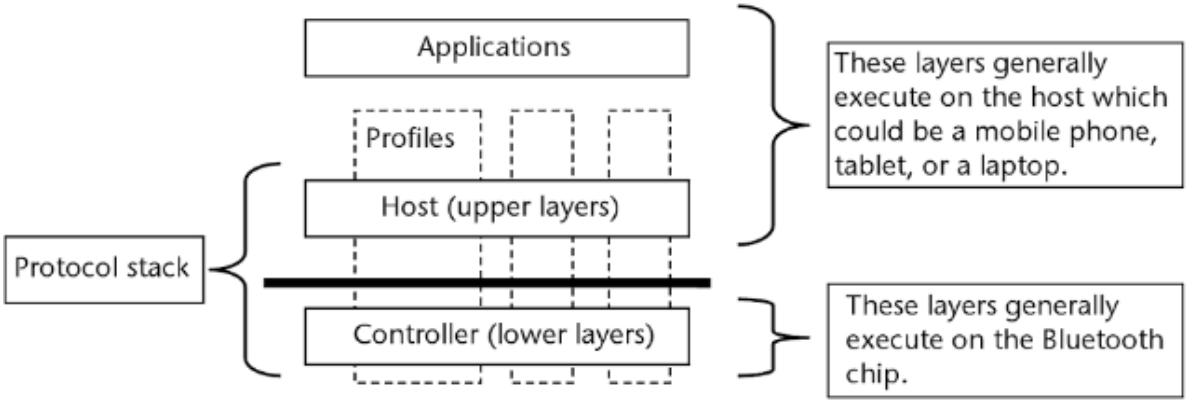

Figure 2.2: The architecture of the BLE protocol stack with the lower layers, 'controller' and the upper layers, 'host'. Source: Gupta [14].

Controller/lower layers: The lower layers of the protocol stack consist of a physical layer and a link layer. The physical layer comprises the operational functionality and the broadcasting frequencies and principles of the BLE system. The link layer comprises the functionality of connecting to other devices, setting up piconets (piconets are explained in section 2.2.2), looking for devices in the vicinity, broadcasting and receiving data, and security [14]. These functionalities are often implemented in a Bluetooth chip and are combined into the Bluetooth Controller. The functionality of the physical layer and the link layer will be elaborated in section 2.2.2. Despite the fact that parts of the BLE Controller features are acquired via the Bluetooth Classic Controller, both Controllers are incoherent with each other. This means that a device embedded with BLE (*a single-mode device*) is not able to communicate with a device equipped with Bluetooth Classic. Therefore, future devices will be implemented with both Bluetooth Classic and BLE protocol stacks, so that the devices are compatible. Devices implemented with both Bluetooth Classic and BLE protocol stacks are known as *dual-mode devices* [11]. Furthermore, the communication between the controller and the host (black solid line in Fig. 2.2) is operated via the Host Controller Interface (HCI).

Host/upper layers: The upper layers are generally executed on the host, which often is a mobile phone, tablet or laptop. The upper layers make use of the lower layers functionality to provide a more complex upper layer functionality [14], such as the Logical Link Control and Adaption Protocol (L2CAP), the Attribute Protocol (ATT), the Generic Attribute Profile (GATT), the Security Manager Protocol (SMP) and the Generic Access Profile (GAP) [11]. Thus, both protocols and profiles can be found in the upper layers. However, profiles can be considered as vertical slices within the protocol stack and provide information about combining protocols to implement a specific usage model [14]. The different protocols/profiles within the upper layers will not be elaborated further, since this is out of scope for this thesis. For more information about the protocols and the upper layers read *'Overview and Evaluation of Bluetooth Low Energy'* by Gomez et al. [11].

Applications: This functionality is not implemented in the BLE protocol stack and the applications depend on the functionality that is expected by the user. An example of an application could be a headset that connects with a laptop via BLE, this needs a specific functionality and will be implemented via the devices.

2.2.2. Bluetooth bandwidth

The Physical Layer

Bluetooth is operating in the unlicensed 2.4 GHz industrial, scientific and medical (ISM) radio frequency (RF) band of the electromagnetic spectrum (Fig. 2.1). Moreover, Wi-Fi devices, microwaves and remote control devices use the unlicensed 2.4 GHz ISM band as well. To reduce the interference between the different devices, Bluetooth uses a frequency-hopping spread-spectrum system (FHSS), transmitting data over different frequencies at different time intervals [1]. This is achieved by hopping to different frequencies in the ISM band and a device makes about 1600 hops per second, spaced out over 1 MHz [8].

Just like classic Bluetooth, BLE uses frequency hopping for communication purposes [10]. The bandwidth of BLE covers 40 channels within the 2.4 GHz band, each with a 2 MHz width, and is moving randomly between the different channels to transmit data [10]. BLE only uses three advertising channels within the 2.4 GHz band. These advertising channels are labeled 37, 38, and 39 and are broadcasting on approximately 2402 MHz, 2426 MHz, and 2480 MHz (Fig. 2.3).

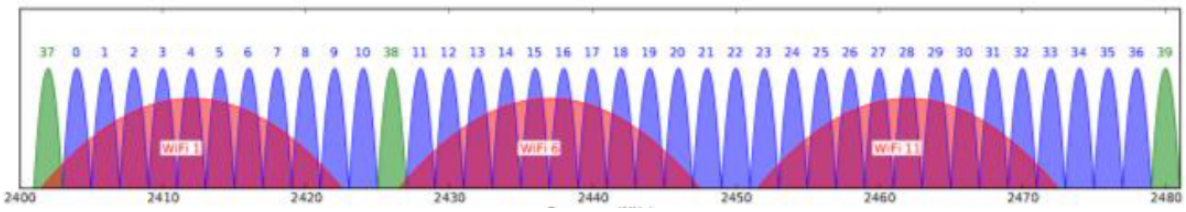

Figure 2.3: The 40 BLE channels (blue) within the unlicensed 2.4 GHz ISM band, including the three advertising channels 37, 38, and 39 (green) broadcasting on respectively 2402 MHz, 2426 MHz, and 2480 MHz. Furthermore, three Wi-Fi channels are depicted as well (red) for comparison, this will be compared in section 2.3.3. Source: Faragher and Harle [10].

The Link Layer

By using BLE, devices are broadcasting data by transmitting data in the form of advertising packages within advertising channels [11]. By limiting the broadcasting through three advertising channels, the receivers need

to do less effort to scan only three channels instead of all 40 channels and thus are save energy while scanning the three advertising channels. Furthermore, devices that are constantly receiving data from the advertising channels and do not broadcast information are called scanners. The network of a device that is broadcasting through advertising channels and scanners is known as a broadcast group (Fig. 2.4).

Besides the scanners that are constantly receiving the broadcasted data from the advertising channels, BLE also allows bidirectional data communication. In contrast to the broadcast group, bidirectional data communication makes it possible for devices to connect with each other and to exchange data. Once a connection is made between two devices, BLE assigns a role, master or slave, to every device within the Link Layer [11]. A set of connected devices is called a piconet (Fig. 2.4) and has a star shaped topology. The device in the center of the piconet adapts the role of master, while all other devices become slaves. The slaves follow the masters lead regarding the information about the frequency hopping sequence. Within a piconet, a master can be served by up to seven slaves simultaneously. However, when the number of seven slaves is exceeded, an additional piconet forms with a newly assigned master. If the piconets need to communicate with each other, a scatternet will form (Fig. 2.4). In a scatternet, multiple piconets are interconnected and the master/slave that connects both piconets is known as bridge node. The bridge node can either be slave in both piconets or master in one and slave in the other [1]. The bridge node is part of different piconets over time. After staying for a certain period in a piconet, the bridge node has the ability to hop to another piconet by switching its hopping sequence [1]. Furthermore, the bridge nodes can transfer information between the piconets.

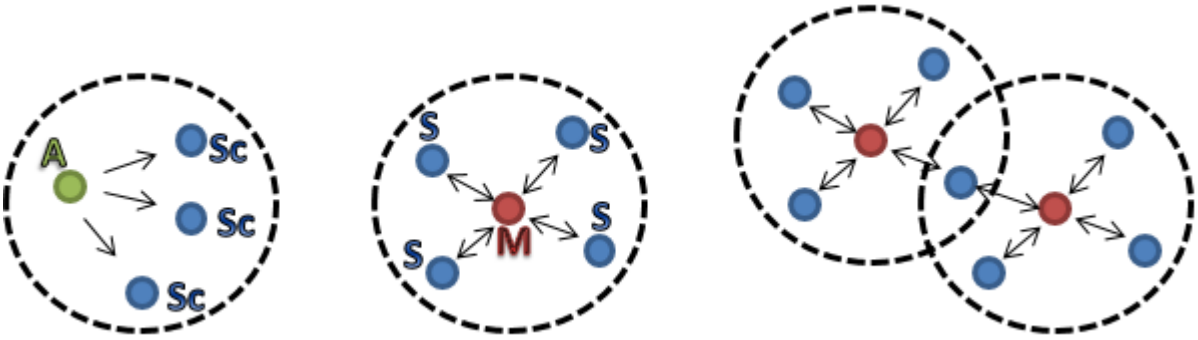

Figure 2.4: Left, a schematic drawing of the broadcast group. One of the devices is broadcasting through the advertisement channel (A) and the scanners (Sc) are scanning and receiving the data. Middle, a piconet with a master (M) device and several slaves (S) which can communicate in bidirectional ways. Right, a scatternet consists of two piconets that are connected with each other via a bridge node, this can either be a slave in both piconets or a slave in one and master in the other.

2.3. Overview of wireless technologies

Before explaining the positioning techniques and measuring principles, alternative wireless technologies that can be used for indoor positioning purposes will be discussed. An overview of the wireless technologies is given in Figure 2.5. In addition, Figure 2.5 includes the typical accuracy, range or coverage, measuring principle and application of the various techniques based on Mautz [23]. It has to be mentioned that there are many exceptions where the accuracy and/or coverage is exceeding the given intervals. Similarly, Mautz [23] only mentioned the main measuring principles and applications and discussed more wireless technologies than presented in Figure 2.5. To limit the scope of this thesis, a small selection has been made and will be discussed. The measuring principles of Figure 2.5, angle measurements, thermal imaging, active beacons and fingerprinting will be described in Chapter 3.

Technology	Typical Accuracy	Typical Coverage (m)	Typical Measuring Principle	Typical Application
Cameras	0.1mm - dm	1 - 10	Angle measurements from images	Metrology, robot navigation
Infrared	cm - m	1 - 5	Thermal imaging, active beacons	People detection, tracking
WLAN/WIFI	m	20 - 50	Fingerprinting	Pedestrian navigation, Location based services
Other Radio frequencies	m	10 - 1000	Fingerprinting, proximity	Person/object tracking
- Zigbee	m	20 - 30	Fingerprinting	Person/object tracking
- Bluetooth	cm - m	5 - 10	Fingerprinting	Person/object tracking

Figure 2.5: Overview of wireless technologies that can be used for indoor positioning purposes. Source: Mautz [23]

To evaluate the different wireless technologies it is useful to compare various factors with their advantages

and disadvantages. The first factor or criteria is that a wireless technology used for indoor positioning purposes has to be well secured and preserves the user's privacy. The privacy and security are the most important criteria and the user's privacy is a common subject of discussion. The indoor positioning techniques mostly need full access to mobile devices in order to track them, meaning that their personal location information and history is known [13]. Since, most users care about their personal information and their past activities, there are all kinds of agreements based on privacy. To preserve the user's privacy, the wireless technology needs to be well secured. For example, Bluetooth is associated with high security, not only because it communicates over short ranges but also due to the authentication process. To prevent the interceptions of a transmitted signal by other receivers, the Bluetooth technology has implemented device authentication. Generally, this means that in order to share information between devices, a shared secret key, or link key, is needed to authenticate each other [8]. After authentication, the paired devices can communicate with each other and pass information back and forth without other devices intercepting the signals.

Another important factor is the cost of the wireless technology. The cost of the system are not only depending on the cost of a positioning device or the cost of maintenance, but also the costs in terms of time and space [13]. The cost in terms of time are related to the installation of the wireless technology and calibration, whereas the cost in terms of space relate to the size and amount of equipment and the requirements regarding the infrastructure of the indoor environment.

Besides security, privacy and the costs, one of the most important factors in the evaluation of wireless technologies for indoor positioning purposes is the system performance. The system performance is depending on several statistical parameters with the accuracy and precision as the main contributors. The accuracy is a standard for the closeness of the measured values with respect to the true value, whereas precision is related to the repeatability or spread in outcomes of the measured values. For clarification, the relation between accuracy and precision is explained in Figure 2.6 on the basis of an archery target and five arrows. Additionally, the statistical parameters influencing the system performance of BLE will be discussed in more detail in chapter 4.

Figure 2.6: The principle of accuracy and precision based on an archery target. The blue and red crosses indicate the locations of the five arrows. The more arrows closer to the gold, the more accurate the shots are. The closer the arrows are together, the more precise the shots are.

2.3.1. Cameras

Cameras belong to the category of optical imaging within remote sensing and operate in the visible light and near-infrared (VNIR) spectrum (Fig. 2.1), between wavelengths of approximately $0.3\mu m$ and $3\mu m$[28]. Optical imaging was one of the first forms of remote sensing and originates back to 1858 when the first aerial photograph was taken by Gaspard-Felix Tournachon made from a balloon above Paris [28]. Currently, optical indoor positioning has many applications, ranging from tracking people during events to tracking and guiding robotic movements in surgery with levels of accuracy up to the sub-mm domain. Furthermore, cameras can be used for optical indoor positioning in two ways, either as an ego-motion system or static sensors that can located moving objects in the images [24]. In contrast to static sensors (i.e. cameras), an ego-motion system is locating the position of mobile sensors relative to the surroundings, so this means that the camera is moving through its surrounding and tries to estimates its position [16]. The main challenge in optical indoor positioning is to translate the primary observations of 2D positions to positions and rotations in a 3D world [24].

The coverage area of cameras is often larger than the coverage area of Bluetooth beacons and an optical in-

door positioning system is relatively cheaper. Although the accuracy levels of current optical indoor positioning system vary between µm and dm, optical indoor positioning has several disadvantages. The visibility of cameras is highly dependent on external light sources and the positioning algorithm can be easily disturbed if the light is too bright or even if there is no light. Furthermore, the acquired data is large which increases the computation time for processing purposes and privacy/security of people must be assured. The user's privacy is an interesting discussion regarding optical indoor positioning, since the system is able to detect anyone without permission whereas in case of crime, accidents and prevention of terrorist attacks this would be a major advantage.

2.3.2. Infrared

The infrared (IR) spectrum (Fig. 2.1) has longer wavelengths than the visible light and is operating between $0.8\mu m$ and $1000\mu m$ [28]. Since the wavelength is longer than the wavelength of visible light, the human eye is not able to see infrared light. One of the methods to use infrared radiation for indoor positioning purposes is by the use of active beacons. The active beacons approach originates from the IR indoor positioning active badge system designed by Want et al. [35] in 1992 and unfortunately the active badge system is closed down and not available anymore [13]. The active badge system comprised a network of static sensors placed in and around the infrastructure of a building, a tag or active badge that emitted an infrared pulse with a unique code every 15 seconds, and a master station that collected the pulses via the sensors, processes the data and visualized the sightings for clients [35]. Typically, the IR sensors of the active badge system had an operating range of 6 meter which also represents the positional accuracy because the active badge system used the Cell-based method (Cell-based method, section 3.1.3) for positioning/localization [23]. However, due to the 15 seconds update rate it was impossible to apply this system for real-time application services and made this technique not feasible for this thesis. Besides the update rate, infrared radiation is unable to penetrate through walls and ceilings and can thus only be used for simple room localization [23]. Another disadvantage of IR localization is that communication between the badge and sensors must be in the line-of-sight (LOS) of the sensors. In contrast to optical indoor positioning, IR indoor positioning is limited to tracking badges, which is an advantage for the privacy discussion. Currently, one of the commercial products on the market is the Firefly system, an IR-based motion tracking system, offering high accuracy (3mm) and update rate (3ms delay) [13]. However, most IR systems are still limited to normal lighting environments and have a small coverage area (Firefly system - 7m), making it not suitable for large open spaces.

Another approach is by tracking humans via thermal infrared radiation ($8\mu m$ to $15\mu m$), so that tags become dispensable. Mautz [23] refers to positioning systems that make use of natural infrared radiation as passive infrared localization systems. The localization of thermal radiation of humans via passive thermal IR sensors is a localization system that has been proposed by Hauschildt and Kirchhof [15] in 2010. Their results showed a sufficient positioning accuracy up to decimeter level, however the effects on the measurements caused by the background radiation has not been investigated further.

2.3.3. WLAN/Wi-Fi

WLAN is an abbreviation for Wireless Local Area Networks which are networks of devices that can exchange data via radio frequency signals and is a very popular technology for indoor positioning. The devices compatible with WLAN within the network are often referred to as Wi-Fi devices, where Wi-Fi is short for wireless fidelity and is a registered trademark of the Wi-Fi Alliance [23]. Furthermore, the wireless networks follow the Institute of Electrical and Electronics Engineers (IEEE) 802.11 standards and operates at the same wavelengths as Bluetooth. Consequently, WLAN is operating in the unlicensed ISM radio frequency band (Fig. 2.1) of 2.4 GHz (2400 – 2484 MHz) and the 5.2 GHz (5150 – 5350 MHz) band [18]. Currently, almost all indoor environments, such as households, airports, train stations, universities, libraries etc., are implemented with WLAN technology. Due to the fact that WLAN-based indoor positioning systems can operate via existing WLAN systems and have been implemented in almost all indoor environments, this IPS becomes relatively cheap and user-friendly. Moreover, the WLAN-based IPS can estimate its user's locations within the network, where the users can be any device that is connected to the WLAN. The WLAN-based IPS has many applications and can be not only be used for tracking persons, but also for Location-Based Services (LBS). The Location-based Services are very relevant for the commercial markets, since LBS can gather information from- and deliver information to -mobile-devices within the WLAN based on their geographical position [23].

Based on the gathered information from an accessible mobile-device, LBS could for example show personal advertisements on billboards within the shopping mall and influence your shopping behavior based on your interests.

The range of the WLAN technology exceeds the range of Bluetooth and the accuracy of the location estimation is dependent on the signal strength of the WLAN [13]. Besides this, BLE indoor positioning has several advantages in comparison with the WLAN-based positioning. Firstly, the Bluetooth chip is less expensive than the costs of Wi-Fi. Secondly, the power consumption of BLE is much lower than Wi-Fi, Bluetooth uses approximately one fifth of the power of Wi-Fi [34]. More and more applications comprise mobile devices with limited operation time (battery), which makes BLE a more preferable positioning technique than WLAN-based positioning systems. Another advantage of BLE over Wi-Fi is the flexibility of the deployment of the system. The beacons can be placed on user-specified locations causing good signal geometries in comparison with the Wi-Fi access points (AP) that often have fixed positions [10].

2.3.4. Alternative RF technologies

ZigBee
Besides Bluetooth there are many other indoor positioning systems operating in the radio frequency band. One of the alternative technologies that has been developed for short-range communication is known as ZigBee which is also operating in the 2.4 GHz (2400 – 2484 MHz) unlicensed ISM frequency band. ZigBee is a low-cost, low-power wireless technology and a ZigBee beacon has a typical signal coverage of approximately 20 to 30 meter in an indoor environment [23]. For example, the battery of a ZigBee beacon endures 3 years of active signal transmission making ZigBee technology a low-power wireless solution. Larranaga et al. [21] presented an indoor positioning algorithm based on ZigBee Wireless Sensor Networks. By deploying a network of 8 ZigBee reference beacons over an area of $432m^2$ and applying their positioning algorithm, Larranaga et al. [21] managed to obtain an average localization accuracy of 3 meter. Furthermore, ZigBee can be used for person/object tracking.

In contrast to BLE, ZigBee does not use a frequency-hopping spread-spectrum system (FHSS) which can cause interference with other radio communication devices operating in the same band, such as Wi-Fi devices, Bluetooth, microwaves and remote controls. Moreover, ZigBee is not supported by mobile devices such as smartphones and tablets, making this solution less favorable for most applications.

Essensium
Essensium is a Belgium company based in Leuven with an expertise in positioning technology. The positioning technology focuses mainly on industrial applications such as smart logistics, container terminals and industrial automation. The main goals are often related to improving visibility, safety, and reducing the cost of operations. Essensium operates a RF single-chip positioning solution within the 2.4 GHz in the ISM-band and is working with two way ranging [7] and provides a 2D positioning solution, since a 3D solution is not necessary yet for their use cases. This is a form of TOA (section 3.2.2) where the two way travel time approach is used in order to overcome clock synchronization. In order to get a high accuracy (<0.5m) the steepness of the signal is directly related to the accuracy, namely the steeper/sharper the edge, the higher the accuracy. The only problem is that the pulse has to travel faster in order to get a sharper edge and if the pulse travels faster, the spectral mask becomes wider. Therefore, Essensium optimizes the accuracy (edge steepness) by using the maximum available instantaneous bandwidth of 200 MHz in the 2.4 GHz ISM-band without violating the ISM spectral mask [7].

To determine a position of a mobile device, the tag sends signal to every reference station at fixed positions to determine its relative distances and eventually the position of the mobile device can be derived by circular intersections each centered at a reference station. Determining positions using circular intersections is a positioning method that is known as trilateration and is further elaborated in section 3.1. The intersection area between the circles is referred to as the Possible Position Zone (PPZ) and has a 100% certainty that a mobile device is located within this area [7]. The more reference stations, the smaller the PPZ becomes which results in a likely position with a higher accuracy.

2.4. BlooLoc technology

The technology that will be used for this thesis is an IPS of BlooLoc, an innovative tech company headquartered in Leuven (Belgium). The term *'BlooLoc'* is a combination of the terms Bluetooth Localization and offers hardware and software for accurate indoor positioning, known as 'yooBee' [2]. In contrast to Essensium, BlooLoc focuses more on consumer type applications and uses Received Signal Strength Indicator values (RSSI, section 3.2.3) instead of time of arrival measurements. As mentioned earlier, a BlooLoc starter kit (Fig. 2.7) has been made available through CGI for experimental purposes. The infrastructure of a starter kit consists of 1 basestation, 15 beacons and 3 tags. Besides the three tags, the system supports the localization of mobile devices as long as the application 'yooBee engine' has been installed on either android or IOS. The starter kit corresponds with a single Cell deployment, referring to the Cell of a single basestation which spans an area of approximately $500m^2$. Since all devices serviced by a Cell should be within the range of the basestation, the range of wireless indoor connections is limited to a recommended $450m^2$ [2]. Furthermore, the cost of a starter kit are 2750€, the update rate (4.1.1 User Requirements) is 1 Hz and the positioning error is less than 1m for 80% of the measurements. The beacons, basestation and tags communicate with each other via RF signals (Bluetooth Low Energy) spread over 40 channels within the ISM 2.4 GHz band, each with a 2 MHz width. Besides the discussed information in this section, more information about the functionality, infrastructure or deployment can be acquired via BlooLoc [2]. This section will explain the infrastructure, functionality and deployment of BlooLoc, and how the infrastructure works for indoor positioning of tags and mobile devices. Note that during this research the yooBee Software Development Kit (SDK) and Application Programming Interface (API) of BLooLoc had version 1.6, however, the functionality of the SDK and the API's are still evolving and thus subject to change.

Figure 2.7: The BlooLoc Starter Kit, 1 basestation, 15 beacons and 3 tags. Source: BlooLoc [2]

2.4.1. Infrastructure, functionality and deployment

The key elements of the infrastructure of BlooLoc are the beacons and the basestations. Since BlooLoc is a multi-purpose solution, both tags and mobile devices can be localized. Furthermore, the communication between the beacons, basestations and tags is wireless and the infrastructure is easy to install and can be quickly deployed.

The Basestations

Every yooBee basestation (Fig. 2.8) covers an area of approximately $450m^2$ and act as a gateway between the beacons, tags, mobile devices and the servers in the Cloud Software Development Kit (SDK). Each cell can host unlimited amounts of mobile devices and up to 256 tags. The functionality of the Cloud SDK includes storing data in a database, fusion of data collected by multiple devices to calculate locations and orientations, monitoring options for the system's status, floorplan configuration, historical location results, and streaming of real-time locations of tags and smartphones [2]. To constantly communicate with the Cloud SDK, the basestations require a connection via either Ethernet or Wi-Fi and need to be powered via a cable. All devices located within the Cell of a basestation are managed and configured by the basestation.


Figure 2.8: YooBee Basestation of BlooLoc. Source: BlooLoc [2]

The Beacons

The yooBee Beacons communicate with the tags, mobile devices and the basestations. The beacons are small (10x10 cm) squared devices with a solar panel covering one side and equipped with a NFC chip for identification purposes (Fig. 2.9). A fully charged beacon can operate between 1 and 3 months and no cables or additional batteries are needed, because the batteries charge themselves by collecting light via the solar panel. The battery status of every beacon within the Cell of a basestation is monitored in the Cloud SDK. So, before deploying the beacons, it has to be considered whether the beacons will be deployed permanent or

temporary. In case of permanent deployment, the beacons require light to recharge the battery and should be located either under light or on a window in direct contact with sunlight.

Figure 2.9: YooBee Beacon of BlooLoc, front (left) and rear (right). Source: BlooLoc [2]

On the other hand, temporary deployment requires the batteries to be fully charged on forehand, so beacons can be mounted temporary to walls and ceiling without the solar panel harvesting light. The beacons can be mounted on windows or smooth surfaces by using the included suction cup tapes and can be attached to walls or other surfaces by using metal brackets with screws. The locations of the beacons are linked to the corresponding locations on the floorplan and act as location references for the tags and mobile devices [2]. Furthermore, the beacons operate with two way communication, meaning that they can both receive and transmit. In order to increase the positioning accuracy and to reduce the calibration time, it is important to indicate the correct height and orientation of the beacons. Therefore, when deploying the beacons, the exact height has to be registered and inserted to the API. The BlooLoc algorithm will use the height and orientation of the beacons in combination with the information of the floorplan (obstacles, scale, walls etc.) to locate tags or mobile devices. Every beacon covers an area of approximately 25 to 30m^2 depending on the walls, meaning the distance between two beacons should be approximately 5 meter.

The Tags

The yooBee tags (Fig. 2.10) are small square devices (31,4 mm x 31,4 mm x 7,7 mm) that can be worn as badge, wristband or necklace and can be attached to objects as a sticker [2]. Similar to the beacons,tags are also embedded with a NFC chip for identification purposes. The motion activated tags are equipped with a replaceable coin cell battery with a lifespan of approximately 1 year and remain in rest mode if not moved. Furthermore, the tags are provided with a push button and a small LED light to signal events for instance in case of emergencies. Not only the beacons battery status, but also the battery status of the tags can be monitored in the Cloud SDK. The tags repeatedly sends (update rate: 1 Hz) BLE signals to its surroundings which can be intercepted by the beacons and basestations. The only downside of the tags and beacons is that they are relatively vulnerable for theft.

Figure 2.10: A yooBee tag of BlooLoc with push button. Source: BlooLoc [2]

2.4.2. Indoor positioning with BlooLoc

The tags use BLE to constantly broadcast data from their inertial sensors as advertise packages within the advertising channels of the Bluetooth band (section 2.2.2 Bluetooth Bandwidth). The broadcasted advertise packages are received by both basestation and beacons. The basestation acts as a scanner and is constantly receiving data from the advertising channels and does not broadcast information itself, whereas the beacons both receive and broadcast data. The beacons collect the data broadcasted by the tags, measure the Received Signal Strength Indicator values (RSSI is explained in section 3.2.3) and the inertial sensor data (section 2.4.3) of the tags and forward it to the basestation using BLE [2]. Simultaneously, the basestation collects all data and transmits it to the Cloud server via Ethernet or Wi-Fi. The cloud server subsequently calculates the positions of the moving tags and visualizes it on the digital floorplan. Moreover, the various received signals are compared to each other in order to eliminate redundant information, increasing the efficiency and run-time of the model. A schematic overview of the communication is illustrated in Figure 2.11.

The positioning of mobile devices is slightly different to the positioning of tags. In case of positioning of mobile devices, the infrastructure only exists of the beacons and an application including the basic yooBee Mobile SDK needs to be installed on the device [2]. Furthermore, the beacons act as the tags in the way that they broadcast advertise packages through the advertising channels in the Bluetooth band. Subsequently, the mobile device is acting as a scanner and is constantly collecting the advertise packages of the beacons and measuring the RSSI values. Furthermore, the mobile device collects the values of its own inertial sensors and then either calculates its position via the Mobile SDK or transmits the data to the Cloud server via Wi-Fi or 3G/4G networks. The latter will finally result in the positions of the mobile devices calculated on the Cloud server and visualization on a digital floorplan.

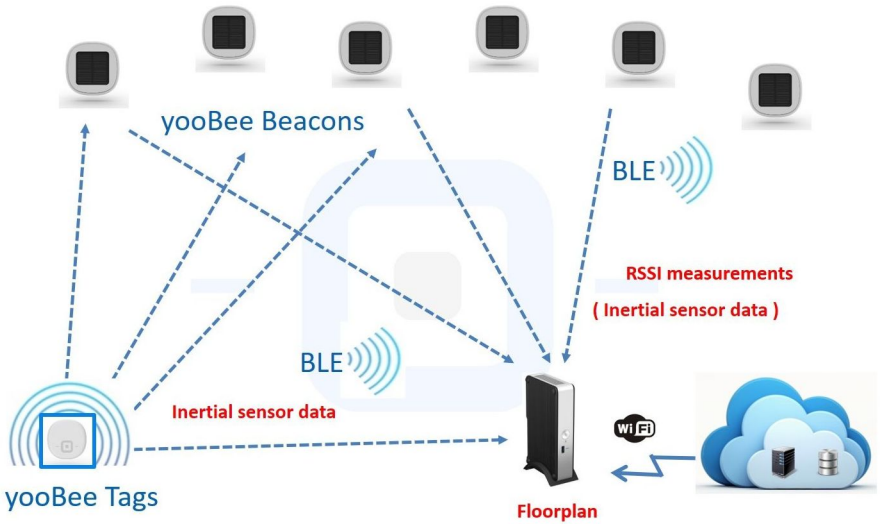

Figure 2.11: A schematic illustration of the communication between tags, beacons, basestation and the Cloud server. Source: BlooLoc [2].

2.4.3. Inertial sensors and sensor fusion principle

The positioning algorithm of BlooLoc uses all information that is present and by deploying more than enough beacons within an indoor environment, there are always beacons in direct LOS with the tag or mobile device. Besides eliminating redundant information from comparing differences in signal strength from the received pulse at various beacons BlooLoc uses the additional inertial sensor data to optimize the positioning algorithm. The inertial sensors of the tags collect information that is transmitted to the beacons. The inertial sensors of the tags contain an accelerometer, magnetometer, thermometer and a gyroscope. The accelerometer measures the motion and vibration of a device and it can detect, in case of human activities, whether people are walking, running or even riding. In contrast to riding, the accelerometer vibrates at every step when a person is walking which results in a significantly different signal. The gyroscope use the Earth's gravitational field to determine orientation, so the gyroscope can detect rotation around a particular axis. Additionally, the magnetometer measures the Earth's magnetic field and since the magnetic field around the Earth has significant values, the magnetometer can be used as a compass. Integrating the information gathered by the three inertial sensors, results in a more accurate positioning, orientation determination and movements detection.

Sensor fusion is the state-of-the-art positioning principle used by BlooLoc to compute the most likely position of a tag or mobile device [4]. The principle sensor fusion comprises the fusion of a RSSI (section 3.2.3) model of the environment, all past inertial sensor data and floorplan information. The RSSI model consists of all past RSSI values between each beacon and every tag or mobile device and is constantly improving and learning from historic data. Moreover, the floorplan information includes all obstacles and infrastructure of the indoor environment such as walls, corridors, doors, obstacles etc. Initially, a burn-in phase is required which is a self-learning auto-calibration system which over time leads to a more and more accurate positioning system by analyzing all gathered data. The more historic data, the better the RSSI model becomes and the more accurate it can account for effects of for instance shadowing and reflection (section 4.2). Finally, a stochastic technique based on a sequential Monte Carlo (particle filter) determines the most likely position [4].

The position information that is displayed on the floorplan contains the users orientation, a real-time position estimate (<2s delay) and a delayed position estimate (16s delay) that is more accurate since it uses future data to compute the most likely position [4]. If the beacons are installed right and the system has self-calibrated properly, a positioning error of approximately 1 meter can be realized and the update rate of the tags is 1 Hz which is sufficient for navigation purposes.

3

Positioning methods and measuring principles of BLE

In this chapter the positioning methods and measuring principles of BLE indoor positioning systems will be explained. The localization of devices using Bluetooth beacons can be obtained via various positioning techniques (section 3.1), such as fingerprinting (FP), triangulation, trilateration, cell-based methods and proximity location sensing technology [5]. The corresponding measuring principles, such as angle of arrival (AOA), time of arrival (TOA), time difference of arrival (TDOA), received signal strength (RSS) etc. will be discussed in more detail in section 3.2. Subsequently, the propagation of the RF signals through the indoor environment can get distorted by several factors, such as moving objects, complex infrastructures that influence the availability of the LOS path, large open rooms and reflecting surfaces that can cause significant multipath [22]. These factors can influence the system performance of the BLE indoor positioning systems. Therefore, it is important to understand the measuring principles of BLE indoor positioning techniques before any experimental setup can be made.

3.1. Positioning methods

3.1.1. Triangulation and trilateration

Triangulation is a geodetic positioning method and can estimate the position of an object relative to multiple reference points. Triangulation requires at least two reference points and an object with an unknown location in 2D. Since the positions of the reference points are known and thus the distance between the reference points, a triangle can be formed between the object and the reference points. The more reference points, the more accurate the position of the object can be localized. Furthermore, triangulation is based on the measuring principle Angle of Arrival (AOA), which will be further elaborated in section 3.2.1.

The triangulation method uses the measurement of angles between a virtual line connecting two reference points or in this case two beacons and the LOS from both beacons to the object [5]. To illustrate the principle of the triangulation method, Figure 3.1 depicts two persons onshore with a known distance L from each other. If one wants to know the distance d from a remote ship to the shore via triangulation, the combination of angles and the known distance between the reference points results in a distance. This will be discussed in more detail in section 3.2.1. According to Chawathe [5] the triangulation method is not suitable for the localization using Bluetooth beacons, because the method is depending on the LOS measurements between the reference beacons and the object. The LOS in an indoor environment can be easily interrupted due to the complex infrastructure, which makes this method dependent on the availability of the LOS path.

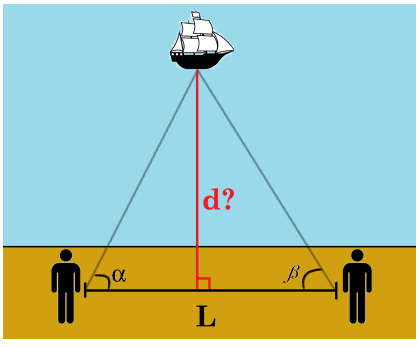

Figure 3.1: The Triangulation method

Trilateration is another geodetic method that uses the geometric properties of triangles. In contrast to triangulation, trilateration is a method that measures the distances from an object to the reference points to get an estimation of the 2D position of the object [22]. The location of the target is estimated by the intersection of multiple circles, where each circle is centered at the location of a reference point of beacon. In addition, the radii of the circles are unique and depend on the received signal strengths (RSS), or on the time of arrival (TOA) of a signal transmitted between the target and the beacon [22]. In contrary, time difference of arrival (TDOA) does not use the radii of circles, but assumes a target must lie on a hyperbola. The measuring principles RSS, TOA and TDOA will be explained in more detail in section 3.2. Furthermore, the intersection points of the circles give an estimation of the targets location. Since the measurements are affected by obstacles (such as furniture), the infrastructure or in other words the basic structure of buildings, multipath reflections and disturbance by other signals operating in the same frequency band, it is almost impossible to get only one intersection point. Additionally, all measurements are subject to noise which will lead to random errors. Therefore, it is common to use an average, or more likely a weighted average of the coordinates of the intersections points to estimate the targets location [34]. As an illustration, Figure 3.2 depicts the principles of the trilateration method with three beacons transmitting omnidirectional signals. In Figure 3.2, the intersections of the circles x_1, x_2 and x_3 are used to estimate the position of the target x. In other words, the average of the three intersection points results in the location of the target x.

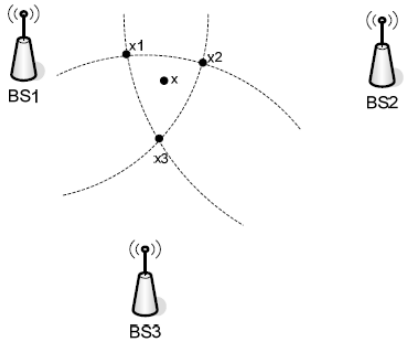

Figure 3.2: The trilateration principle of target x. Source: Wang et al. [34]

3.1.2. Fingerprinting

Until recently, the Fingerprinting (FP) positioning method was the state-of-the-art indoor positioning technique and is also available on most smartphones. FP requires premeasured features (fingerprints) related to a certain location in space and subsequently estimates its target's location by corresponding online measurements with the closest premeasured fingerprint [22]. According to Faragher and Harle [10] (2014) a fingerprint refers to

> *"The pattern of radio signal strength measurements recorded at a given location in space and consists of a vector of signal identity information (such as cellular Cell-IDs, or Wi-Fi MAC addresses) and a corresponding vector of Received Signal Strength (RSS) values".*

Typically, the FP method comprises two phases, namely the offline training phase and the online position determination phase [13]. Firstly, the location of interest, for example an office floor, is divided into grid cells of size x,y and stored in a database. Subsequently, the offline phase is collecting location related data for every grid cell within the area of interest. The locations of the fixed reference stations (beacons) and the various signal strengths from nearby stations are measured and collected for every grid cell [31]. However, the offline phase is collecting the location based data multiple times in order to improve the accuracy of the fingerprints which results in the fact that the offline phase is a rather time consuming process.

During the online phase, the signal strengths and location related data of the target are measured. These values can be compared to the premeasured data collected in the offline phase in order to make an estimation for the target's location [13]. Therefore, it is profitable that the offline phase is gathering the location based data multiple times, because it results in a more accurate comparison with the data that is collected during the online phase. The more accurate comparison will eventually lead to a more accurate estimation of the target's location. Furthermore, the online position determination phase uses the k-nearest neighbor algorithm to determine the target's position. The k-nearest neighbor algorithm will be explained in section 3.2.4. To conclude, the advantage of this technique is the more accurate positioning estimations, although the offline phase is very time consuming. A major downside is however that the way the device is held during the offline training phase influences the various location related signal strengths and can result in locations with an offset is the devices is held differently during the online phase. Additionally, every time the infrastructure within the indoor environment changes, the offline phase needs to be done once again. This makes fingerprinting a rather doubtful positioning method.

3.1.3. Cell-based method

In contrast to the previous indoor positioning methods, the cell-based method requires knowledge about the visibility all beacons individually without using angle or distance measurements [5]. Subsequently, a network of cells based on the limited range of the beacons can be setup to localize targets within the network. Furthermore, it is not required that the target is visible to all beacons. For instance, let's consider the schematic situation depicted in Figure 3.3 with an indoor positioning network of five beacons A, B, C, D and E and the corresponding cells related to their range. If a target is within the range three beacons *(beacons B, C, and D in Fig. 3.3)*, it can be localized within the region of intersection of the corresponding cells. The other two beacons *(A and E in Fig. 3.3)* in the network are not able to locate the target, because it is out of range. Generally, cell-based methods use information on both the visibility and non-visibility to locate the target.

The irregular shapes of the beacons cells are a consequence of the often complex infrastructure of an indoor environment. The shape and size of the cells is directly related to the range of its beacon. For outdoor applications, the shapes would be more regulars, such as circles or ellipsoids. However, indoor environments go hand in hand with signal attenuation, reflections and multipath. The consequence is that the Bluetooth signals get distorted and the cells transform into irregular shapes (Fig. 3.3).

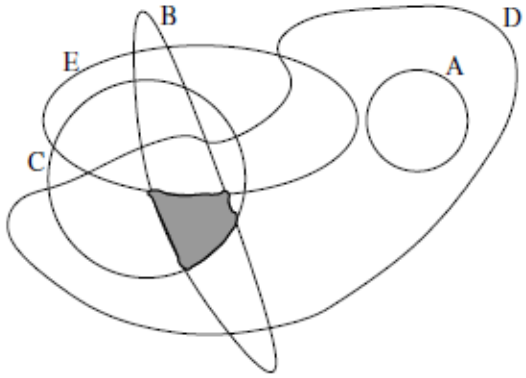

Figure 3.3: The principle of Cell-based localization. The target is visible in the cells of beacons B, C, and D and is located in the intersection region (grey). The target is out of range for beacon A and E. Source: Chawathe [5]

The Cell-based method is also referred to as the proximity location sensing technique which locates a target relative to a known reference point or area [13]. This technique does not give an absolute or relative estimation of the targets position, it only detects whether a target is within the proximity area or not. Therefore, the Cell-based method is a useful technique for various applications, for example, the proximity area of a detector can represent a room in a hospital and a target can be some medical equipment or a patient.

3.2. Measuring principles

3.2.1. Angle of Arrival (AOA)

The Angle of Arrival measuring principle is using the angles between the target and two fixed reference points to determine the position of the target. Figure 3.4 illustrates the basic principle of triangulation, the object is located at point C and the two locations of the reference points are point A and B. Since the positions of A and B are fixed and known, the baseline L between A and B can be easily computed. Moreover, with help of the measurement angles α and β in the LOS from C to each of the reference points, the location of point C can be found. Firstly, by applying the rules of sine for the unknown sides AC and BC can be expressed (Fig. 3.4).

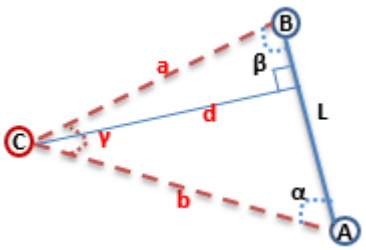

Figure 3.4: The Triangulation principle.to find the location of point C.

$$\text{Side BC} \rightarrow a = L \times \frac{\sin(\alpha)}{\sin(\gamma)}, \text{Side AC} \rightarrow b = L \times \frac{\sin(\beta)}{\sin(\gamma)} \qquad (3.1)$$

In equation 3.1 the angle of γ can be expressed as $\gamma = 180 - \alpha - \beta$ or $\pi -$

$\alpha - \beta$. By substituting this in the sinus and taking account the properties of trigonometric functions $\sin(\gamma) = \sin(\pi - (\alpha + \beta)) = \sin(\alpha + \beta)$, equation 3.1 can be rewritten as

$$\text{Side BC} \rightarrow a = L \times \frac{\sin(\alpha)}{\sin(\alpha+\beta)}, \text{ Side AC} \rightarrow b = L \times \frac{\sin(\beta)}{\sin(\alpha+\beta)} \tag{3.2}$$

Finally, the following expression for the length of the height of the triangle d can be formed via basic goniometric principles

$$d = \sin(\alpha) \times b \rightarrow d = \frac{L\sin(\alpha)\sin(\beta)}{\sin(\alpha+\beta)} \tag{3.3}$$

A major disadvantage of the AOA measuring principle is that the receivers need several antennas for accurate angle measurements which are often expensive. Furthermore, AOA is not suitable for the localization using Bluetooth beacons, because the method is depending on the LOS measurements between the reference beacons and the object. The LOS in an indoor environment can be easily interrupted due to the complex infrastructure, which makes this method dependent on the availability of the LOS path. This makes AOA less favorable for indoor positioning systems that prefer locating mobile devices and tags.

3.2.2. Time of Arrival (TOA) and Time Difference of Arrival (TDOA)

The principle of Time of Arrival (TOA) computes the distance of a target based on the travel time of a signal from a transmitter to a receiver, for instance BLE beacons and mobile devices. This means that the TOA principle measures the one-way propagation time and since the signal travels with a known velocity and the absolute time of arrival is measured, the distance relative to a beacon can be calculated. The TOA measurements of two beacons will narrow the position of the mobile device down to two possibilities and a third beacon will result in a precise location of the mobile device. Unfortunately, the TOA principle is dependent on a precise time synchronization between all beacons and mobile units [34]. To get a better idea about the precise time synchronization, for instance, a nanosecond error between the transmitter and the receiver already translates into a distance error of 30 cm if RF signals are used [23]. To overcome the clock synchronizing of the transmitter and receiver, the two-way travel time approach can be used. So instead of measuring the travel time of a pulse traveling from transmitter to receiver, the travel time of a pulse propagating back and forth between transmitter and receiver is measured. In this way, clock synchronization becomes redundant, however a correction in time has to be made. When the receiver intercepts a pulse, it instantly sends a pulse back to the transmitter, however the instant between receiving and transmitting causes a fixed delay in time.

Another measuring principles that is often mistaken for being similar to TOA is the Time Difference of Arrival (TDOA). However, the difference between TOA and TDOA can be found in how the distance is calculated. In TDOA the target (source) transmits a signal that is received by all fixed reference stations (receivers) and based on the difference in time of arrival of the signal at the receivers, an estimation of the targets location can be made [34]. Additionally, an advantage of TDOA in comparison with TOA is that the mobile devices do not have to be time synchronized with the beacons [36]. Once the difference in distances between the mobile device and two reference stations is known, it is assumed that the target must lie on a hyperbola that is defined to be the set of all points which have a constant range difference with respect to two reference stations [19, 36]. Therefore, the position of the mobile device is limited to the hyperbolas between the reference stations and the hyperbola can be computed by using the following equation

$$R_{i,j} = \sqrt{(x_i - x)^2 + (y_i - y)^2 + (z_i - z)^2} - \sqrt{(x_j - x)^2 + (y_j - y)^2 + (z_j - z)^2} \tag{3.4}$$

where (x,y,z) represent the position of the target and $(x_i, y_i, z_i), (x_j, y_j, z_j)$ represent the position of the fixed reference stations i and j [22]. Furthermore, the fixed reference points are known as *foci* and represent for instance two BLE beacons deployed for indoor positioning purposes. The process of positioning using the range differences and hyperbolas is denoted as hyperbolic lateration.

At first, consider a 2D case with two fixed BLE beacons and a target (Fig. 3.5), where the range between the target and the first beacon is given by r_1 and the range to the second beacon by r_2. The range difference $\Delta d = r_2 - r_1$ is constant and limits the targets position to a set of points that lie on a hyperbola [19]. Additionally, a third beacon in the system will generate another hyperbola between for instance the first and the third beacon. Finally, the intersection point of both hyperbolas defines the targets position (Fig. 3.5). The positioning becomes more complex for a 3D case, since in 3D the constant range difference is not given by a hyperbola

but by the surface of a hyperboloid. Therefore, at least three hyperboloids are required to determine the 3D position of the target.

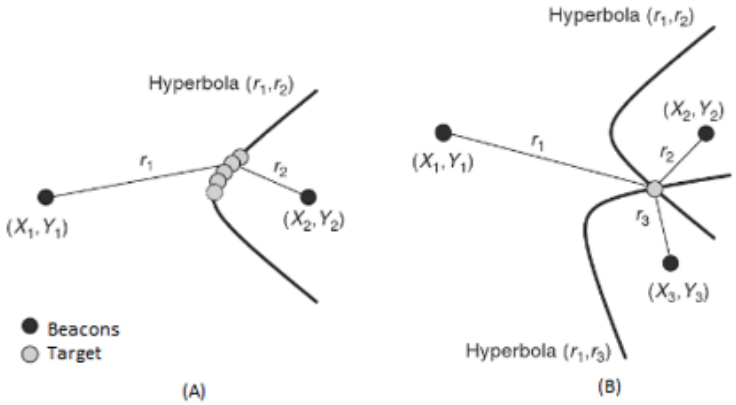

Figure 3.5: The principle of hyperbolic lateration for a 2D case. Source: Küpper [19]

3.2.3. Received Signal Strength (RSS)

Additionally, Received Signal Strength Indicator (RSSI) is a measuring principle based on wave propagation and its corresponding signal attenuation in order to estimate the distance between transmitters and receivers. The RSSI are based on the observed Received Signal Strength (RSS) values that have been averaged over the sampling period [23]. This measuring principle is based on signal attenuation, meaning that the original signal strength from the transmitter is compared to the decreased signal strength at the receiver. The decrease of the signal strength relative to its original intensity is depending on the distance the signal has to propagate [31]. Furthermore, the received power (P_R) of an electromagnetic wave is inversely proportional to the square of the distance (d) to the source [27] and can be expressed as follows:

$$P_R \propto \frac{1}{d^2} \tag{3.5}$$

The received power is not only depending on the distance from the source, but is also related to the transmitted power (P_T). The relation between the received power, transmitted power and the distance can be expressed in the attenuation model [23],

$$P_R \propto P_T \frac{G_T G_R}{4\pi d^p} \tag{3.6}$$

where (P_T) represents the transmitted power at the source, (G_R) and (G_T) are representing the antenna gains of both transmitter and receiver and the p is the path loss exponent. The path loss exponent represents the attenuation rate of the propagation signal with increasing distance and commonly takes values between 4 and 6 for indoor environments [23]. Thus, the distance to every beacon can be derived in case the path loss exponent, the transmitted power at the emitter, the received signal power at receiver and the antenna gains of the transmitter and receivers are known. Theoretically, the distances that have been estimated from the RSSI values to multiple beacons can be used to determine the receivers position by trilateration. However, in the real world, interference, multipath and the presence of obstacles and people leads to a more complex spatial distribution of the RSSI values [23]. BlooLoc uses the fusion of a RSSI model of the environment, all past sensor data and floorplan information to estimate positions (section 2.4.3).

3.2.4. K-nearest neighbor classification

The fingerprints gathered during the online position determination phase are assigned to the premeasured data by using the k-Nearest Neighbor (k-NN) algorithm. The k-Nearest Neighbor algorithm is a simple classification method where new data is compared to the premeasured data of its k nearest neighbors. The value of k is a positive user-defined integer and is often a relative small number. It represents the amount of neighbors that is taken into account during the execution of the algorithm. The k-NN classification method will be explained on the basis of a simple example. Assuming the dataset of Figure 3.6, with the red circles and green triangles representing different classes of signal strengths measured in the offline phase of the FP method and

the star represents the signal strength of the target measured in the online phase of the FP method. The algorithm assigns the test point to a class according to the class that is most frequent among the k nearest points. To find the nearest neighbors, the distance (commonly the Euclidean distance) between the test point and the surrounding points has to be calculated. So, for k=3 the test point will be assigned to the signal strengths of the red circles since the majority of the three nearest points are circles, whereas for k=5 the test point is classified to the signal strengths of the triangle class (Fig. 3.6).

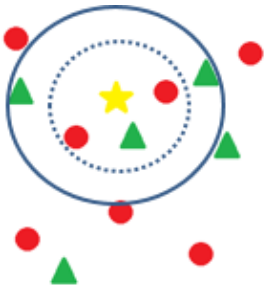

Figure 3.6: An example of k-NN classification. The test point (star) will be assigned to the class that is most frequent among its k nearest points. In case of k=3 (dotted circle), the test point is assigned to the circle class (red) and in case of k=5 (solid circle) it is classified as a triangle (green).

4

Use Cases, requirements and system performance

The second part of the main research question (section 1.3.1) for this thesis states *'to enable the required system performance for given use cases'* and is referring to two major terms, namely the system performance and the use cases. The system performance and the use cases are closely correlated, since the required system performance is mainly dependent on the defined use case. In this chapter, several examples of use cases will provide an overview of their corresponding user requirements. The use cases define both the user requirements and the system performances. Furthermore, the term *'system performance'* will be elaborated focusing on statistical quantities, such as accuracy, precision and reliability. Besides the explanation of system performances, the most important factors that influence the system performances will be discussed. Next, the user requirements form the basis for the theoretical design computations and the practical experiments, which will be explained in the methodology (chapter 5).

4.1. User requirements and use cases

Not only the interest in indoor position systems is continuously growing, but along with it grows the amount of applications. As previously stated, some examples are described (section 1.1.2) to get an indication of the wide-spread field where indoor localization is applicable. The different applications come with various use cases that are defined by user requirements. Before continuing with the user requirements and use cases, it is important to understand that indoor positioning systems can have several objectives, for instance navigation, tracking and LBS.

Navigation has several definitions, where the first definition is the determination of a position, speed and heading of an object [23]. The second definition comprises indoor wayfinding and provides the user with an optimal route based on a start and end point, where the optimal route is often based on factors as costs, time and distance. For example, a business man has to catch his flight on Schiphol and wants to know the fastest route to his gate. The computation of the optimal path can take real-time information of the queue time at the check-ins and security lanes into account and suggest an alternative route that may be longer in distance, but shorter in time. At last, the third definition of navigation relates to the guidance of an object along a path and constantly take the changing current position and the planned path into account [23].

Tracking is defined by Mautz [23] (2012) as *"the repeated positioning of a moving object or person over time"*. In contrast to navigation, tracking does not require the information about the current position to be available at the mobile device [23]. If an object or mobile device is being tracked, its previous locations and current location can be monitored, even without the fact that the object or mobile device is aware of being tracked. Therefore, tracking is often associated with privacy issues if applied on for indoor positioning of mobile devices. A well-known example of tracking, is the track and trace service of parcel services, that provide a constant update of where a parcel is currently located and when it will arrive at its destination.

Another term that is often used, is ***Location-Based Services (LBS)***. As mentioned earlier, LBS are relevant

for the commercial markets, since LBS can gather information from- and deliver information to -mobile-devices within the WLAN based on their geographical position [23]. Next to navigation and tracking, which are also forms of LBS, geographical advertisement is becoming a common application of LBS. Geographical advertisement gathers information from accessible mobile-devices, and show personal advertisements on for example billboards within a shopping mall and influence your shopping behavior based on your personal interests.

4.1.1. User requirements

The objective of an IPS influences the user requirements of the use cases. Before the use cases can be defined, it is important to describe the user requirements in more detail. Since the user requirements differ for every application, a weighting system can test the user requirements against each other to obtain the optimal system for a given application. For this research, the main user requirements will be briefly discussed and are schematically illustrated in Figure 4.1. Mautz [23] defined up to 16 user requirements and for this research, a selection of user requirements has been made and two user requirements, precision and reliability, have been added since these are the major requirements in this research. For more information about the user requirements study the habitation thesis "Indoor Positioning Techniques" of Mautz [23] (2012).

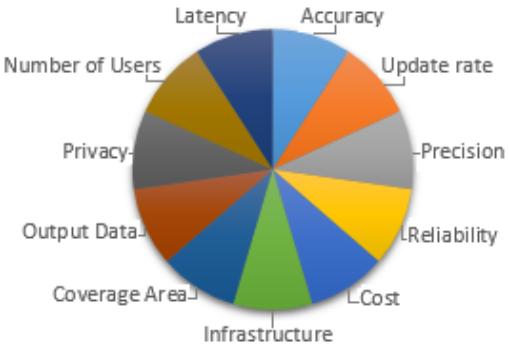

Figure 4.1: Overview of the main user requirements

• **Accuracy**: *The closeness of a measured value to the true value or the measurement uncertainty (Fig. 2.6). Mostly, the accuracy is divided in a horizontal and vertical accuracy.*

• **Precision**: *The precision is related to the repeatability or spread in outcomes of the measured values (Fig. 2.6). Furthermore, precision is also the term that is used to describe the uncertainty in observational data or in modelled data. Precision will be further elaborated in chapter 5.*

• **Reliability**: *The reliability is a term explaining the performance of statistical testing for validation and describes the ability of the observation system to check (itself) for modelling errors [32]. Reliability is often expressed in terms of internal- and external reliability and will be elaborated further in chapter 5.*

• **Cost**: *The costs of the system, maintenance costs, costs in space and time (see section 2.3).*

• **Infrastructure**: *The required infrastructure in terms of basestation, beacons, tags and mobile devices. The necessary infrastructure correlates with the cost of the system, the coverage area and the number of users.*

• **Coverage Area**: *The coverage area is limiting the indoor environment to the area where the system will be setup. If the coverage area increases, so does the infrastructure and thus the cost of the system. Mostly, the coverage area of an indoor environment is defined by a local area, however the coverage area can extent up to global coverage. For example, the GNSS system covers the whole globe and can be received almost everywhere.*

• **Privacy**: *Active or passive devices. Furthermore, the privacy of the devices must be guaranteed and well secured (see section 2.3).*

• **Output Data**: *The output data can consist of 2D/3D coordinates and can present either an absolute or relative position. Furthermore, the output data is mostly given as a location or in more specific cases a location within a geofence. The output data also comprises dynamic parameters such as speed, heading, uncertainty and variances [23].*

• **Update Rate**: *The update rate refers to the frequency at which the user's location is updated. The update rate can be on request or for example every second, this is highly dependent on the use case.*

• **Number of Users**: *The number of users that must be monitored by the system, this can either be tags or mobile devices (active or passive).*

• **Latency**: *The latency refers to the delay in the representation to the user of the requested information or location. In other words, real-time applications have almost no latency which may result in a less precise location, whereas applications with a positioning delay (higher latency) are often coherent with a higher precision.*

4.1.2. Use cases

Several examples of applications for indoor localization have been described in section 1.1.2 to get a better understanding of the wide-spread field, wherein indoor localization is applicable. Based on these applications, various use cases can be defined for further analysis. For every use case, the user requirements (section 4.1.1) will be analyzed and discussed so that the differences in user requirements for different use cases become clear. The analysis on the values of the user requirements has been performed in consultation with Robert Voûte (CGI) and are based on both assumptions and previous applications.

Smart grocery shopping
The first use case defines indoor localization using smartphones and tags to do smart grocery shopping and is one of the examples provided by BlooLoc to promote their product. By giving a shopping list as input, the system provides you a smart and efficient way to walk through the supermarket. Since the grocery shopping is often done within one single supermarket the coverage area is limited to the size of the supermarket. For instance, the average area of a Jumbo (major Dutch supermarket chain) supermarket is approximately $1180m^2$ [17]. This use case is applicable for two different groups, namely the costumers of the supermarkets and the shopping carts. The costumers will most likely be tracked and navigated via their smartphones which requires an horizontal positioning accuracy of less than 1 meter. Furthermore, since the costumer uses navigation an update rate of 1 second is required with a latency of < 2 seconds. Since it is most likely that the shopping carts will be equipped with a tag and costumers want to locate their cart once in a while, an accuracy of <1m is desired. Additionally, an update rate of 5 seconds with a latency of < 2 seconds will be sufficient for locating a shopping cart. Given the fact that the BlooLoc starter kit covers approximately $500m^2$ and costs 2750€ [2], at least three starter kits are necessary to obtain a good accuracy and cover the whole supermarket. This means that the average costs to cover a Jumbo supermarket would be around 8250€. The maintenance cost of the batteries of the tags and beacons will add up to the initial costs, where the cost made by the costumers is limited by the use of smartphones. Furthermore, the costumer is not interested in his absolute position, but most likely to his relative position with respect to a local reference. In addition, the shopping cart will not change in height meaning that a 2D position in the supermarket would be sufficient. If all shopping carts would be equipped with a tag, the shopping behavior of the costumers and the store layout can be analyzed on the basis of heatmaps. Subsequently, real-time information about queue time for every cash register can be implemented, so that customers can be distributed over the cash registers or personal can be warned in case of large numbers of customers. The privacy of the costumers will be guaranteed fully, whereas privacy on the shopping carts is not necessary. For completeness, the user requirements of this use case are summarized in Figure 4.2.

User Requirement	Description
Coverage Area	Average size of a supermarket: 1180 m^2
Infrastructure	3 BlooLoc kits, 3 Basestations, 45 Beacons
Cost	3 BlooLoc starter kits (2750€ per kit) and maintenance cost
Privacy	Privacy of the costumers is maximal, no privacy for carts
Number of Users	Available shopping carts and visitors of supermarket
Update Rate	Shopping Carts: 5 sec; People: 1 sec
Latency	For both Carts and People <2 sec
Horizontal Accuracy	High accuracy for detemining different lanes, <1 meter
Vertical Accuracy	Not applicable
Output Data	Relative 2D locations

Figure 4.2: Summary of the user requirements for the use case “Smart grocery shopping” with the IPS of BlooLoc as example.

Hospitals and Care Centers

In addition, the second use case is related to another important indoor localization application, namely hospitals and care centers. Since hospitals and care centers have different user requirements, they will be analyzed separately. As mentioned earlier, hospitals offer countless possibilities for both tags (for tracking patients, finding equipment, etc.) and smartphones or tablets (for location medical staff or visitor navigation) [33]. Generally, hospitals cover larger areas than supermarkets and often have multiple floors within the buildings. Larger areas automatically come with a larger infrastructure and higher costs. For instance, the Westfriesgasthuis hospital in Hoorn (Netherlands) with an average coverage area of 86000m^2 is chosen as an example [25]. The average coverage area of the hospital includes the GGZ (Mental healthcare), clinics, offices and the parking garage [25]. To cover an area like this, at least 172 BlooLoc kits are needed, worth 473000€. Additionally, the maintenance cost of the energy levels of beacons and tags have to be taken into account. Furthermore, the patients can be tracked by a low cost temporary bracelet. The infrastructure would consist of 172 basestations and 2580 beacons. The requirements such as accuracy, update rate, privacy and number of users can vary, because there are multiple objectives for indoor localization in hospitals. The objectives for this use case can be subdivided in three groups namely equipment, staff and patients. Since staff members in hospitals must be located quickly in case of emergencies, the update rate of the staff is required to be < 1 second with a latency of < 2 seconds. The horizontal accuracy to locate the staff is required to be < 1 meter. On the other hand, patients are most likely not changing positions that frequent, thus an update rate of 10 seconds with a latency of < 5 seconds and a horizontal accuracy of < 2 meter is sufficient. Finally, for the localization of equipment (wheelchairs, infusion pumps etc.) room level accuracy will be sufficient (< 5 meter) and the update rate will most likely be on request or 1 minute with a latency of < 5 seconds. The privacy of both patients and staff has to be guaranteed externally, however, internally privacy is less since it is important for staff to locate other staff members and patients within the hospital. The equipment does not need privacy. Furthermore, the number of users depends on the amount of patients, staff, visitors and equipment that is being tracked. Finally, the user requirements of this use case are summarized in Figure 4.3.

User Requirement	Description
Coverage Area	Area of an hospital (Westfriesgasthuis) 86000 m^2
Infrastructure	172 BlooLoc kits, 172 Basestations, 2580 Beacons
Cost	172 BlooLoc starter kits (2750€ per kit) and maintenance costs
Privacy	Privacy of the staff, patients and visitors is maximal, no privacy for equipment
Number of Users	Depending on patients, staff, visitors and equipment
Update Rate	Equipment: 1 min; Staff: 1 sec; Patients: 10 sec
Latency	Equipment: <5 sec; Staff: <2 sec; Patients: <5 sec
Horizontal Accuracy	Staff <1 m, Patients <2 m, Equipment <5 m
Vertical Accuracy	Not applicable
Output Data	Relative 2D locations

Figure 4.3: Summary of the user requirements for the use case “Hospitals” at the Westfriesgasthuis in Hoorn (Netherlands) with the IPS of BlooLoc as example.

Besides hospitals, it is possible to track elderly people in care centers by using a geofence such that an alarm is triggered when a patient with dementia would exit a designated area [2]. In order to track the patients in care centers within a geofence, the update rate should be < 1 second with a latency of < 2 seconds. Horizontal positioning accuracy of < 2 meter would be sufficient for patients, whereas room level accuracy (< 5 meter) would be sufficient for the staff members. Furthermore, staff members are less urgent to locate than in a hospital and therefore an update rate of 10 seconds with a latency of < 5 seconds is acceptable. The privacy of both staff and patients has to be guaranteed externally, however, internally the staff members will have access to the locations of the patients, to locations of other staff members etc. By way of example, following the construction standards of care centers in the Netherlands, the average area is 840m^2. This results in two BlooLoc starterkits with 30 beacons to cover a care center. Finally, an overview of the user requirements of this use case is summarized in Figure 4.4.

User Requirement	Description
Coverage Area	Area of a care center (Construction standards) 840 m^2
Infrastructure	2 BlooLoc kits, 2 Basestations, 30 Beacons
Cost	2 BlooLoc starter kits (2750€ per kit) and maintenance costs
Privacy	Privacy of the staff, patients and visitors is maximal
Number of Users	Staff and 30 patients
Update Rate	Staff: 10 sec; Patients: 1 sec
Latency	Staff: <5 sec; Patients: <2 sec
Horizontal Accuracy	Staff <5 m, Patients <2 m
Vertical Accuracy	Not applicable
Output Data	Relative 2D locations + Geofence for designated areas

Figure 4.4: Summary of the user requirements for the use case "Care centers" according to the construction standards in the Netherlands with the IPS of BlooLoc as example.

Airports, Train/Subway Stations and Shopping Malls

The third use case is related to airports, shopping malls, and train/subway stations. Airports and train/subway stations are often complex buildings with many facilities and many travelers need to find their way under time pressure. Regarding airports, an indoor localization system could guide people in a smart and quick way to the right place, gives information about queue time at the security and can tell you to avoid crowded places if you are in a hurry. On the other side, if you have some time left before departure and the system can find the nearest shops and facilities for you. Similarly, train/subway stations are often crowded and commonly associated commuters. Real time information about delays, platform changes, interference and planned maintenance can help the commuters saving precious time. Furthermore, the staff can be tracked as well and receive a warning in case of emergencies or if there are changes in their schedule. In contrast to airports and train/subway stations, shopping malls host people that have no time pressure and most likely are day trippers. An indoor localization system in shopping malls can guide people to their favorite places, locate ATMs, analyze the shopping behavior and provide an anti-theft system in the form of geofencing [2]. The similarity between shopping malls and airports, train/subway stations, is that the buildings are often complex and contain large open spaces with high ceilings. It is also very common to have several sublevels within one large open space, for example an open cafeteria above check-in counters at an airport.

User Requirement	Description
Coverage Area	Area of train station (Utrecht Centraal) 25000 m^2
Infrastructure	50 BlooLoc kits, 50 Basestations, 750 Beacons
Cost	50 BlooLoc starter kits (2750€ per kit) and maintenance costs
Privacy	Privacy of the staff and people is guaranteed
Number of Users	Amount of travellers/staff per day at Utrecht Centraal
Update Rate	Staff: 10 sec; People: 5 sec
Latency	Staff: <1 sec; People: <2sec
Horizontal Accuracy	Staff <5 m, People <5 m
Vertical Accuracy	Not applicable
Output Data	Relative 2D locations + possible sublevels

Figure 4.5: Summary of the user requirements for the use case "Airports, Train/Subway Stations and Shopping Malls" specified for the Utrecht Central train station (Netherlands) with the IPS of BlooLoc as example.

The user requirements accuracy, update rate, output data and privacy are approximately the same for airports and train/subway stations, as well as for shopping malls. Obviously, the coverage area, cost, infrastructure and number of users vary for all locations. A horizontal accuracy of 5 meter or less would be more than sufficient for locating people and staff. For navigation purposes an update rate of 5 seconds with a latency of < 2 seconds for navigation purposes. The update rate for locating staff is a little lower, 10 seconds, with

a latency of < 1 second. Furthermore, the privacy of the people or travelers must be guaranteed, while for staff the privacy is only guaranteed externally. Similarly to the previous use case, the output data will be 2D relative positions with respect to a local reference. To illustrate the user requirements for the train station of Utrecht Central, a summery is given in Figure 4.5, note that the accuracy, privacy, output data and update rate are approximately the same for airports, subway stations and shopping malls.

Warehouses and Distribution Centers
The final example use case comprises the application of indoor localization in warehouses and distribution centers. Warehouses and distribution centers are often large open spaces filled with an infrastructure of large racks and shelves to store all kind of orders. Generally, forklifts are driven around to either store a package until further notice or retrieve it for further delivery. Adapting an indoor environment with a positioning system has many benefits and will increase the efficiency and productivity of the warehouses. The forklifts can be attached with a tag, which makes it possible for the drivers to respond to an order and to be guided through the warehouse to the right place. Furthermore, the system can monitor locations of free space on the shelfs for additional storage. Another benefit is that packages or orders can be tagged as well, so that it is possible to locate an order on request and translate it into an order status for the client. Additionally, the inverse principle of geofencing can be applied. For example, instead of triggering an alarm if a package leaves an area, a warning can be sent out if a package is still in the warehouse after a delivery due date.

As illustration for this use case the coverage area of a warehouse of an e-commerce company called Zalando and bol.com is used. The coverage area of the warehouse in Venlo (Netherlands) is approximately 130000m^2. To fully cover an area of these proportions, 260 BlooLoc kits are need including 260 basestations and 3900 beacons worth in total 715000€. Such an investment will eventually be profitable and cause more efficiency, productivity, less waste time and thus more income/profit. Furthermore, both horizontal and vertical accuracy for locating products has to be < 1 meter with an update rate of 1 minute and a latency of < 10 seconds. The vertical accuracy has to be less than a meter in order to locate products on different shelves. To guarantee the safety of the employees driving the forklifts, the horizontal accuracy has to be < 0.5 meter with an update rate of 0.5 seconds and almost no latency (< 0.5 seconds) such that collisions can be prevented. Besides the high horizontal accuracy and update rate for locating the forklifts, the output data will be a 2D location with a dynamic geofence. Instead of a room or space, the geofence represents a forklift in this case and will prevent collisions by warning the drivers in case two forklifts tend to collide. The privacy of the employees is guaranteed externally, however internally the privacy is less so that the system can function optimal. The amount of users is highly dependent on the amount of orders and the amount of forklifts that will be tagged for localization. To conclude, a summary of the user requirements are illustrated by means of Figure 4.6.

User Requirement	Description
Coverage Area	Area of e-commerce company (Zalando, Venlo) 130000 m^2
Infrastructure	260 BlooLoc kits, 260 Basestations, 8900 Beacons
Cost	260 BlooLoc starter kits (2750€ per kit) and maintenance costs
Privacy	Privacy of the staff is guaranteed, no privacy for products
Number of Users	Amount of orders and forklifts present in the warehouse
Update Rate	Staff/forklifts: 0.5 sec; Products: 1 min
Latency	Staff/forklifts: <0.5 sec; Products: <10sec
Horizontal Accuracy	Staff/forklifts: <0.5 m, Products <1 m
Vertical Accuracy	Products <1 m
Output Data	Relative 2D locations, Dynamic geofencing, stock heights

Figure 4.6: Summary of the user requirements for the use case “Warehouses and Distribution Centers” specified for the an e-commerce warehouse of Zalando and bol.com in Venlo (Netherlands) with the IPS of BlooLoc as example.

4.1.3. The use case represented in this thesis

The most representative use case was chosen based on the user requirements and goals of this thesis, namely the use case *"warehouses/distribution centers"*. The other use cases are challenging as well, however the accuracy in both horizontal and vertical directions has to be high in the use case of the warehouses. The required

horizontal and vertical accuracy in this use case is an interesting challenge to investigate and in addition the use case corresponds with large open spaces.

4.2. System performance

The system performance is depending on several statistical parameters with the accuracy and precision as the main contributors. The accuracy is a standard for the closeness of the measured values with respect to the true value, whereas precision is related to the repeatability or spread in outcomes of the measured values (Fig. 2.6). However, the accuracy and precision are depending on many factors that can influence the system performance. The accuracy and precision are both largely dependent on range, whereas the observed range is depending on factors as signal attenuation, transmitting power, path loss and noise. Before elaborating on the statistical parameters of the system performance, the factors that influence the system performance will be elaborated.

4.2.1. Geometry

The challenges of an indoor environment come together with factors influencing the system performance. If the wavelength is long enough, RF signals can penetrate a wall which leads to signal attenuation but a signal can also be reflected by the wall. The characteristics of an indoor environment (walls, obstacles, etc.) play a major role in the disturbance of the signals. Besides the characteristics of an indoor environment, the geometry of the IPS plays a major role in whether or not a certain level of precision can be realized. The main contributor to obtain a certain degree of precision is a factor solely influenced by geometry, namely the Geometric Dilution of Precision (GDOP). Furthermore, a combination of both geometry and the indoor environment leads to factors as multipath, signal fading, NLOS and shadowing.

Dilution of precision (DOP)
The geometry of the infrastructure has large influences on the precision and accuracy of the positioning system. The relation between the geometry of the positioning system and the measurement precision is called Geometric Dilution of Precision (GDOP). Basically, the Dilution of Precision (DOP) represents a measure reflecting the geometric configuration of the IPS and is therefore useful in determining the optimal configuration of an IPS. To illustrate GDOP imagine a RF positioning system with two static transmitters and one mobile receiver. Due to trilateration, the receiver is located on the intersection of the circular lines centered at the transmitters. In the first situation (Fig. 4.7a) the transmitters are distant with respect to each other and direction wise transmitter 1 lies orthogonal to transmitter 2. This results in x and y coordinates of the receiver with equal precision [20]. In comparison with the second situation (Fig. 4.7b), the transmitters are much closer to each other and not orthogonal anymore, resulting in a larger uncertainty region and no equal precision in x and y coordinates. In this case (b) the precision is diluted in comparison to the first situation (a) as a consequence of geometry.

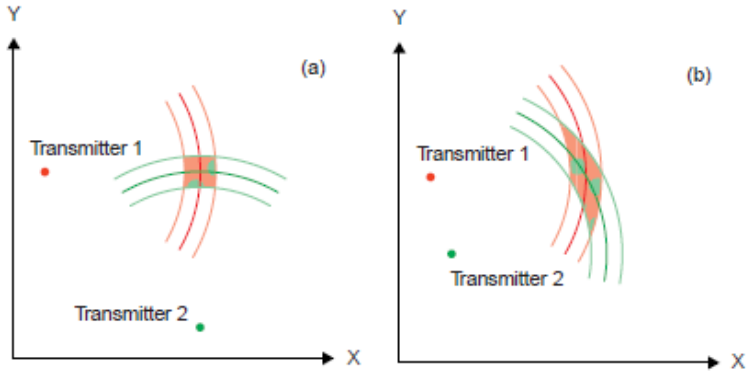

Figure 4.7: a) The position uncertainty is small (low dilution of precision) and in b) the position uncertainty is larger (high dilution of precision) as a consequence of geometry. Source: Langley [20]

Besides GDOP, other flavors of dilution of precision (DOP) occur in most solutions. Generally, the more transmitters that are present in a solution, the smaller the DOP values and thus the smaller the uncertainty. In

many cases, the beacons of an indoor positioning solution are placed at a certain height relative to the mobile receiver. To look at this from another prospective, assume you are standing in a field with a GPS receiver and want to know your position in both horizontal and vertical directions. The vertical position errors are most of the times higher than the horizontal errors. This effect is due to the positioning of the satellites with respect to the receiver. All satellites are above the receiver and no signal is received from below because RF waves cannot travel through the Earth's surface [20]. In contrast, the horizontal coordinates do not suffer from this since they receive signals from all horizontal directions. The position errors related to the horizontal and vertical directions are known as Horizontal Dilution of Precision (HDOP) and Vertical Dilution of Precision (VDOP). Furthermore, the DOP values are highly dependent on the amount of satellites that are visible for the receiver. Increasing the amount of visible satellites will lead to a decrease in DOP and thus a higher precision. The DOP will be elaborated further in chapter 5 to illustrate how the DOP is implemented in the theoretical design computations.

4.2.2. Multipath and fading

Multipath is caused by reflections (Fig. 4.8) of the signal on walls, shiny surfaces and obstacles and influences both TOA and RSSI measurements. Multipath simply means that there are multiple paths for a signal to travel between transmitter and receiver. The reflections will lead to various arrival times and angles at the receiver while the direct signal assuming LOS conditions will always arrive first. Although the direct wave arrives first, it can be attenuated as a consequence of a partially obstructed direct path. The direct wave can be isolated more easily from reflections if the signal consists of a short and sharp pulse, however, this coincides with shorter wavelengths which are much faster blocked by walls and obstacles [4]. Additionally, multiple waves each traveling a unique path arrive at the receiver and can either be in phase with each other or not. If the relative phase of the arriving waves coincides the signal becomes stronger, a principle often referred to as constructive interference at the receiver [4]. On the other hand, if the relative phase of the arriving waves is out of phase the signal weakens and becomes a *'fading'* signal, also known as destructive interference at the receiver. According to Callaerts [4] (2016) constructive and destructive interference at the receiver is often experienced over short distances, typically half wavelength distances, and is known as fast fading (Fig. 4.8). The multipath and fading effects can be analyzed on the basis of practical experiments, where different types of building material have a major influence. For instance, concrete walls cause different reflections in comparison with metal plates that are attached to the walls. The effects of both fading and multipath should therefore be taken into discussion when analyzing the results of the practical experiments.

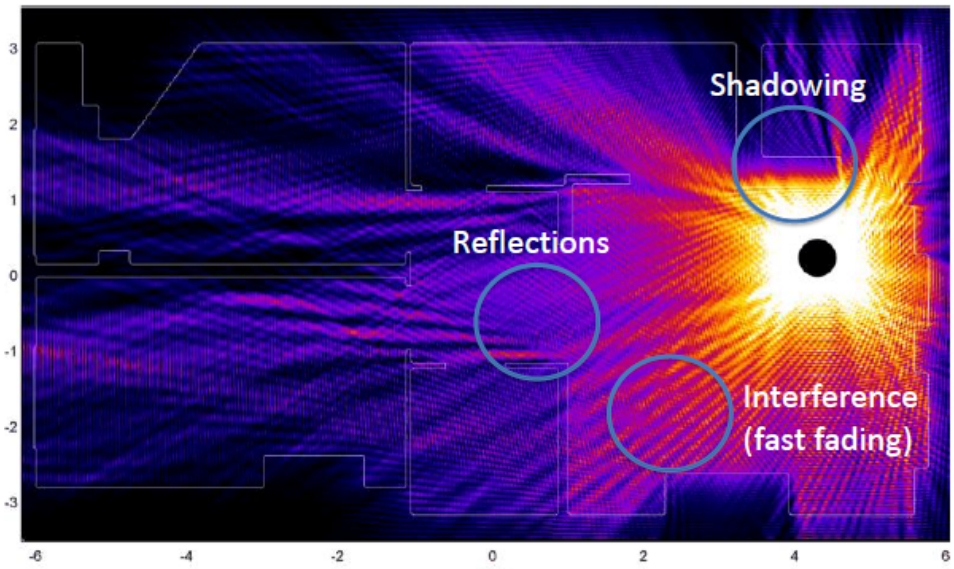

Figure 4.8: Visualization of an RF signal propagating in an indoor environment showing the effects of reflections, interference and shadowing. Source: Callaerts [4]

4.2.3. Non-Line-of-Sight and shadowing

In case a direct wave propagates through a wall or obstacle, the signal attenuates rapidly. In case of open corridors partially blocked by walls (such as in Fig.4.8), the signal partially propagates trough the wall while the rest of the signal propagates along the wall through the opening. This results in an area that is 'shadowed' and provides a weak signal. Besides shadowing by walls or obstacles, a human body can cause shadowing as well, a principle called body shadowing. The RF signals are blocked by water and since an adolescent human body consists for 65% of water, persons cause attenuation of the signal as well. If the signal in the shadowing zone becomes significantly weak, the area becomes a Non-Line-of-Sight (NLOS) situation. Such a NLOS situation can be the consequence of for instance thick walls of certain material and the presence of highly reflective obstacles. In a NLOS situation, the direct path remains undetected and only multipath waves are detected [4]. NLOS conditions are a significant problem for indoor localization and cannot be solved solely by one of the measuring principles (RSSI, T(D)OA or AOA). Furthermore, both shadowing and NLOS conditions lead to an increase in distance errors and influence the system performance.

5

Methodology

5.1. Theoretical design computations

The knowledge about statistical phenomena and processes that are influenced by the factors described in the previous section 4.2 have to be well understood in order to validate your observational data with a theoretical model. Before any observational data will be acquired, the quality of the estimated parameters can be examined on forehand. This will be done based on theoretical design computations, which will assess the quality of estimated parameters with multiple hypothetical geometries. The design computations take all information that is known on forehand into account, such as the amount of beacons (up to 15), geometry, the intitial standard deviation of the observations etc. The main purpose of the theoretical model will be to assess the quality of an IPS based on a predefined geometry. Several situations with different geometries will be tested in order to find the optimal configuration. However, before describing the setup and results of the theoretical design computations, it is necessary to clarify some definitions related to quality control and the corresponding statistical background.

5.1.1. Linear functional models, precision and residuals

As stated earlier, the system performance is depending on several statistical parameters with the accuracy and precision as the main contributors, where the accuracy is a standard for the closeness of the measured values with respect to the true value and precision is related to the repeatability or spread in outcomes of the measured values (Fig 2.6). A more accurate definition of precision is given by Teunissen et al. [32]:

> *"Precision describes the spread or variability in the (estimation) result, that can be expected when the process or phenomenon would be observed again under similar circumstances."*

The spread or variability is mainly a consequence of *random errors*. The impact of random errors decreases if measurements are repeated multiple times, since the expectation of the random errors equals zero. In other words, if a measurement would be repeated frequently enough under similar circumstances, the average of the random errors should equal zero. In order to estimate unknown parameters from uncertain data, the acquired data can be used in a mathematical model. The mathematical model consists of a functional model: $E(\underline{y}) = Ax$, and a stochastic model: $D(\underline{y}) = Q_{yy}$. The underlined variables $\underline{y}$ represent random variables, which are functions to map random processes to numbers. For example, a random process could be flipping a coin where the random variables are the quantified outcomes (heads or tail) of the random process. Furthermore, the functional model describes the linear relation between a vector of m observations $\underline{y}$ and a vector of n unknown parameters x, whereas the stochastic model relates to the uncertainty of the observations $\underline{y}$ expressed in the covariance matrix (Q_{yy}). Dissimilarities between the observational data and the model can highlight the presence of significant errors. Additionally, linear systems do not necessarily have a solution and are called consistent if there is at least one solution. In case the linear system has one unique solution, it satisfies $m = n = rank(A)$. In case of $rank(A) < n$ the linear system is consistent and underdetermined, since there will be more than one solution. However, if $rank(A) = n < m$ the system becomes inconsistent and overdetermined, since there will be generally no solution.

To solve an inconsistent system of equations and to find the discrepancies between the observations and the model the Weighted Least Squares Estimation (WLSE) or Best Linear Unbiased Estimation (BLUE) are used. In case of WLSE, the solution is given as

$$\underline{\hat{x}} = (A^T W A)^{-1} A^T W \underline{y} \tag{5.1}$$

and is identical to the solution of BLUE by substituting $W = Q_{yy}^{-1}$ which results in the following solution

$$\underline{\hat{x}} = (A^T Q_{yy}^{-1} A)^{-1} A^T Q_{yy}^{-1} \underline{y}. \tag{5.2}$$

The A matrix represents the measurement design matrix and is highly dependent on the type of observational data and unknown parameters. The precision of $\underline{\hat{x}}$ is dependent on the redundancy between the observations and the unknown parameters $(m-n)$, the design matrix A and the precision of the observations Q_{yy}. Furthermore, the precision is represented by the diagonal of the variance matrix $Q_{\hat{x}\hat{x}} = (A^T Q_{yy}^{-1} A)^{-1}$ expressed as the variance, additionally the standard deviation can be obtained by taking the square root of the variance. The discrepancies between the observational data and the model are expressed by the residuals $(\underline{\hat{e}} = \underline{y} - A\underline{\hat{x}})$, where large residuals indicate a rather poor fit, whereas the smaller the residuals, the better the fit.

5.1.2. Non-linear functional models

The BLUE can only be used to solve linear relationships. However, in case of non-linear estimations the approach is slightly different. The theoretical design computations that are used in this research are based on a non-linear problem, because there is a system of m non-linear equations in 3 unknown parameters $(x_{tag}, y_{tag}, z_{tag})$ which makes the this an inconsistent system in case $m > 3$, since it meets the requirement of $rank(A) = n < m$. As explained earlier, a tag sends an omnidirectional BLE pulse to several beacons with fixed locations. All beacons that are able to receive the BLE pulse, collect the data and calculate the distances to the tag based on trilateration, which will eventually result in a position of the tag. For the theoretical design computations, it is assumed that x_i, y_i, z_i for $i = 1, \ldots, m$, are the known locations of the beacons. The BlooLoc set that is used for the experiments contains 15 beacons, so the maximum value of m will be 15. The unknown position of the tag is represented by 3 unknown parameters $x_{tag}, y_{tag}, z_{tag}$. The unknown distance from the beacon j to the tag can then be determined by

$$d_j = \sqrt{(x_j - x_{tag})^2 + (y_j - y_{tag})^2 + (z_j - z_{tag})^2}. \tag{5.3}$$

Considering the amount of beacons $i = 1, \ldots, m$ $(m \leq 15)$ the system of nonlinear equations becomes

$$\begin{bmatrix} d_1 \\ \vdots \\ d_m \end{bmatrix} = \begin{bmatrix} \sqrt{(x_1 - x_{tag})^2 + (y_1 - y_{tag})^2 + (z_1 - z_{tag})^2} \\ \vdots \\ \sqrt{(x_m - x_{tag})^2 + (y_m - y_{tag})^2 + (z_m - z_{tag})^2} \end{bmatrix} \tag{5.4}$$

It has to be mentioned that this is not exactly how the BlooLoc IPS works (see section 2.4.2), but this allows the design computations to assess geometrical strength. Since the least-squares principle is not restricted to linear systems of equations ($y \approx Ax$, the least-squares principle can also be used to solve a non-linear vector function ($y \approx A(x)$) [32]. In the non-linear functional model, the solution for x is chosen such that $A(x)$ is as close as possible to the given measurement vector y, where 'closeness' is measured by the weighted sum of squares of the entries of $y - A(x)$ [32].

Linearization

Since there is no analytical solution for a non-linear system, the model has to be linearized. According to Teunissen et al. [32] the principle of linearization is based on Taylor's theorem. Assume a vector θ exists in between x and x_0

$$a_i(x) \approx a_i(x_0) + [\delta_x a_i(x_0)]^T (x - x_0) + \tfrac{1}{2}(x - x_0)^T \delta^2_{xx^T} a_i(\theta)(x - x_0) \tag{5.5}$$

where the gradient vector $\delta_x a_i(x_0)$ (Jacobian) and the Hessian matrix $\delta^2_{xx^T} a_i(\theta)$ are used in the 1^{st} order and 2^{nd} order term of Taylor's theorem. Furthermore, the x_0-term describes the initial value or the approximated values. To solve the system of non-linear equations, the 2^{nd} and higher order terms of Taylor's theorem have been ignored. The linear approximation can then be written as $a_i(x) \approx a_i(x_0) + [\delta_x a_i(x_0)]^T (x - x_0)$, where

$\delta_x a_i(x_0)$ represents the $m \times n$ Jacobian matrix *(J)* of the partial derivatives. The linear approximation of *A(x)* is given as

$$y - A(x_0) \approx \delta_{x^T} A(x_0)(x - x_0) \tag{5.6.1}$$

$$\Delta y_0 \approx \delta_{x^T} A(x_0)\Delta x_0 \tag{5.6.2}$$

with $\Delta y_0 = y - A(x_0)$ and $\Delta x_0 = (x - x_0)$. Eventually, the linear approximation can be written as

$$\Delta y_0 \approx J * \Delta x_0 \tag{5.7}$$

with the gradient vector $J = \delta_x a_i(x_0)$ (Jacobian) in between x and x_0.

Precision

After composition of the linear approximation, the WLSE and BLUE can be used to estimate the $\Delta\hat{x}_0$. The WLSE can be formulated as $\Delta\hat{x}_0 = (J^T W J)^{-1} J^T W \Delta y_0$ and the BLUE is the WLSE in case of substitution of $W = Q_{yy}^{-1}$, resulting in $\Delta\hat{x}_0 = (J^T Q_{yy}^{-1} J)^{-1} J^T Q_{yy}^{-1} \Delta y_0$, where the uncertainty of the observations Δy_0 is expressed by the covariance matrix Q_{yy}. Furthermore, the precision is estimated by computing the variance matrix $Q_{\hat{x}\hat{x}} = (J^T Q_{yy}^{-1} J)^{-1}$, where the diagonal is representing the variance. Eventually, the total precision or the PDOP (see section 4.2) can be derived by

$$\sigma_T = \sqrt{\sigma_x^2 + \sigma_y^2 + \sigma_z^2} \tag{5.8}$$

where the standard deviations σ_x, σ_y and σ_z are computed by the model via the square root of the diagonal of the variance matrix $Q_{\hat{x}\hat{x}}$.

Dilution of precision

Since the major challenge to overcome is to determine an optimal configuration in terms of geometry, LOS, signal strengths etc. for a given set of beacons within a 3D space. In other words, given a limited amount of beacons and a predefined 3D space, how should the beacons be deployed such that the geometry, LOS, signal strengths etc. provide the required precision and reliability?

An optimal positioning solution for a given measurement error is the one that minimizes the GDOP [30], although it has to be noted that the measurement error is not only dependent on the geometry. In turn, the GDOP can be minimized for a certain user location by optimizing the geometry of the beacons within the 3D space. The deployment of an IPS can be compared with the configuration of the GPS up to a certain degree. The position dilution of precision (PDOP) of GPS is depending on the total precision and can be expressed as $\sigma_T = \sqrt{\sigma_x^2 + \sigma_y^2 + \sigma_z^2}$ for three dimensions *(x,y,z)* and the users clock bias error estimate (σ_b). The precision in *(x,y,z)* can be retrieved via the square root of the diagonal of the variance matrix $Q_{\hat{x}\hat{x}}$ resulting from a Least Squares solution, which contains the contribution to the position error of both the geometry and the random measurement error [29]. Since $Q_{\hat{x}\hat{x}} = (J^T Q_{yy}^{-1} J)^{-1}$ and the Q_{yy} matrix is assumed to be diagonal with an initial standard deviation (σ) of 1 meter, Q_{yy} can be expressed as $Q_{yy} = \sigma^2 * I$ where I is the identity matrix. Subsequently, the variance matrix becomes $Q_{\hat{x}\hat{x}} = (J^T \frac{1}{\sigma^2} J)^{-1}$ or $Q_{\hat{x}\hat{x}} = \sigma^2 (J^T J)^{-1}$, where σ refers to the intial standard deviation and $(J^T J)^{-1}$ relates to the geometry only. Eventually, according to Langley [20] and Rizos [29] several relations of the DOP can be expressed depending on the coordinate component, or a combination of the coordinate components

$$GDOP = \frac{1}{\sigma}\sqrt{\sigma_x^2 + \sigma_y^2 + \sigma_z^2 + \sigma_b^2}. \tag{5.9}$$

By excluding the users clock bias error estimate, the GDOP can be simplified to the position dilution of precision PDOP

$$PDOP = \frac{1}{\sigma}\sqrt{\sigma_x^2 + \sigma_y^2 + \sigma_z^2} \tag{5.10}$$

where the GDOP can be subdivided into horizontal-, vertical-, and time DOP. The HDOP, VDOP and TDOP can be expressed as

$$HDOP = \frac{1}{\sigma}\sqrt{\sigma_x^2 + \sigma_y^2} \tag{5.11}$$

$$VDOP = \frac{\sigma_z^2}{\sigma} \tag{5.12}$$

$$TDOP = \frac{\sigma_b^2}{\sigma} \tag{5.13}$$

From these expressions it can be concluded that $PDOP^2 = HDOP^2 + VDOP^2$ and $GDOP^2 = PDOP^2 + TDOP^2$. Because the various DOP relations are functions of both receiver and satellite coordinates, the DOP relations can be predicted for any given set of satellites and receiver locations. This principle will be applied in the theoretical design computations where the location of the receiver (tags/mobile phones) are combined with different beacon configurations which will act as satellites.

5.1.3. Internal vs. External reliability

A statistical evaluation of the test experiments can be discussed on forehand by elaboration of the term reliability. The reliability is a term explaining the performance of statistical testing for validation and describes the ability of the observation system to check (itself) for modeling errors [32]. The initial data analysis, existing of a functional model and least square estimations, is able to detect disturbances, outliers and other biases. However, some errors are left undetected by the statistical testing and the reliability helps to discuss the statistical possibility that errors are left undetected during the test experiments. The reliability will be explained according to the internal reliability and the external reliability.

Internal reliability

The internal reliability is often expressed as the Minimal Detectable Bias (MDB) ∇ in one of the observations. The internal reliability is describing the possibility that a bias in the observations can be detected. In order to find the MDB values for one of the observations $i = 1, \ldots, m$ alternative hypotheses have to be tested. The null hypothesis is defined as $H_0 : E(\underline{y}) = Ax$, where the m alternative hypotheses are described by $H_{a,i} : E(\underline{y}) = Ax + C_{yi}\nabla_i$. The matrix C_{yi} is an indicator for the observation that contains an error:

$$C_{y1} = \begin{pmatrix} 1 \\ 0 \\ \vdots \\ 0 \end{pmatrix}, C_{y2} = \begin{pmatrix} 0 \\ 1 \\ \vdots \\ 0 \end{pmatrix}, C_{ym} = \begin{pmatrix} 0 \\ 0 \\ \vdots \\ 1 \end{pmatrix} \tag{5.14}$$

and ∇_i is the corresponding MDB value. To compute the MDB, the probability or power (γ) that an error can be detected and the non-centrality parameter (λ) which is depending on the size of the bias are depending on the level of significance α. In practice, the level of significance is often set to $\alpha = 0.001$. Subsequently, the power becomes $\gamma_0 = 0.80$ and the non-centrality parameter is set to $\lambda_0 = 17.0747$ [32]. By fixing the values of the power and the non-centrality parameter, the MDB values can be derived by

$$|\nabla| = \sqrt{\frac{\lambda_0}{C_y^T Q_{yy}^{-1} Q_{\hat{e}_0 \hat{e}_0} Q_{yy}^{-1} C_y}} \tag{5.15}$$

where the Q_{yy} matrix represents the precision of the observations y and the variance matrix of the residuals $Q_{\hat{e}_0 \hat{e}_0} = Q_{yy} - Q_{\hat{y}\hat{y}}$ with $Q_{\hat{y}\hat{y}} = J(J^T Q_{yy}^{-1} J)^{-1} J^T$. Finally, Teunissen et al. [32] defines the MDB as *"the size ∇, that the error specified by C_y should have in order to be detected with probability γ_0."*

External reliability

The external reliability is defined as the bias in the estimates due to a bias $C_y|\nabla|$ in the observations. It is the impact that an error $C_y|\nabla|$ (when undetected) has on the estimator $\hat{\underline{x}}_0$ of the null hypothesis. The null hypothesis was defined as $H_0 : E(\underline{y}) = Ax$ and the corresponding m alternative hypotheses are described by $H_{a,i} : E(\underline{y}) = Ax + C_{yi}\nabla_i$ with $i = 1, \ldots, m$. In case of the null hypothesis, the best estimator of vector x for a linearized model is than given by

$$E(\Delta\hat{\underline{x}}_0) = (J^T Q_{yy}^{-1} J)^{-1} J^T Q_{yy}^{-1} E(\Delta\underline{y}_0) \tag{5.16}$$

where the vector of m observations is given as $E(\Delta\underline{y}_0) = Jx$. However, in the alternative case the best estimator $\Delta\hat{\underline{x}}_0$ of H_a can be expressed as follows

$$E(\Delta\hat{\underline{x}}_0 | H_a) = (J^T Q_{yy}^{-1} J)^{-1} J^T Q_{yy}^{-1} E(\Delta\underline{y}_a) \tag{5.17}$$

where the vector of m observations is now given as $E(\Delta\underline{y}_a) = Jx + C_y\nabla$ and substitution of $\Delta\underline{y}_a$ gives

$$E(\Delta\hat{\underline{x}}_0 | H_a) = (J^T Q_{yy}^{-1} J)^{-1} J^T Q_{yy}^{-1} (Jx + C_y\nabla). \tag{5.18}$$

After elaborating this further and applying the distributive law, it becomes

$$E(\Delta\hat{\underline{x}}_0|H_a) = (J^T Q_{yy}^{-1} J)^{-1} J^T Q_{yy}^{-1} Jx + (J^T Q_{yy}^{-1} J)^{-1} J^T Q_{yy}^{-1} C_y \nabla \tag{5.19}$$

where the first part of the equation $(J^T Q_{yy}^{-1} J)^{-1} J^T Q_{yy}^{-1} Jx$ is equal to x, since $(J^T Q_{yy}^{-1} J)^{-1} J^T Q_{yy}^{-1} J$ cancel each other out. The best estimator of H_a can be written as

$$E(\Delta\hat{\underline{x}}_0|H_a) = x + \nabla\hat{x} \tag{5.20}$$

where the second part is referred to as the external reliability

$$\nabla\hat{x} = (J^T Q_{yy}^{-1} J)^{-1} J^T Q_{yy}^{-1} C_y \nabla. \tag{5.21}$$

Generally, the theoretical design computations simulate possible positions of a tag in a local *x,y,z* grid. For every virtual tag position, the distances to the m beacons are computed, linearization of the non-linear system will be performed, in order to compute the precision from the variance matrix and both internal- and external reliability.

5.2. Detection Identification Adaption procedure

Observational data acquired in the field is usually biased resulting in significant errors in the estimated model. The biases can be classified in three types of measurement errors, namely *random errors*, *systematic errors* and *outliers*. As mentioned earlier, the impact of random errors decreases if measurements are repeated multiple times, since the expectation of the random errors equals zero. In case all measurements or a subset of the measurements are affected by a constant or variable error, the error is a systematic error. Finally, outliers are non-random errors in a single measurement often obtained by the user during the measurements. Therefore, when the presence of an error is suspected to exceed the range of the random errors, the data should be validated and if necessary corrected for these outliers. The observational data can be corrected for outliers by using the Detection, Identification and Adaption (DIA) procedure to provide validated measurements for further analysis and interpretation. Generally, the DIA procedures detects (Detection) outliers based on the validity of a predefined null-hypothesis (H_0). Subsequently, if H_0 appears to be invalid, a test will be performed in order to locate (Identification) the error and finally the located error will be removed or taken into account (Adaption) [32]. Since the practical experiments will contain many measurements consistent with measurement errors, the DIA procedure will be applied to the data.

5.2.1. Overall Model Test

Generally, the overall model test (OMT) is an initial check (Detection) determining whether or not the H_0 hypothesis (section 5.1.1) is rejected. If the H_0 hypothesis gets rejected, either the model is wrong or outliers/systematic errors are present in the data and these should be identified and adapted. In order to check if the null hypothesis gets accepted or rejected, the OMT uses the test statistic $T_{q=m-n}$ and a critical value K. The test statistic of the OMT is defined as

$$T_q = \hat{\underline{e}}_0^T Q_{yy}^{-1} \hat{\underline{e}}_0 \tag{5.22}$$

where the size of the residuals $\hat{e}_0$ is compared to the precision of the observations Q_{yy}. In this research the Q_{yy} matrix is assumed to be a diagonal matrix and by elaborating the equation for T_q it can be written as

$$T_q = \frac{\hat{\underline{e}}_1^2}{\sigma_1^2} + \frac{\hat{\underline{e}}_2^2}{\sigma_2^2} + \frac{\hat{\underline{e}}_3^2}{\sigma_3^2} + \ldots + \frac{\hat{\underline{e}}_m^2}{\sigma_m^2} = \sum \frac{\hat{\underline{e}}_i^2}{\sigma_i^2}. \tag{5.23}$$

Therefore, in case of a diagonal Q_{yy} matrix the test statistic T_q can be defined as the weighted sum of the squared residuals. To test if the residuals are too large, the T_q is tested against a critical value K. Since T_q is not a linear function of $\hat{\underline{e}}$ it is not normally distributed. Instead, T_q has a chi square distribution $\chi^2(q,0)$ where $q = m - n$ represents the redundancy and in this case q would be equal to $q = 15 - 3 = 12$. Based on the chi square distribution of T_q the critical value K can be determined based on an α related to a certain confidence interval, which is in most cases the 95 % confidence interval ($\alpha = 0.05$). Thus, when the value of $T_q > K$ the outcome is considered to be unlikely and an error is detected, or in other words the H_0 hypothesis is rejected.

5.2.2. W-test

The OMT is a good indicator for detecting whether or not outliers are present, but it is not identifying and adapting for the error. Besides the OMT, there are several tests that can be used for the identification of measurement errors in the observed data and for this research the w-test will be applied. The w-test is a more specific test trying to identify a single observational discrepancy in the data and removes the discrepancy after identification. The outlier detection and identification is done based on a certain threshold with respect to the null-hypothesis. The null-hypothesis has been defined in section 5.1.1 and is $H_0 : E(\underline{y}) = Ax$. To detect an outlier in one of the observations, there are m alternative hypotheses described by $H_{a,i} : E(\underline{y}) = Ax + C_{yi}\nabla_i$, where $i = 1, \ldots, m$. Since the Q_{yy} matrix is assumed to be diagonal, the test criteria of the w-test ($|\underline{w}|$) can be defined as

$$|\underline{w}| = \frac{\hat{\underline{e}}_i}{\sigma_{\hat{\underline{e}}_i}} \tag{5.23}$$

where $\hat{\underline{e}}_i$ represents the residual of the i^{th} observation and $\sigma_{\hat{\underline{e}}_i}$ is the standard deviation of the corresponding residual and can be derived via the diagonal of the variance matrix of the residuals $Q_{\hat{e}_0\hat{e}_0} = Q_{yy} - Q_{\hat{y}\hat{y}}$. Since the residuals are needed for the test value $|\underline{w}|$, firstly the functional model $E(\underline{y}) = Ax$ and its corresponding stochastic model $D(\underline{y}) = Q_{yy}$ are defined. The design matrix A contains data on the independent variables which attempt to explain the observed data. The uncertainty of the observations $\underline{y}$ per beacon is expressed in the Q_{yy} matrix and together with the solution of the BLUE (section 5.1.1), the residuals $\hat{\underline{e}}_i$ per observation and the standard deviation of the residuals $\sigma_{\hat{\underline{e}}_i}$ can be derived. Subsequently, to determine whether a single observational discrepancy is present or not, the maximum value of $|\underline{w}|$ is checked against the critical value k_a. Since $|\underline{w}|$ is a linear function of $\hat{\underline{e}}_i$ the $|\underline{w}|$ is normally distributed. Therefore, the critical value k_a is based on a normal distribution and the 95% confidence interval ($\alpha = 0.05$). The null-hypotheses is rejected in case it satisfies to $|\underline{w}| > \sqrt{k_a}$. If H_0 is rejected, the location of the maximum value of $|\underline{w}|$ is used to remove this outlier and the iteration continues until H_0 is accepted and all outliers are removed.

5.3. The initial model

The initial model that has been created for the theoretical design computations requires the amount of beacons and the size of the theoretical 3D space as input by the user. The shape of the theoretical 3D space is assumed to be a cube, since most indoor environments can be described by rectangular spaces. Furthermore, the locations of the beacons have to be predefined by the user such that the beacons are located within the predefined cube. The point density within the cube can vary and depends on the user requirements. In this case, the points represent possible locations for a mobile device and are used to calculate the precision, internal reliability (MDB) and external reliability (section 5.1). The denser the points, the more possible locations for a mobile device and the more insight the user gets in the distribution of the statistical parameters. To get a better understanding of the theoretical 3D space and the locations of the beacons, three geometric scenarios will be elaborated.

5.3.1. Three geometric scenarios

The geometry of the infrastructure has large influences on the precision and accuracy of the positioning results. In order to test the influences of geometry, the IPS several geometric situations are simulated in the model. The initial model requires the user to predefine the locations of the beacons based on a certain geometric solution. The predefined situations are theoretical assumptions, where the dilution of precision (section 4.2 and 5.1.2) plays a major role. Since the model describes a theoretical 3D space, both horizontal and vertical dilution of precision are taken into account. The geometry of the infrastructure can result in a larger uncertainty region and no equal precision in *x, y* and *z* direction. To obtain a high precision, the beacons will have to be geometrically spread/distributed over the area. Besides the high precision, the measurements need to be reliable. To obtain a good reliability, it's necessary to place the beacons in each other vicinity. Therefore, the geometry of the infrastructure influences both the precision and reliability.

Three geometric situations are simulated in the model to test the precision and reliability. For all three situations, the initial uncertainty of the observations $\underline{y}$ was set to 1 meter and the range between two beacons is limited to a maximum of 5 meter (section 2.4). The three situations with different geometric configurations are visualized in Figure 5.1. The first situation is described by configuration with 12 beacons aligned both

horizontally as vertically at a height of $z = 1$ and $z = 5$ and three beacons aligned in the center of the cube at height $z = 3$. The second situation is almost similar to the first situation, except that there is no vertical alignment. Similarly to the first situation, 12 beacons are aligned horizontally at a height of $z = 1$ and $z = 5$, while in vertical direction, the beacons at $z = 1$ shifted 2.5 meter to the center of the cube. Finally, the third situation is almost identical as the second configuration, however the beacons at $z = 3$ are now not horizontally aligned, but form a triangle. Furthermore, the size of the third 3D space is 7x10x6 which is approximately the size of one of the test locations.

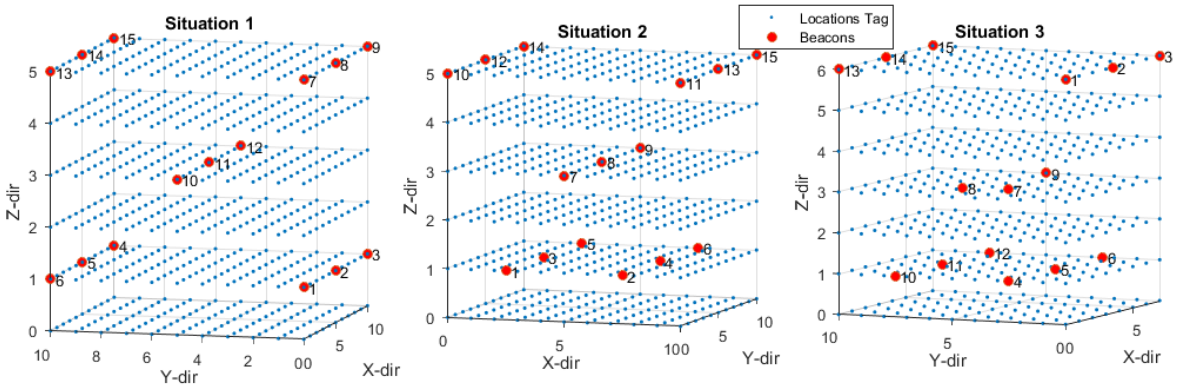

Figure 5.1: The three scenarios that will be simulated in the initial model.

6

Theoretical and experimental results

6.1. The practical experiments

The practical experiments can be divided in two types of experiments, namely the range-related and the geometric related experiments. Basically, the range-related experiments will provide insight in the signal strength of the beacons, tags and mobile phones and evaluate the characteristics of the BlooLoc IPS, whereas the geometric related experiments will provide insight to the precision based on the geometric composition of the beacons. Therefore, the results of the range-related experiments of the beacons can be used to update the theoretical design computations. The theoretical design computations are in their turn input for the geometric related experiments. The practical experiments are performed with the starter kit of BlooLoc including 15 beacons, 1 basestation and three tags. Additionally, three smartphones are used in the experiments as mobile devices, two android operated smartphones (LG Spirit and Motorola Moto G) and one IOS operated smartphone (Iphone 5C). All three smartphones are compatible with Bluetooth 4.0 (BLE) which makes it possible to compare the measurements with each other. The Leica DISTO A3 laser distance meter is used to measure accurate distances with an accuracy of 1.5 mm up to 30 meter. The precision results of the model can be compared with the precision results of the geometric experiments and can be used as a validation of the design computation. A comparison between the results will be made in chapter 7.

6.1.1. Range experiments

The range experiments provide insight in the signal strength of the basestation, beacons and mobile devices. Two different type of range related signal strength tests will be performed, the first test will evaluate the signal strengths of the advertise packages of all 15 beacons over distance, whereas the other test relates to the difference between two smartphones with the same Bluetooth chip. The different options for the range related signal strength experiments are illustrated schematically in Figure 6.1. Both experiments will be performed in an empty hallway in the basement of the Civil Engineering and Geosciences (CiTG) building at the Delft University of Technology.

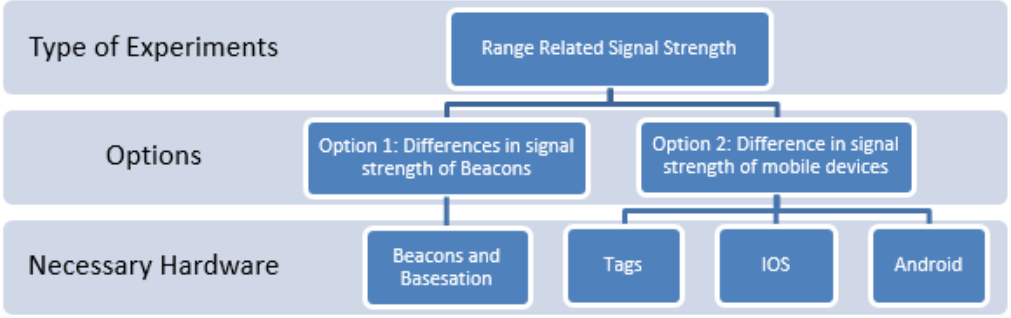

Figure 6.1: Schematic overview of the practical experiments

Option 1: Difference in signal strength of the beacons
To evaluate the characteristics of the BlooLoc IPS, a performance test of the BLE signal strengths of the different beacons is used. The BlooLoc starter kit consists of 15 beacons broadcasting BLE advertising packages. In order to make a distinction in signal strengths for the 15 beacons, all beacons will be tested individually. One by one, a beacon is stuck to a glass door and subsequently the signal strengths are measured every 0.5 meter increasing away from the beacon up to 10 meter by using the Bluetooth RSSI application on the Motorola Moto G. The exact distances will measured with the laser distance meter. The signal strengths experiments are repeated three times per beacon in order to increase the statistical coverage of the measurements, resulting in a total of 60 measurements per beacon and 900 measurements in total. The measurements also provide insight in the variances and standard deviations with respect to the distance.

In addition to the 10 meter range measurements, another experiment will be performed to test the range over which the broadcasted BLE advertising packages can be received. This experiment is almost similar to the 10 meter experiments, however, the signal strengths will be measured every 5 meter up to 50 meter distance away from the beacon. The 50 meter experiments will be performed for three different beacons and will be repeated 4 times to increase the statistical coverage of the measurements, resulting in 40 measurements per beacon and 120 measurements in total.

Option 2: Difference in signal strength of mobile devices
In order to evaluate the different BLE signal strengths of an IOS phone and an Android phone, the Iphone 5C is tested against the LG Spirit. Besides the phones, the initial idea was to measure the signal strengths of the three Bluetooth tags too, however, the Bluetooth chips of the tags do not broadcast advertising packages like the beacons. Instead of advertising packages, the tags implement their own multicast protocol to communicate efficiently with the beacons without collisions and this communication cannot be intercepted with a BLE chip. Therefore, the mobile device tests will be limited to an IOS operated and an Android operated device. To test the BLE signal strength, both phones will be placed on a mark that corresponds to the zero meter distance with their Bluetooth turned on. Subsequently, the signal strengths are measured every 0.5 meter increasing to a distance of 10 meter by using the Bluetooth RSSI application on the Motorola Moto G. The exact distances will measured with the laser distance meter. The distance measurements are perfumed three times for both phones to get a better statistical coverage.

6.2. Results of the range experiments

6.2.1. Signal strength of beacons

In order to distinguish the 15 beacons on base of their signal strength behavior, the 15 beacons have been tested individually. One by one, a beacon hang on a door at a height of 1.45±0.03 meter in the basement of the CiTG building. The floor was marked at every 0.5 meter away from the beacon up to a maximum distance of 10 meter. Once the beacon stuck to the door and was broadcasting its advertising packages via BLE, the signal strength was measured at every 0.5 meter advancing away from the beacon resulting in 20 received signal strength measurements. The whole test was repeated three times per beacon (60 measurements) resulting in a total of 900 measurments for the 15 beacons. Additionally, the average RSS values of the three tests has been computed for every beacon and an overview of the acquired data is illustrated in Figure 6.2.

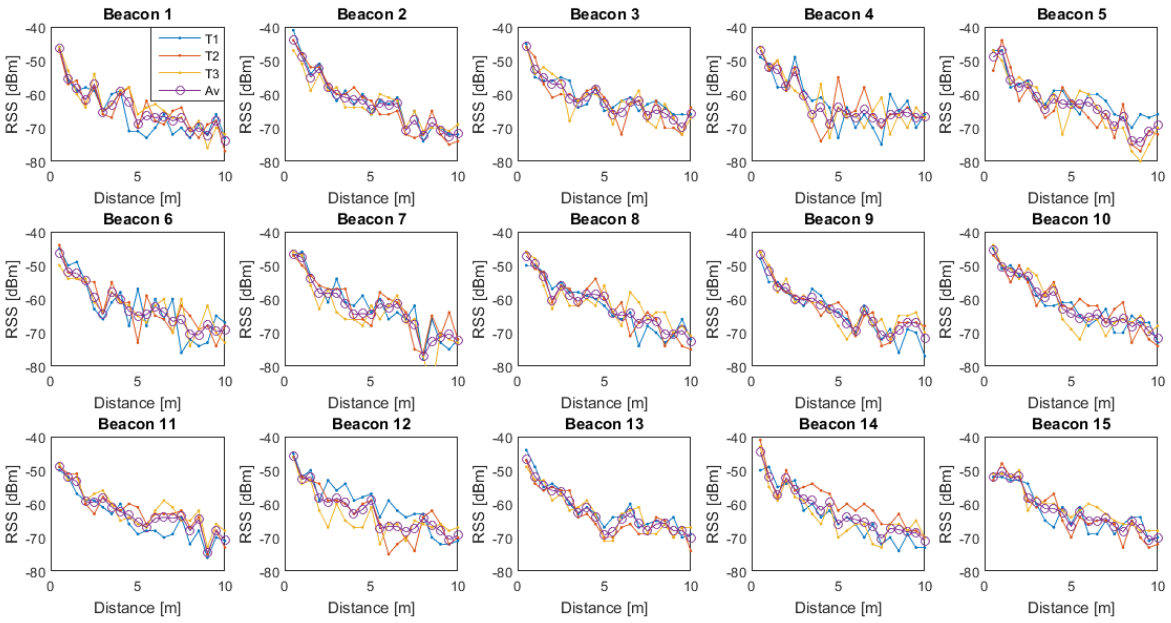

Figure 6.2: An overview of the acquired data for the received signal strengths of all beacons. The three tests per beacon (blue, red and yellow solid lines) and the average (purple dotted line) of the three tests are depicted per beacon.

By taking a closer look to the acquired data in Fig. 6.2, all plots tend to show the same type of trend. Generally, it can be stated that the acquired RSS values decrease with increasing distance from the beacon. The overall trend shows a quadratic or exponential decay of the RSS values over distance. Furthermore, the three test plots vary per beacon and are in some cases very close to each other, for example beacons 2, 9 and 13 in Fig. 6.2, while in other cases, beacons 4, 6, and 12 in Fig. 6.2, they are very wide spread. The overall trend comes forward by looking at the 15 average RSS plots in Figure 6.3. Based on Fig. 6.3 the RSS values close to the beacon (1-3 m) are less spread than the RSS values at larger distances. This is an indication for the precision of the measurements which tends to be higher near the beacon and decreases with increasing distance. To draw conclusions from the acquired data, the data has to be tested for outliers by using the DIA procedure (section 5.2).

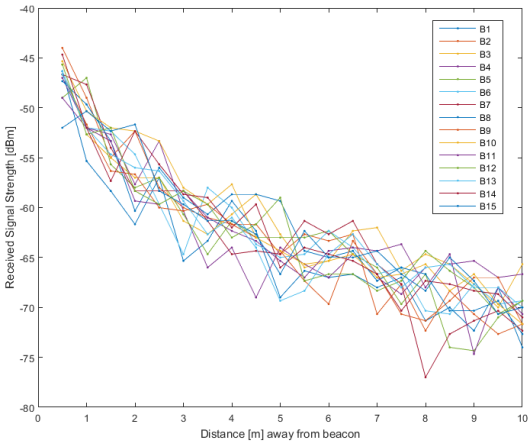

Figure 6.3: The average RSS values per beacon.

The other range experiments focus on the maximum range over which the broadcasted BLE advertising packages can be received. For three different beacons (beacon nr. 4, 9 and 15) the range experiments were repeated four times and received signal strengths were measured every 5 meter up to 50 meter away from the beacon. By looking at the results in Fig. 6.4, the graphs show a similar pattern as in the overview of all bea-

cons show in Fig. 6.2. However, it must be noticed that the decrease in signal strength is faster for the first 20 meter away from the beacon than for the distance 25 - 50 meter. The estimated trend of the average values of the three beacons show a gentle, almost horizontal slope. Furthermore, the average values are depicted with the corresponding standard deviations per distance unit. The BLE signal is still received at 50 meter distance from the beacon, although it seems to approach a constant value. Therefore, the range was extended up to the end of the basement hallway (approximately 175 meter away from the beacon) and the BLE signals of the beacon were still reaching the mobile device. The fact that the BLE signals are still received at 175 meters from the beacon, could be a consequence of the signal propagation through the hallway. The basement hallway is approximately 2 meters wide and is completely empty. There is no furniture or obstacles that could block or attenuate the signal that is propagating through the hallway.

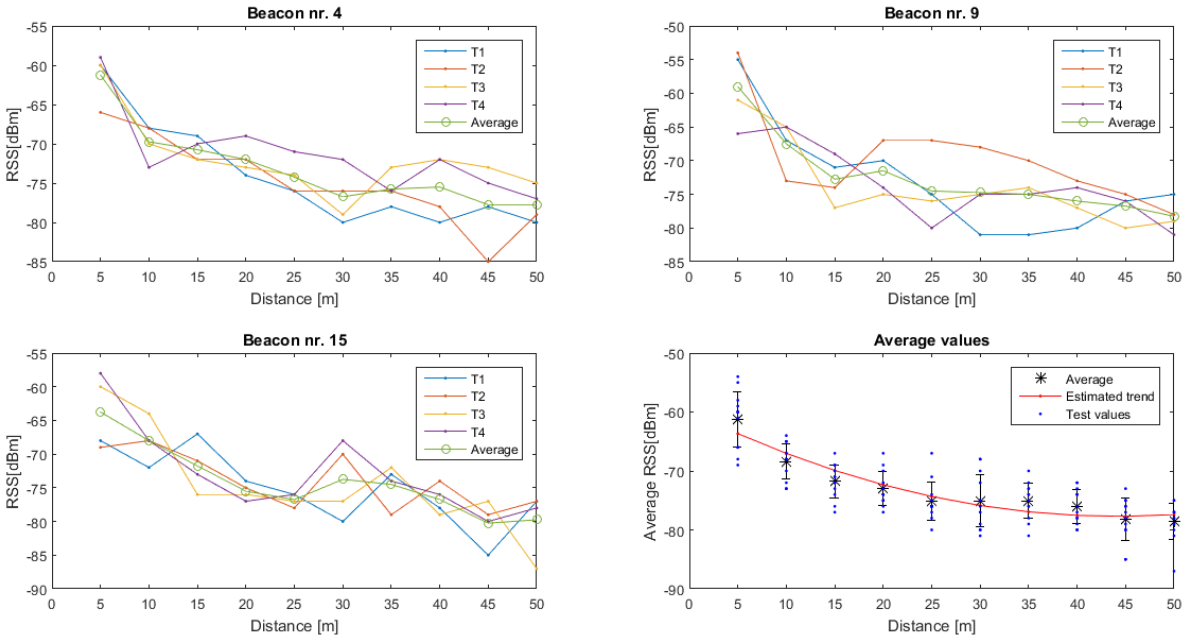

Figure 6.4: An overview of the acquired data from the 50m range experiments with three beacons.

Applying outlier detection

To apply outlier detection in order to provide validated measurements for further analysis and interpretation, the design matrix A and Q_{yy} matrix have to be defined. The indicated trend of Fig. 6.2 and 6.3 showed a quadratic or exponential decay of the RSS values over distance. Therefore, the design matrix A ($n \times 3$) is based on a quadratic polynomial or second order polynomial and consists three columns, where the first columns consists of 1's, the second represents the distance (d) and the third column is the squared distance (d^2). Furthermore, the diagonal of the Q_{yy} matrix is defined by the uncertainty of the observations $\underline{y}$ per beacon in the form of the variance. After defining the design matrix and the Q_{yy} matrix, the w-test was performed and iterated until all outliers were removed that did satisfied $|\underline{w}| > \sqrt{k_a}$. Eventually, H_0 was accepted after removing 171 data points of the in total 900 measurements. Both before and after applying outlier detection, the variance and corresponding standard deviation was computed for every distance unit. The original dataset and the data after outlier detection and removal are visualized in Figure 6.5. The average standard deviation of the initial data is 3.5982 dBm which reduces to 3.0032 dBm after applying outlier detection. Additionally, the average values per distance unit, their error range based on the standard deviation per distance unit and the estimated trend are plotted in Fig. 6.5. Comparing the initial data to the corrected data, it can be concluded that the standard deviation per distance unit decreased as a consequence of outlier detection. Furthermore, the residuals between the observed average values and the estimated trend are smaller after applying outlier detection.

In addition, the standard deviation appears to increase slightly with increasing distance from the beacon in both cases (Fig. 6.5). To verify whether the standard deviation increases with distance or not, the standard deviations of both the initial data and the data after applying outlier detection are shown in Figure 6.6. The standard deviation after applying outlier detection is lower than before, where the difference between the

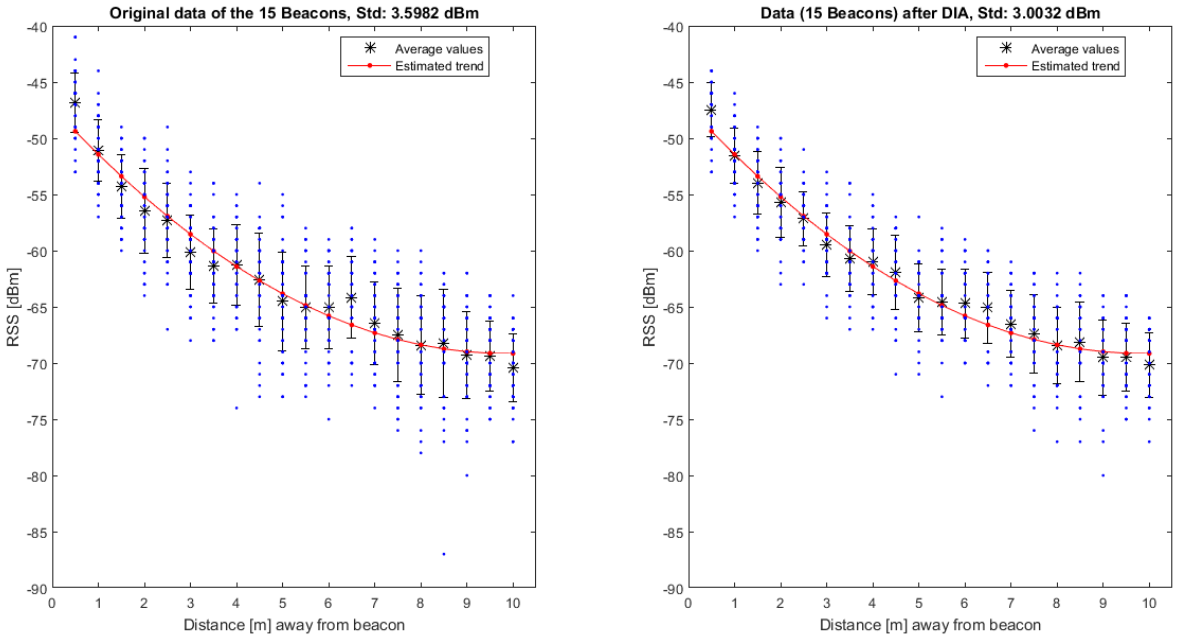

Figure 6.5: A) Left, the original dataset (blue dots), the average values (black stars) with error bars corresponding to the standard deviation per distance unit and the estimated trend (red solid line). B) Right, the dataset (blue dots) after applying outlier detection, the average values (black stars) with error bars corresponding to the updated standard deviation per distance unit and the estimated trend (red solid line).

original standard deviation and the standard deviation after outlier detection is also given in Fig. 6.6. Analyzing the standard deviations, it can be concluded that the standard deviations increase slightly with increasing distance away from the beacon. For clarification, the standard deviations has also been visualized in Figure 6.6, where the overall trend confirms the slight increase of the standard deviation.

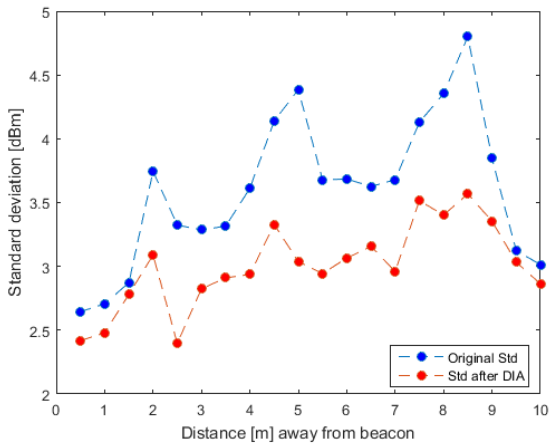

Distance (m)	Initial Std (dBm)	Std (dBm) after outlier detection	Diff (dBm)
0.5	2.644	2.418	0.226
1	2.707	2.479	0.227
1.5	2.872	2.780	0.092
2	3.745	3.090	0.655
2.5	3.324	2.397	0.927
3	3.286	2.825	0.461
3.5	3.315	2.910	0.405
4	3.612	2.938	0.675
4.5	4.139	3.329	0.810
5	4.385	3.038	1.347
5.5	3.678	2.944	0.735
6	3.685	3.066	0.619
6.5	3.627	3.156	0.471
7	3.679	2.960	0.718
7.5	4.129	3.515	0.614
8	4.353	3.403	0.951
8.5	4.801	3.568	1.233
9	3.846	3.354	0.492
9.5	3.122	3.033	0.089
10	3.014	2.863	0.151

Figure 6.6: Left, the original standard deviations (blue) and the standard deviation after outlier detection (red) per distance unit. Right, overview of the standard deviations, both original and after outlier detection.

Subsequently, outlier detection has also been applied on the data from the 50 meter range experiments. The same design A matrix and Q_{yy} matrix as for all 15 beacons, since the indicated trend of Fig. 6.4 also shows a quadratic or exponential decay of the RSS values over distance. By applying outlier detection, 22 data points were detected, identified and removed of the in total 120 measurements. The average initial standard deviation was 3.349 dBm and 2.9016 dBm after applying outlier detection. The average values of both the initial and corrected data set are illustrated in Fig. 6.7 together with the estimated trend and the error range based on the standard deviation per distance unit. The estimated trend both show a similar quadratic decay gradually decreasing in slope towards a distance of 50 meter. The results of the 10- and 50 meter experiments both show the same trend which seems to gradually approach a constant value.

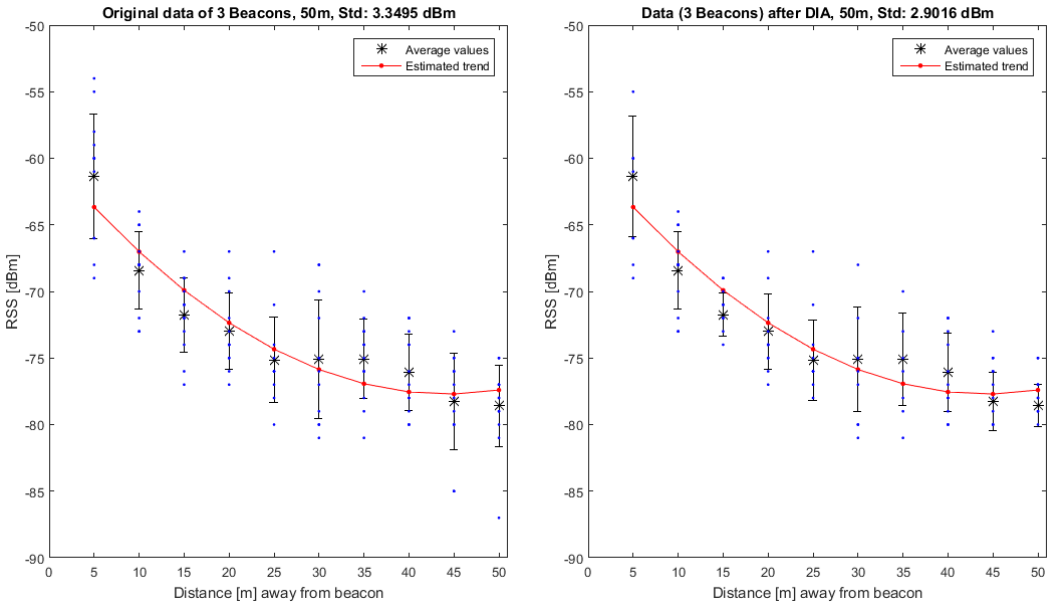

Figure 6.7: Left, the original dataset, average values and the estimated trend for the 50 meter experiment. B) Right, the dataset (blue dots) after applying outlier detection for the 50 meter experiment.

In contrast to Fig. 6.6, the standard deviations of the 50 meter experiments does not show (Figure 6.8) the slight increase in standard deviation with increasing distance. Instead, the standard deviation is fluctuates a over distance, both decreasing and increasing. Considering the signal attenuation of the BLE signals, it is expected that the standard deviation would increase over distance. However, based on the results of Fig. 6.6 and Fig. 6.8 it can be concluded that the standard deviation fluctuates over distance, but does not necessarily decrease with increasing distance. A possible explanation could be that the amount of disturbances increase over distance, this can vary per measurement location. The measurements were taken in a long hallway with no obstacles, however the hallway became wider at certain locations, which could have lead to signal disturbance. Furthermore, the number of measurements is to low in order to estimate a good standard deviation.

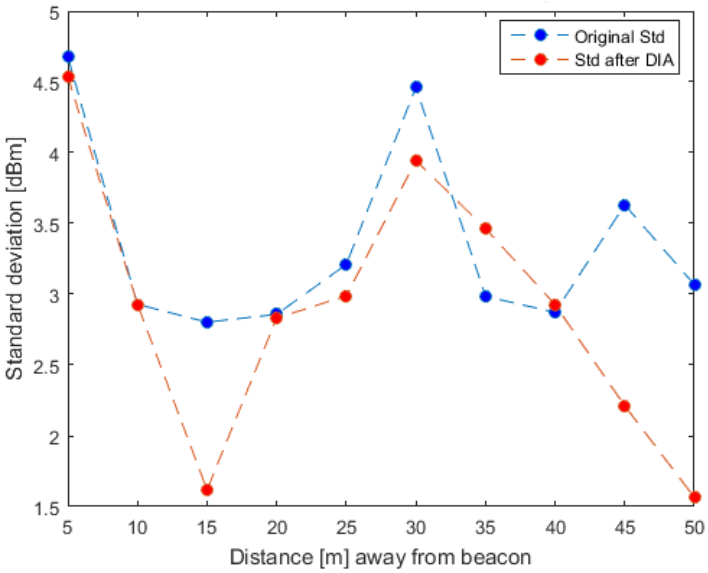

Figure 6.8: A) The standard deviations (blue) per distance unit of the original data for 50 meter (left) and B) the standard deviations (red) per distance unit after applying outlier detection (right).

6.2.2. The relationship between distance and signal strength

The relationship between distance and signal strength can be derived via the estimated trends that are shown in Fig. 6.5. The estimated trend is based on a quadratic polynomial or second order polynomial, where the estimated parameters can be used in order to determine a distance relationship. The second order polynomial can be defined as follows

$$RSS(d) = p_3 + p_2 d + p_1 d^2 \tag{6.1}$$

where p_1, p_2 and p_3 represent the coefficients of the polynomial, d is the distance and RSS the received signal strength. The coefficients for the original estimated trend are slightly different than the coefficients of the estimated trend after applying the DIA procedure. The original coefficients are $p_1 = 0.2262$, $p_2 = -4.457$ and $p_3 = -47.21$, whereas the coefficients after applying the DIA procedure are $p_1 = 0.2053$, $p_2 = -4.254$ and $p_3 = -47.38$. Since the corrected data is more reliable, these coefficients will be used in order to compose the relation between distance and signal strength. By substituting the coefficients in the second order polynomial it becomes

$$RSS(d) = -47.21 - 4.454d + 0.2053d^2. \tag{6.2}$$

By using the quadratic formula, the relation between distance and signal strength can also be expressed as

$$d = \frac{-p_2 \pm \sqrt{p_2^2 - 4p_1(p_3 - RSS)}}{2p_1} \tag{6.3}$$

with the second order polynomial coefficients of $p_1 = 0.2053$, $p_2 = -4.254$ and $p_3 = -47.38$. Subsequently, the average RSS values after outlier correction (Fig. 6.5) and the corresponding standard deviations (Fig. 6.6) were used to determine the empirical standard deviations related to the distance (σ_d). For every distance unit d_i, a random vector chosen from the multivariate distribution with as mean the average value of RSS_i and the variance σ_i^2 was generated 100000 times. The random vector with 100000 RSS values was used as input for equation 6.3 together with the coefficients of the polynomial given in equation 6.2. Eventually, the standard deviation σ_d was computed from the computed random vector with distances for every distance unit. An overview of the empirical standard deviations over distance is illustrated in Figure 6.9. The standard deviation related to the distance shows an increase with increasing distance away from the beacon. Furthermore, the average σ_d is 1.74 meters, which is higher than the initial standard deviation of $\sigma = 1$ that is used in the design computations. Throughout the thesis, the initial standard deviation was set to $\sigma = 1$ and had no distance relationship. However, in theory there is a distance relation regarding the empirical standard deviation which could be implemented in a future model.

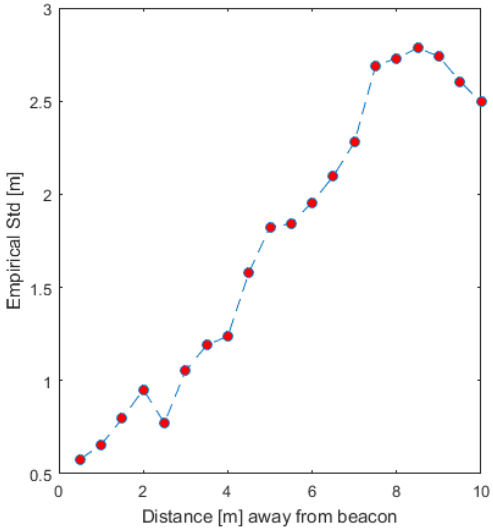

Distance (m)	Std (m)
0.5	0.576
1	0.656
1.5	0.797
2	0.951
2.5	0.774
3	1.051
3.5	1.197
4	1.229
4.5	1.587
5	1.821
5.5	1.836
6	1.952
6.5	2.095
7	2.276
7.5	2.694
8	2.731
8.5	2.790
9	2.739
9.5	2.609
10	2.489

Figure 6.9: The empirical standard deviations related to the distance.

6.2.3. Signal strength of mobile devices

Indoor positioning systems can track and locate several mobile devices such as tags, smartphones and tablets. Therefore, a small sub-experiment has been performed to evaluate the BLE signal strengths of an IOS phone

and an Android phone, the IPhone 5C was tested against the LG Spirit. As discussed earlier, the initial idea was to include measurements of the signal strengths of the three Bluetooth tags, but since the tags implement their own multicast protocol to communicate efficiently with the beacons without collisions, the communication cannot be intercepted with a BLE chip. Therefore, the mobile device tests were limited to an IOS operated and an Android operated device.

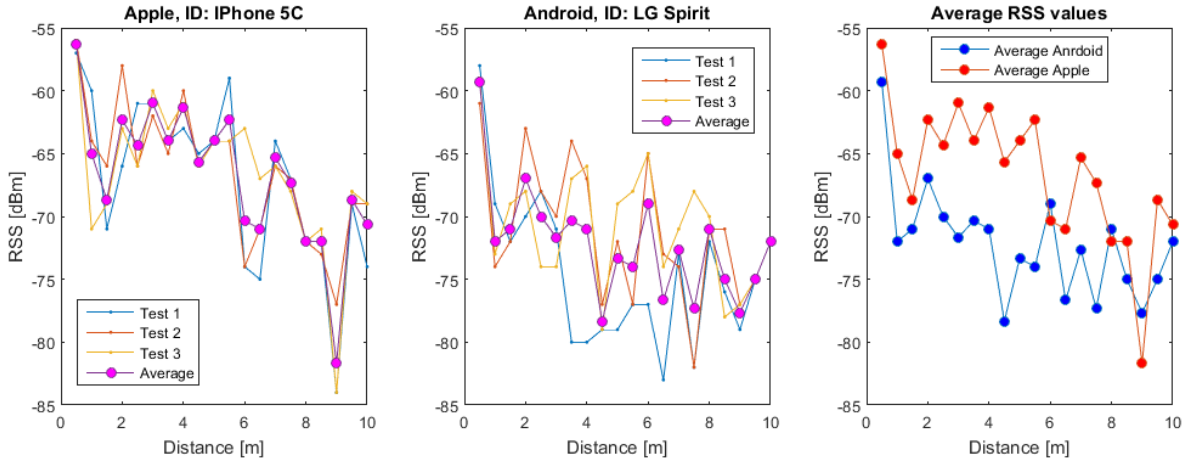

Figure 6.10: A) The acquired data from the IOS IPhone 5C (left), B) the Android LG Spirit phone (center) and C) their average RSS (right) values.

The test setup was similar to the experiments of the RSS values of the beacons, so the floor was marked at every 0.5 meter away from the beacon up to a maximum distance of 10 meter. Instead of beacons, the one of the mobile devices was placed on the zero mark with Bluetooth enabled. Subsequently, every 0.5 the signal strength was measured with increasing distance away from the mobile device resulting in 20 received signal strength measurements. Similar to the beacons, the signal strength measurements were repeated three times to reduce the random errors in the measurements. The test has been done separately for both the LG Spirit and the IPhone 5C to reduce the effect of signal interference. Both phones are implemented with the same Bluetooth chip (Bluetooth 4.0, BLE) which makes it possible to test them against each other and to compare the results. The results of the three tests per phone and their average RSS values are depicted in Figure 6.10. It has to be noted that the results of the three different test are less spread for the IOS phone than for the Android phone. Furthermore, the average RSS values of the IPhone are generally higher than those of the LG Spirit. Similarly to the beacons, the signal tends to decrease slightly with increasing distance away from the mobile devices.

6.3. Results of the theoretical design computations

6.3.1. Results of the first scenario

The precision values for every possible position of a mobile device have been computed with a point density of 1 meter for the first scenario and the precision is illustrated in Figure 6.11. The visualized precision corresponds to the total precision, which is derived by $\sigma_T = \sqrt{\sigma_x^2 + \sigma_y^2 + \sigma_z^2}$, where the σ_x, σ_y and σ_z are computed by the model via the square root of the diagonal of the variance matrix $Q_{\hat{x}\hat{x}}$ (section 5.1). The computed total precision indicates that this geometry has a relatively higher precision (lower standard deviation) when the mobile device is located at the same elevation as the beacons at$z = 1$ and $z = 5$ with a minimum standard deviation of 0.7871 meter. However, the precision becomes significantly lower towards the center of the 3D space as a consequence of the geometry. The total precision decreases up to a maximum standard deviation of 1.124 meter at $z = 3$. The gradual decrease in precision towards the center of the 3D space is caused by the vertical alignment of the beacons at $z = 1$ and $z = 5$. Due to the vertical alignment, the precision error increases in the z-direction towards the center. The precision error in the z-directions decreases again towards the edges as a consequence of the triangle formation of the beacons. Therefore, the PDOP increases towards the center and decreases towards the edges, see Figure 4.7 in section 4.2.

Besides the total precision, the corresponding MDBs (section 5.1) have been calculated at every location

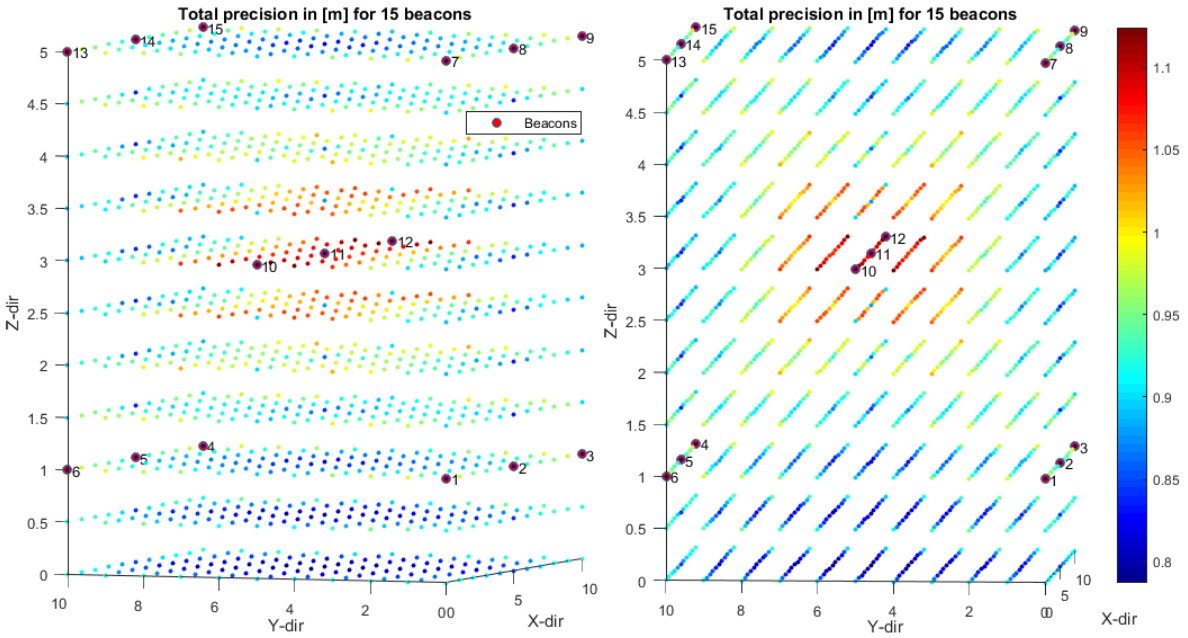

Figure 6.11: Two different view angles of the 3D space showing the total precision for every possible position within the first geometry.

with respect to every beacon. Since the MDB values contain 15 values for every possible tag location, only the maximum MDB values have been plotted in Figure 6.12 along with the corresponding beacon number. Besides the precision, the reliability of the observations is also dependent on the geometry. The maximum MDB values indicate that it is possible to have a relatively large bias in the positioning results, without being detected. The increase in reliability is caused by the fact that beacons can verify each others measurements. The maximum MDB values are located in between the beacons at $y = 4-6$ and at $z = 3$, the beacons validate the positioning results at these locations more than at the locations towards the sides of the 3D space. By looking at the corresponding beacons, often the beacons furthest away from the tag location coincide with the maximum MDB. For example, the maximum MDB values at *z=1* coincide with the beacons at *z=5*, meaning that the positioning error at these locations can be relatively large, without the possibility of detecting the bias caused by an error in the corresponding beacon.

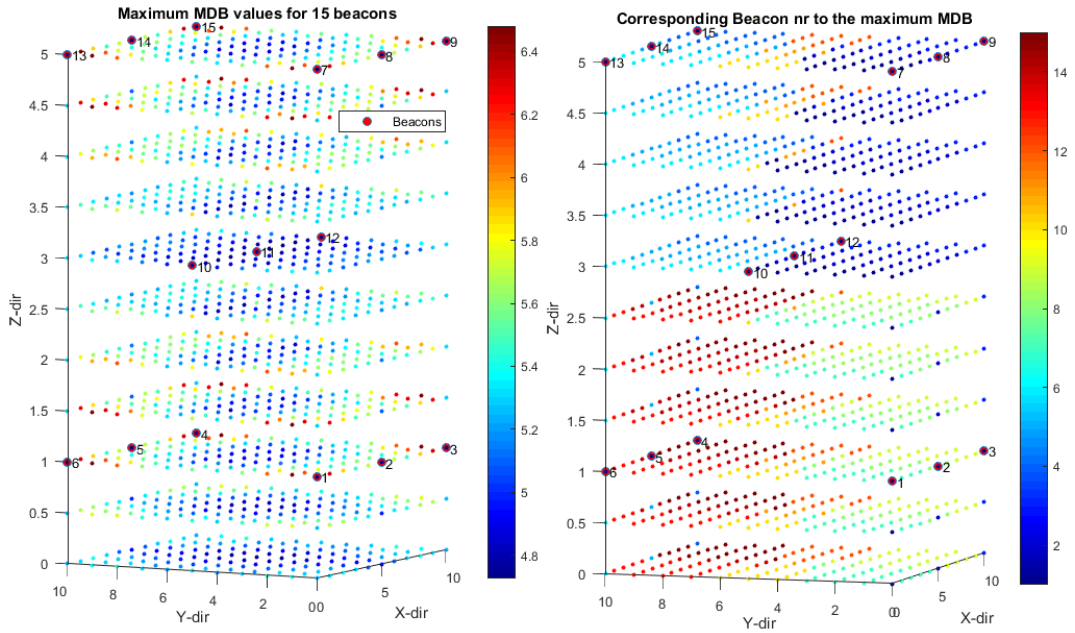

Figure 6.12: A) Left, the maximum MDBs [m] for every location of a mobile device and B) right, the beacon number corresponding to the maximum MDBs.

Additionally, the maximum MDBs were used to compute the corresponding external reliability $|\nabla \hat{x}|$ or Minimal Detectable Effect (MDE) indicating the effect of the MDB on the estimated position. Similar to the MDB, every possible tag location contains 15 MDE values related to an error in one of the 15 beacons. The MDEs are depicted in Figure 6.13 and show a similar pattern as the total precision (Fig. 6.11) gradually increasing MDEs towards the center of the 3D space. The external reliability shows the effect on the estimated positions due to a bias $C_y|\nabla|$ in one of the beacons. Since beacons are validating the positioning estimates for beacons in close proximity, the effect on the estimated positions is minimum at the locations coinciding with the highest precision (lowest std's), namely between $z = 0-1.5$ and $z = 4-5$. The tag locations towards the center of the cube have the largest impact on the estimated positions, since the positioning estimates are validated less. As a consequence, the effect on the position estimates becomes larger in case an error in a beacon remains undetected for the given geometry.

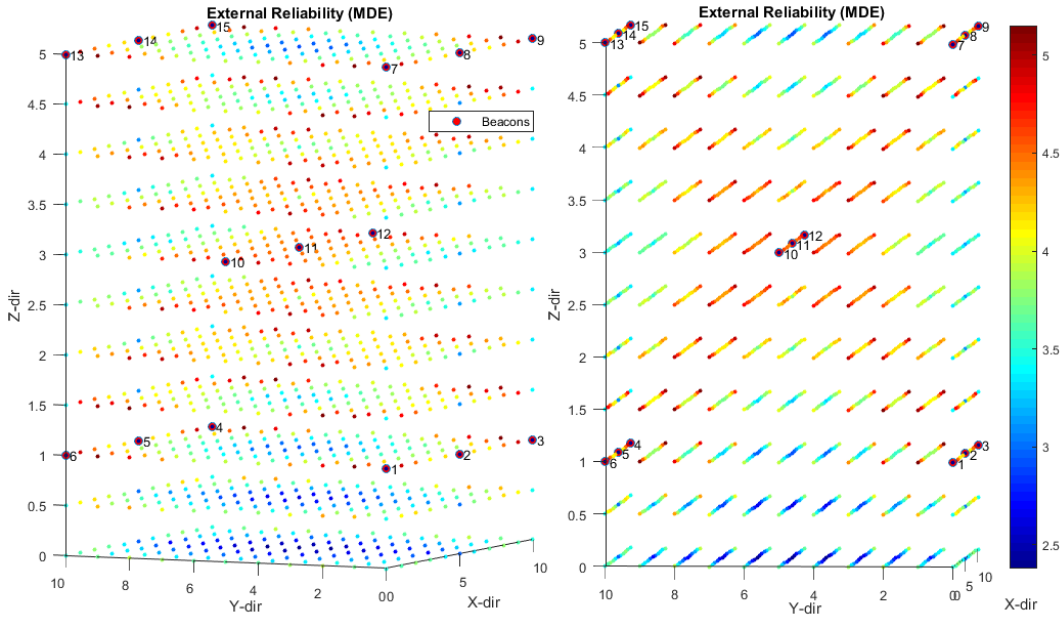

Figure 6.13: Two different view angles of the 3D space showing the external reliability or MDE [m] for every possible position within the first geometry.

6.3.2. Results of the second scenario

Similar to the first scenario the total precision, maximum MDBs and the corresponding beacon number and MDEs have been computed. Since the beacons are not vertically aligned in this scenario, the results differ significantly from the first scenario. Compared to the first situation (Fig. 6.11), the total precision has generally increased (smaller standard deviation, minimum of 0.7816 meter) which indicates that this geometry gives a better result than the first scenario. The total precision is evenly spread over the 3D space, except for some locations at the edges of the 3D space at $z \geq 3.5$ with a maximum standard deviation of 1.1757 meter. The precision shows a symmetrical pattern, with a increase in precision towards the center of the 3D space. Some of the tag locations towards the edges of the 3D space show a decrease in precision (higher standard deviation). The direct relationship between the precision and geometry is reflected in the center points ($x = 2-8, y = 0-10, z = 0-1.5$ and $z = 4-5$). In contrast to the first scenario, the beacons are not vertically aligned anymore which reflects in an decrease in PDOP or in other words an increase in precision. Due to the shift of the beacons at $z = 1$ towards $x = 2$ and $x = 8$ the precision in the z-direction increases in the center, resulting in an overall decrease of the PDOP.

Comparable to the first geometric configuration, only the maximum MDB values have been plotted in Figure 6.15 along with the corresponding beacon number. The maximum MDB values in Fig. 6.15 have their lowest values centered in between the beacons. The increase in reliability is caused by the fact that beacons closer to each other can verify each others measurements. Furthermore, beacons can also verify each others measurements in at least one direction, when two beacons are located opposite of each other. For example, the increase in MDB towards the center at $z = 5$ is caused by the fact that the beacons 10, 12 and 14 are located opposite of beacons 11, 13 and 15 and they verify each others measurements in the x-direction. The beacons

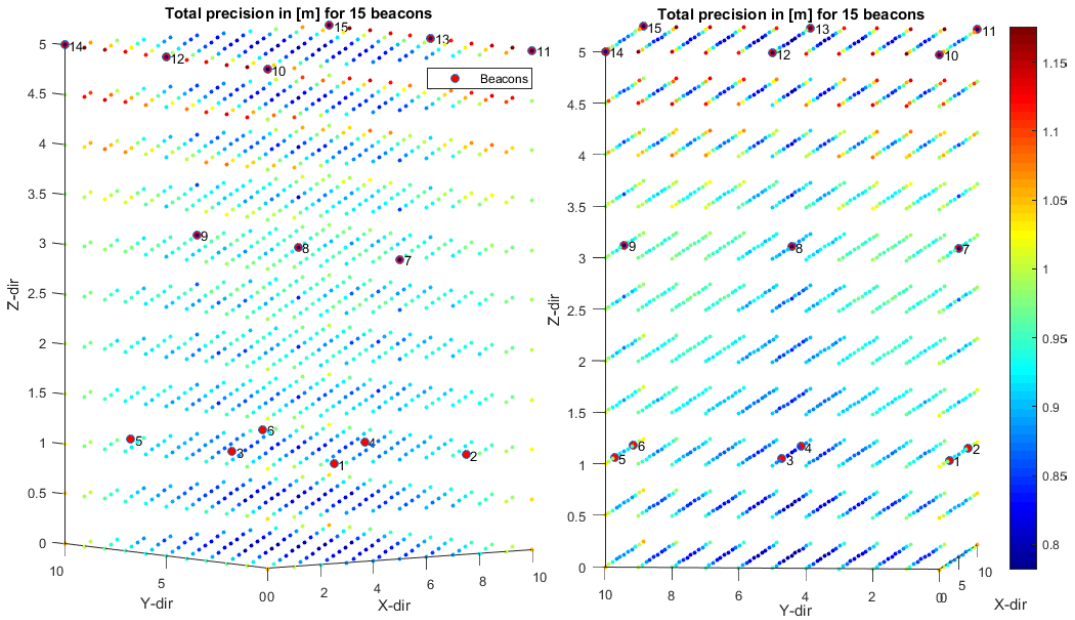

Figure 6.14: Two different view angles of the 3D space showing the total precision for every possible position within the second geometry.

corresponding with the maximum MDBs are still the beacons furthest away from the tag location, meaning that the positioning error at these locations can be relatively large, without the possibility of detecting the bias caused by an error in the corresponding beacon.

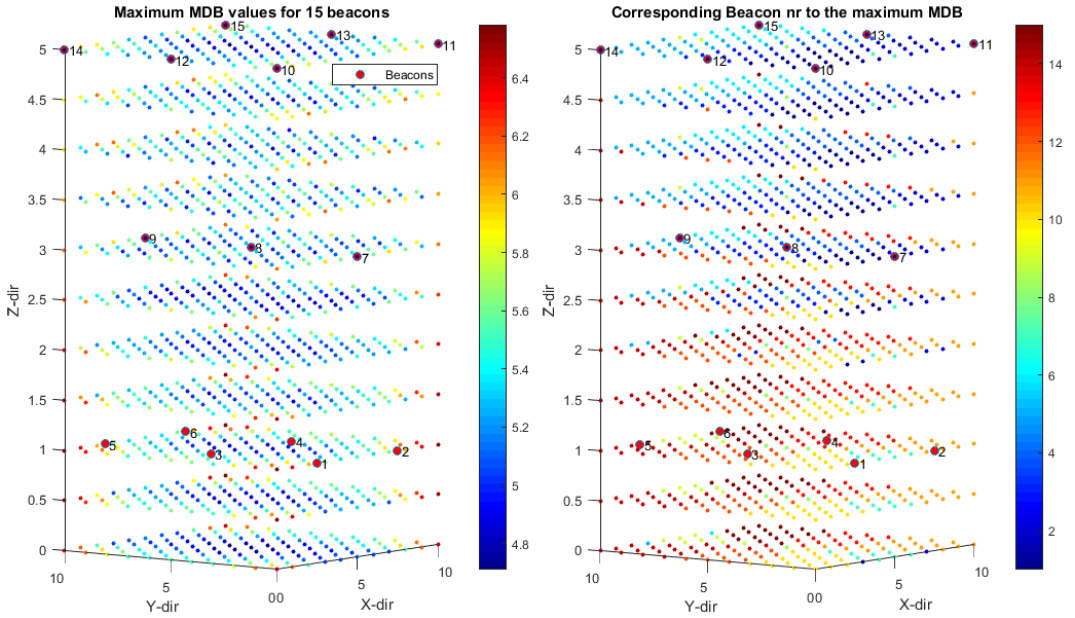

Figure 6.15: A) Left, the maximum MDBs [m] for every location of a mobile device and B) right, the beacon number corresponding to the maximum MDBs.

Similar to the MDB, every possible tag location contains 15 MDE values related to an error in one of the 15 beacons. Therefore, only the MDE values corresponding with the maximum MDB values of Fig. 6.15 are illustrated in Figure 6.16. In comparison with the MDEs of the first geometry (Fig. 6.13), the MDEs have generally lower values and have some higher values near the edges of the cube. The pattern of MDEs is similar to the precision pattern of Fig. 6.14. The external reliability shows the effect on the estimated positions due to a bias $C_y|\nabla|$ in one of the beacons. Since beacons are validating the positioning estimates for beacons in close proximity, the effect on the estimated positions is minimum at the locations coinciding with the highest precision (lowest std's), namely between $x = 2-8, y = 0-10, z = 0-1.5$ and $z = 4-5$. The tag locations at the edges of the cube have the highest effect on the estimated positions, since the positioning estimates are

validated by less beacons. This results in a larger effect on the position estimate if an error in a beacon remains undetected for the given geometry.

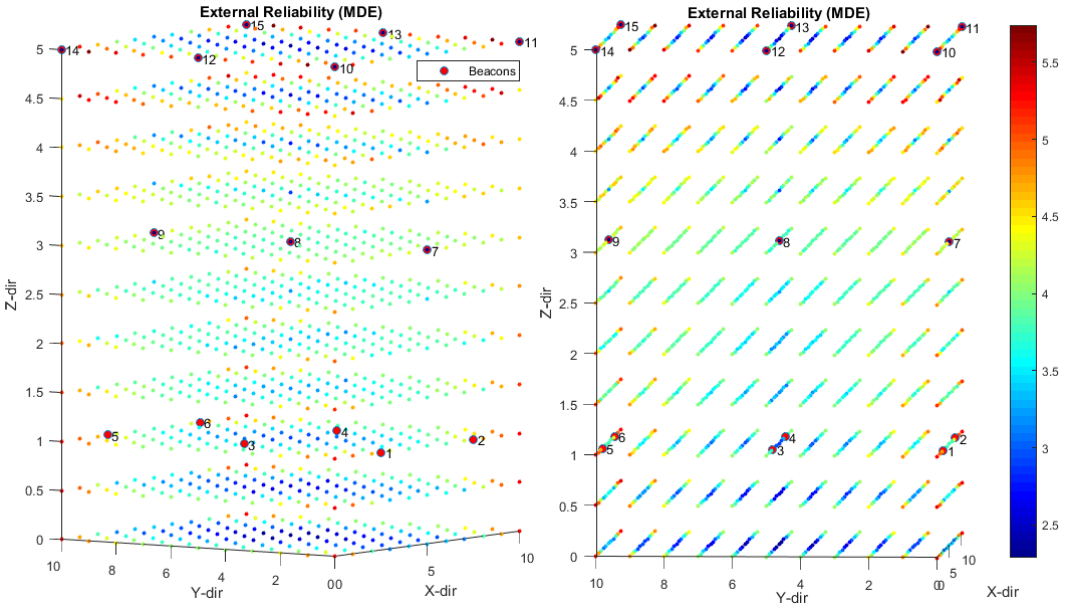

Figure 6.16: Two different view angles of the 3D space showing the external reliability or MDE [m] for every possible position within the second geometry.

6.3.3. Results of the third scenario

The total precision of the third geometric configuration is visualized in Figure 6.17 with a minimum of 0.7854 meter and maximum of 1.0744 meter. The precision shows a symmetrical pattern, with an increase in precision towards the center of the 3D space. The tag locations towards the edges of the 3D space show a decrease in precision (higher standard deviation). The direct relationship between the precision and geometry is reflected in the center points ($x = 0-7, y = 3-7$ and $z = 0-6$). In these regions, the precision is high in both x,y and z direction resulting in an increased total precision. By comparing the precision results with the first and second scenario, the geometry of the beacons of the third situation is close to the second situation. The beacons at $z = 1$ and $z = 5$ are not vertically aligned, causing a decrease of PDOP in the center region and thus a relatively high precision.

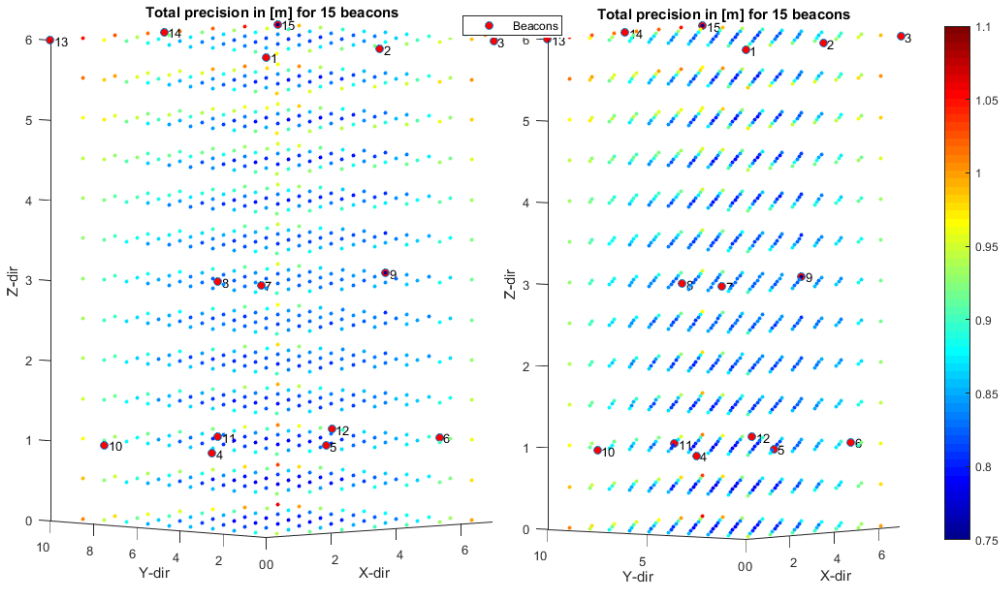

Figure 6.17: Two different view angles of the 3D space showing the total precision for every possible position within the third geometry.

Subsequently, the maximum MDBs were computed and are shown in Figure 6.18. The maximum MDB values indicate that it is possible to have a relatively large bias in the positioning results, without detecting that the bias is caused by an error in the system. The maximum MDB values in Fig. 6.18 have their lowest values centered in between the beacons. The increase in reliability is caused by the fact that beacons closer to each other can verify each others measurements. As mentioned earlier, beacons can also verify each others measurements in at least one direction, when two beacons are located opposite of each other. For example, the increase in MDB towards the center at $z = 6$ is caused by the fact that the beacons 1, 2 and 3 are located opposite of beacons 13, 14 and 15 and they verify each others measurements in the y-direction. By looking at the corresponding beacons, often the beacons furthest away from the tag location coincide with the maximum MDB. For example, the maximum MDB values at *z=1* coincide with horizontal positions of the beacons at *z=5*, meaning that the positioning error at these locations can be relatively large, without the possibility of detecting the bias caused by an error in the corresponding beacon.

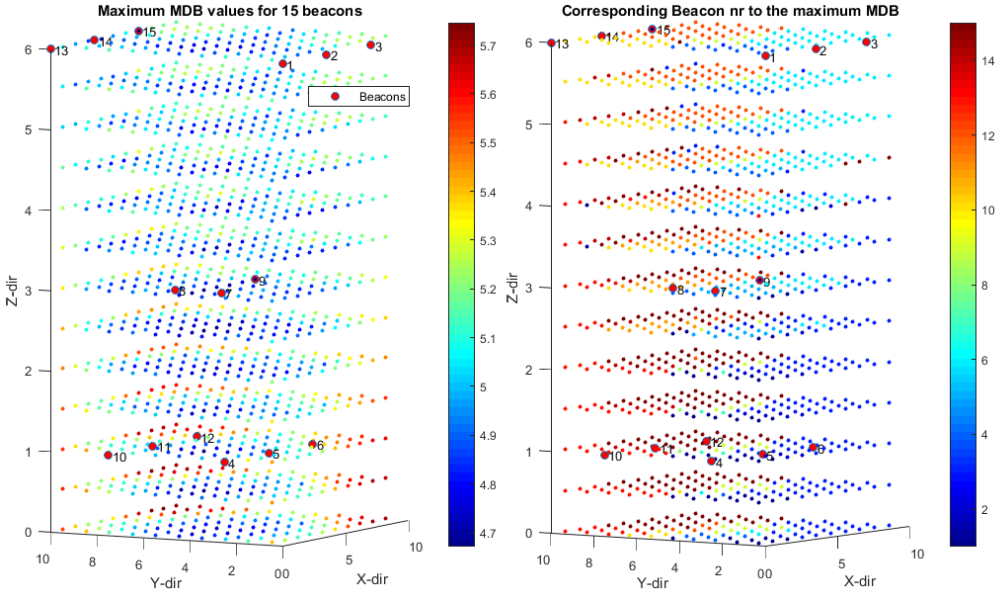

Figure 6.18: A) Left, the maximum MDBs [m] for every location of a mobile device and B) right, the beacon number corresponding to the maximum MDBs.

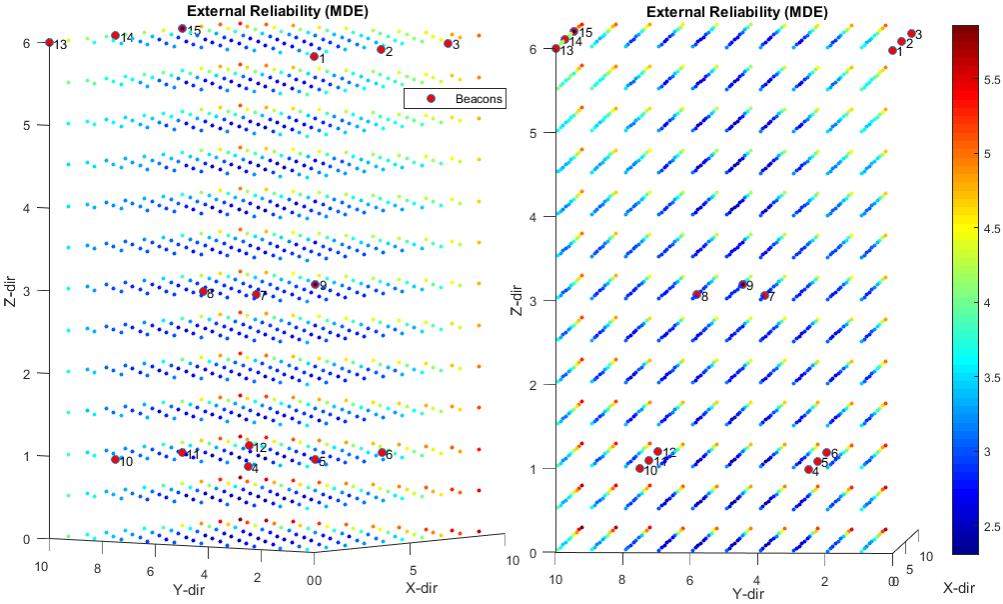

Figure 6.19: Two different view angles of the 3D space showing the external reliability or MDE [m] for every possible position within the third geometry.

The final result of the initial geometry computations is the external reliability as a consequence of the third geometry (Fig. 6.19). The external reliability shows the effect on the estimated positions due to a bias $C_y|\nabla|$ in one of the beacons. Since beacons are validating the positioning estimates for beacons in close proximity, the effect on the estimated positions is minimum at the locations coinciding with the highest precision (lowest std's), namely between $x = 0-7, y = 3-7$ and $z = 0-6$. The tag locations at the edges of the cube have the highest effect on the estimated positions, since the positioning estimates are validated by less beacons. As a consequence, the effect on the position estimates becomes larger in case an error in a beacon remains undetected for the given geometry. To conclude, the third situation resulted in the highest overall precision followed by the second situation.

6.4. Geometric experiments

The geometric experiments can be compared with the results derived from the theoretical design computations to validate the model. The theoretical set-ups can be computed from 4 beacons up to 15 beacons within predefined area and the locations of the beacons can be set manually. Particular theoretical geometries will have different results and predictions for precision that can be obtained. The geometry of the experimental set up will be based on the geometries that are tested in the theoretical design computations, such that a comparison can be made between the predicted precision and the obtained practical precision. The geometric experiments will be performed on the first floor at the office of the student association PS (Practische Studie) in the CiTG building at the Delft University of Technology.

Geometric experiment 1

The geometric experiments are based on the results derived from the theoretical design computations. Since the theoretical design computations provide measures for precision, internal (MDB) and external reliability for different theoretical set-ups, a validation can be done by a practical experiment. The geometry of the practical experimental set up is based on the geometry that is tested in the theoretical design computations, such that a comparison can be made between the predicted precision and the obtained practical precision. The practical experiment will be carried out in a hallway at the first floor of the CiTG building at the TU Delft. Assuming the first floor begins at $z = 0$ meter, the ceiling height is $z = 5.993$ meter. The 2D floorplan of practical experiment is illustrated in Figure 6.20.

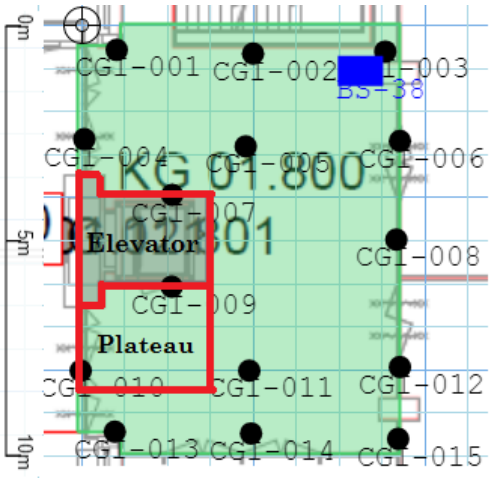

Figure 6.20: Test area with the locations of the beacons (black), basestation (blue) and the elevator shaft (red).

The test area is approximately 7x10x6 meter, equal to the 3D space defined in the design computations. The 15 beacons (black circles) have been deployed according to the third geometric configuration of Fig. 5.1. Beacons 1-3 and 13-15 were deployed at the ceiling ($z = 5.993$ m), beacons 4-6 and 10-12 at $z \approx 1$ m and beacons 7-9 in the center row at $z = 3.00$ m. The measurements with the BlooLoc tag are done according to a 1 meter grid in x and y direction with its origin in the upper-left corner of the test area (Fig. 6.20). In order to prevent signal attenuation by the human body, the tag will be placed on a tripod. The tripod with the tag was placed on a virtual 1 by 1 meter grid and measured for at every location for 90 seconds, resulting in numerous positioning estimates at each of the, in total 46, measurement locations of Figure 6.21. The measurement at location 28 contained no data and has not been used for further analysis. Furthermore, the test area consists of hallway without obstacles, where the only exceptions are an elevator shaft located between ($x = 0-2$ and $y = 3-6$) and a big rock (Fig. 6.21, circle). The elevator has an exit to a plateau at a subfloor floor at $z = 2.55$ m which might cause some signal attenuation or distortion for measurements taken underneath the plateau. Note that during this research the yooBee Software Development Kit (SDK) and Application Programming Interface (API) of BLooLoc had version 1.6, however, the functionality of the SDK and the API's are still evolving and thus subject to change.

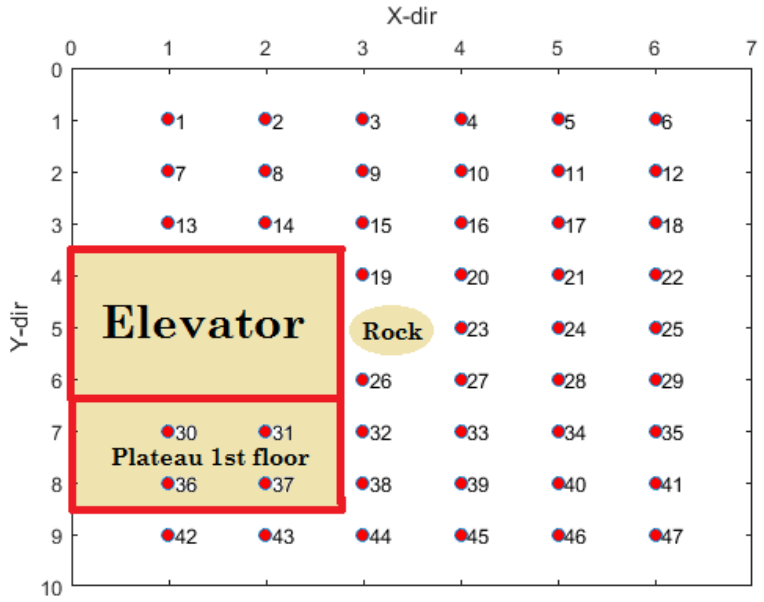

Figure 6.21: The measurement locations (red dots) in the test area.

Geometric experiment 2

The second practical experiment will be carried out on the first floor near the office of the study association 'Practische Studie' (PS) in the CiTG building at the TU Delft. Assuming the first floor begins at $z = 0$ meter, the ceiling height is $z = 5.283$ meter. Furthermore, the first floor contains several meeting rooms with a sublevel floor on top. The floors of these sublevel areas lie at $z = 2.55$ meter and are not surrounded by walls, but are fenced by a meter high glass fence. The open sublevel floor makes this an interesting location for testing the geometry and the corresponding precision results with the BlooLoc IPS. The 2D floorplan of practical experiment is illustrated in Figure 6.22.

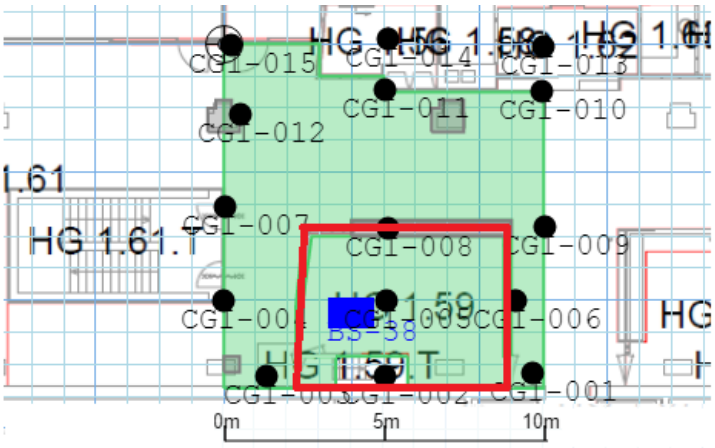

Figure 6.22: The test area (green) with the locations of the beacons (black), basestation (blue) and the meeting room/subfloor (red).

The test area is approximately 10x10x5 meter, equal to the 3D space defined in the design computations. The 15 beacons (black circles) have been deployed based on the second geometric configuration of Fig. 5.1 (Situation 2). Beacons 1-3 and 13-15 were deployed at the ceiling ($z = 5.283$ m), beacons 4-6 and 10-12 at $z \approx 1$ m and beacons 7-9 in the center row at $z = 3.00$ m.

The measurement locations are done according to a 2 meter grid in x and y direction with its origin in the upper-left corner of the test area and are visualized in Figure 6.23 for $z = 1$ (1-24) and $z = 4$ (25-34). From Fig. 6.23 can be seen that the upper part of the test area is an open space $y < 5$ and the lower part (red square) contains a meeting room with a open subfloor on top. Note that measurement location numbers 15-17 and

21-23 lie within the meeting room and are separated from the rest of the area by concrete walls and a glass wand. Measurement locations 18 and 24 are covered by the subfloor, but in contrast lie in a hallway and are therefore not located within a separate room. Besides the subfloor, other obstacles are two concrete pillars (gray squares in Fig. 6.23) and a wooden wall extension from $x \approx 3.5 - 10$ and $y \approx 0 - 1$.

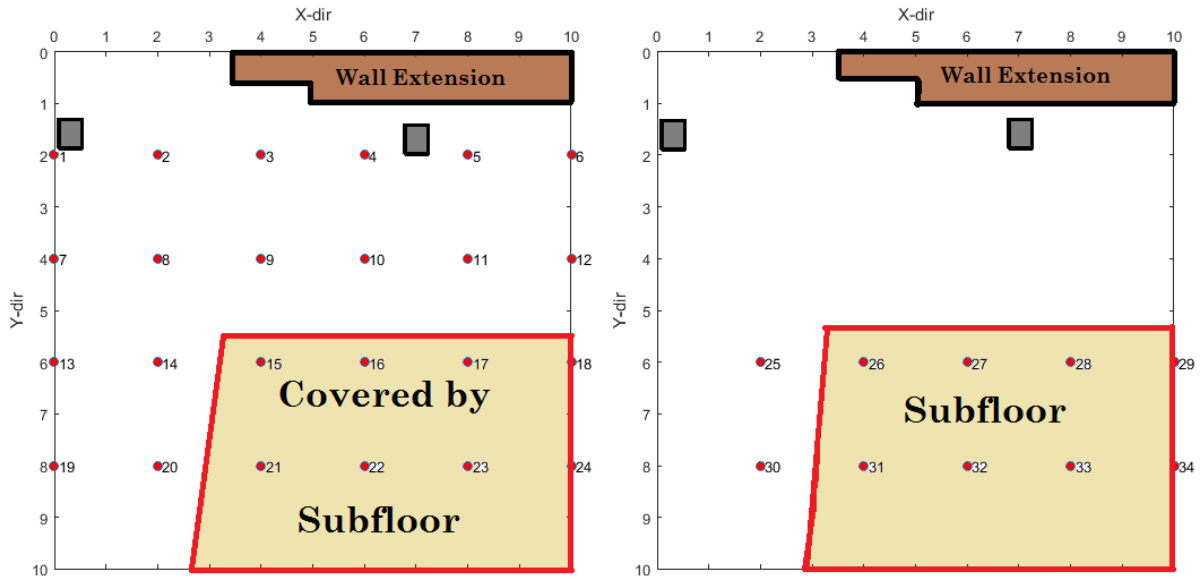

Figure 6.23: The measurement locations (red dots) in the second test area at *z=1* (left) and *z=4* (right).

6.5. Results of the geometric experiments

6.5.1. Geometric experiment 1

The BlooLoc beacons were deployed according to the third geometric configuration of Fig. 5.1. For every possible tag location at $z = 1$ (Fig. 6.21), the position in x and y coordinates was calculated along with a standard deviation for both x and y direction for approximately 90 seconds. Since the BlooLoc tag has an update rate of 1 Hz, this should result in 90 measurements per location, however in practice this slightly less and differed a bit per measurement location. Eventually, the positioning estimates were averaged over all measurements taken at a measurement location and compared to the true location. The distance d between the true locations and the corresponding estimated positions has been used to filter out the points that had been estimated at $d > 1.5$ meter from their true location, resulting in the removal of 19 points. Since the accuracy is a standard for the closeness of the measured values with respect to the true values, the accuracy results are visualized in Figure 6.24 (left). It is hard to distinguish a pattern, since some estimates have a high accuracy or in other words, are relatively close to their true positions (nr. 2, 4, 29, 39, 43, 45), while others have a significant offset (nr. 5, 17, 21, 46, 47) and thus a low accuracy. However, it is remarkable that all points underneath the plateau at the first floor have been removed due to a offset of $d > 1.5$ meter. The removal of these points is most likely due to a combination of NLOS and shadowing. Most of the position estimates that are closest to their true locations are found at $x = 4$. The higher offsets next to the elevator shaft are most likely caused by reflections and multipath due to the metal elevator shaft.

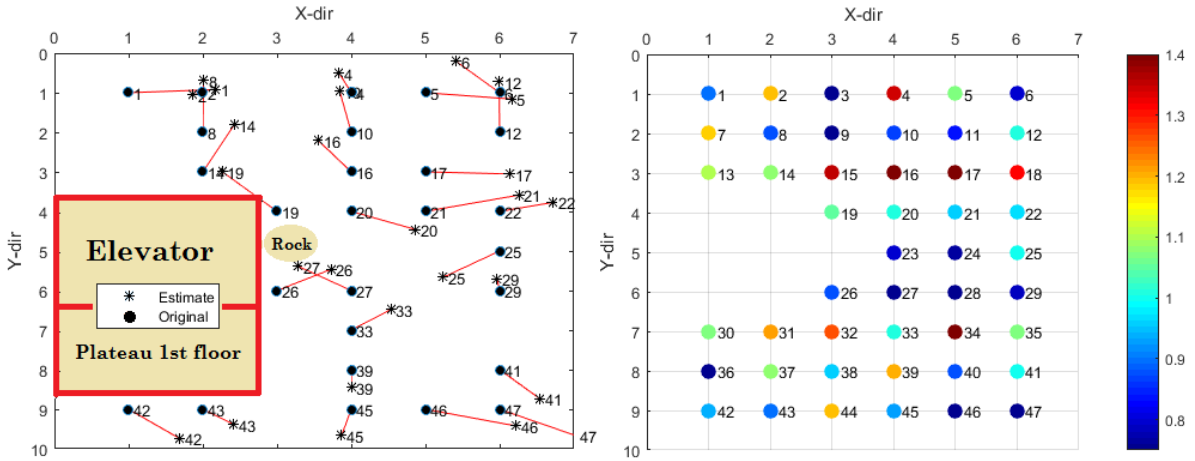

Figure 6.24: Left, the accuracies of the practical results from the first experiment visualized by the difference of the measured positions with respect to the true positions. Right, the estimated total precision or HDOP by the BlooLoc IPS in [m].

The standard deviations of the estimated positions, σ_x and σ_y, were used to calculate the horizontal precision or the HDOP at $z = 1$ by using equation 5.11 (section 5.1.2) with an initial standard deviation of $\sigma = 1$. Similar to the position estimates, the computed horizontal precision values were averaged for every measurement locations. For convenience, the horizontal precision of the measurements has been visualized at their true locations in Figure 6.24 (right), but take into account that the estimated positions differ from the true locations (Fig. 6.24, left). From Fig. 6.24 (right) can be seen that the estimated precision of the IPS ranges from 0.75-1.5 meter where the majority of the estimated precision lies between 0.75 and 1.1 meter. The highest precision is found in the center of the area, whereas at some places the precision values of the IPS shows a significant decrease in precision (nr. 15 - 18 and 34) as a consequence of either systematic errors or due to signal reflections of the metal elevator shaft. Furthermore, the precision has only been validated at one height level $z = 1$. This height level has been chosen because most people wear mobile devices in their pockets at approximately $z = 1$ meter. Since BlooLoc only provides a 2D solution (x, y), the theoretical design computations can be used to give the user insight in distribution of the standard deviations in the z-direction.

To get a better insight in the data acquired with the BlooLoc IPS, the data measured at three random points with location number 8, 18 and 27 (Fig. 6.24) has been visualized in Figure 6.25. The scatter plots of Fig. 6.25 show the positioning errors of the measured positions with respect to their true position and the spread in the measurements. Location numbers 8 and 27 (Fig. 6.25, left and right) correspond with a higher precision since the spread in the measurements is smaller and the positioning errors relatively small. For instance, the

positioning errors of the measurements with respect to location number 8 (Fig. 6.25, left) are relatively low in the x-direction and slightly higher in the y-direction. In contrast to location number 18 (Fig. 6.25, middle), which corresponds with a low accuracy and a low precision as a consequence of the increased spread of the measurements and the increased distance between the measured positions and the true position. Furthermore, the positioning errors do not show an elliptical distribution around the true location but clearly indicate an offset with respect to the true position. Since the positioning errors do not show an elliptical distribution around the true location and the majority of the measurements shows the same offset, the errors can be classified as systematic errors.

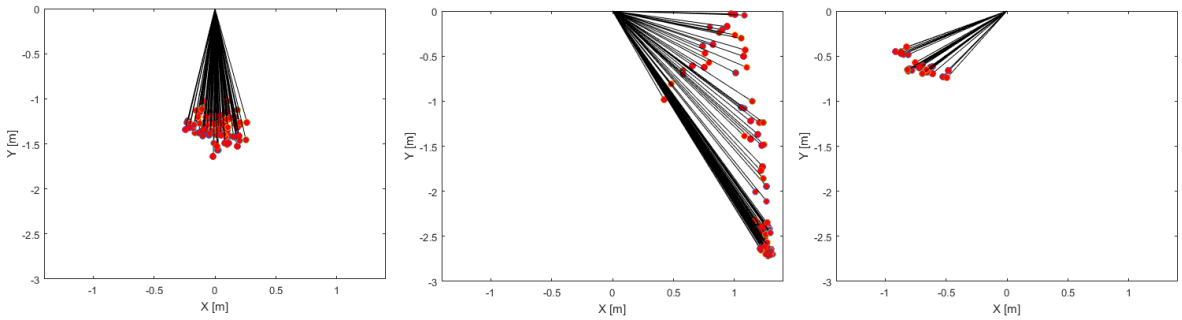

Figure 6.25: Visualization of the positioning errors (red) with respect to their true locations at, from left to right, location 8, 18 and 27.

6.5.2. Geometric experiment 2

For the second experiment, the BlooLoc beacons were deployed according to the second geometric configuration of Fig. 5.1. Similar to the first experiment, for every tag location at $z = 1$ and $z = 4$ (Fig. 6.23), the position in both x and y coordinates was estimated along with the corresponding standard deviations. To analyze the accuracy of the measurements, the positioning estimates were averaged and compared to their true location. The closeness of the measured values with respect to the true values is depicted in Figure 6.26 for $z = 1$ (left) and $z = 4$ (right). In contrast to the accuracy of the first practical experiment, the accuracy is much lower in this case at $z = 1$ and $z = 4$. Subsequently, the estimated points at distance $d > 1.5$ meter from their true location have not been filtered out, since this yields for the majority of the points. Several points have a high accuracies (nr. 3, 6, 11, 12, 13, 19, 24 at $z = 1$), whereas the rest of the measurement locations coincides with a significant offset and thus low accuracies. Generally, the accuracy at $z = 4$ is very low and coincides with large offsets, except for location nr. 31 (Fig. 6.26, right). Since the calibration of the BlooLoc IPS was successfully carried out, it is unlikely that the large offsets are caused by a systematic error. Furthermore, the offsets show different magnitudes and directions. Therefore, it is more likely to explain the majority of the higher offsets by NLOS and shadowing caused by the subfloor.

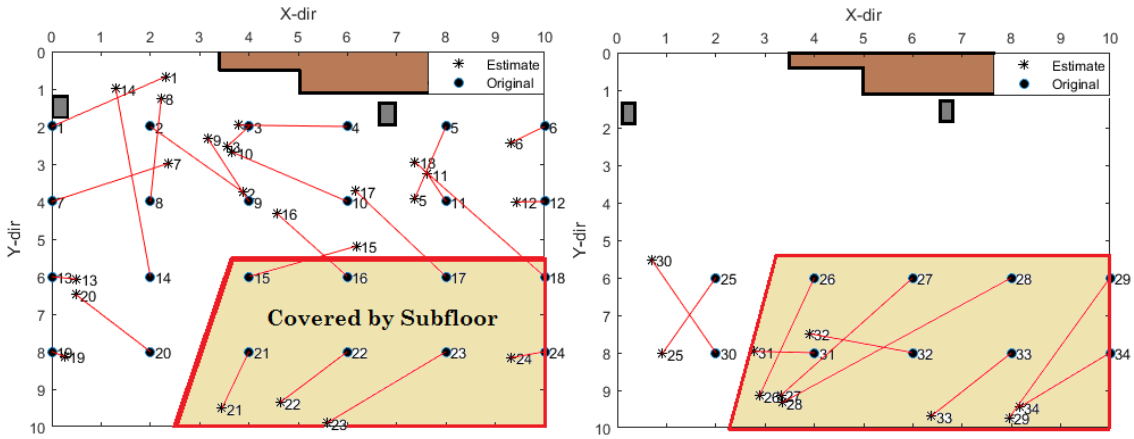

Figure 6.26: The accuracies of the practical results from the second experiment visualized by the estimated positions and the true locations at z=1 (left) and at the subfloor z=4 (right).

In addition to the accuracy, the horizontal precision or HDOP was computed from the estimated standard

deviations, σ_x and σ_y at $z = 1$ and $z = 4$ by using equation 5.11 (section 5.1.2) with an initial standard deviation of $\sigma = 1$. The standard deviations were averaged for every measurement location. Once more, it has to be mentioned that the horizontal precision is visualized at their true locations for interpretation purposes in Figure 6.27 at $z = 1$ and $z = 4$, but take into account that the estimated positions differ from the true locations (Fig. 6.26). Overall, the horizontal precision at $z = 1$ ranges from 0.5 - 1.15 meter and is low, or in other words, the standard deviations are high. From Fig. 6.27 (right) can be seen that the highest precision at $z = 1$ is found at $y = 8$, which is counterintuitive with the expected precision pattern. Since $y = 8$ is mainly covered by the subfloor, the measurement locations were inside a meeting room which was expected to lead to a decrease in precision. In addition, the lowest precision was found at $y = 4$, $z = 4$ which is within the area that was not covered by the subfloor. The precision at $z = 4$ ranges from 0.7 - 1.3 meter, meaning that the precision is lower for the measurement locations on the subfloor.

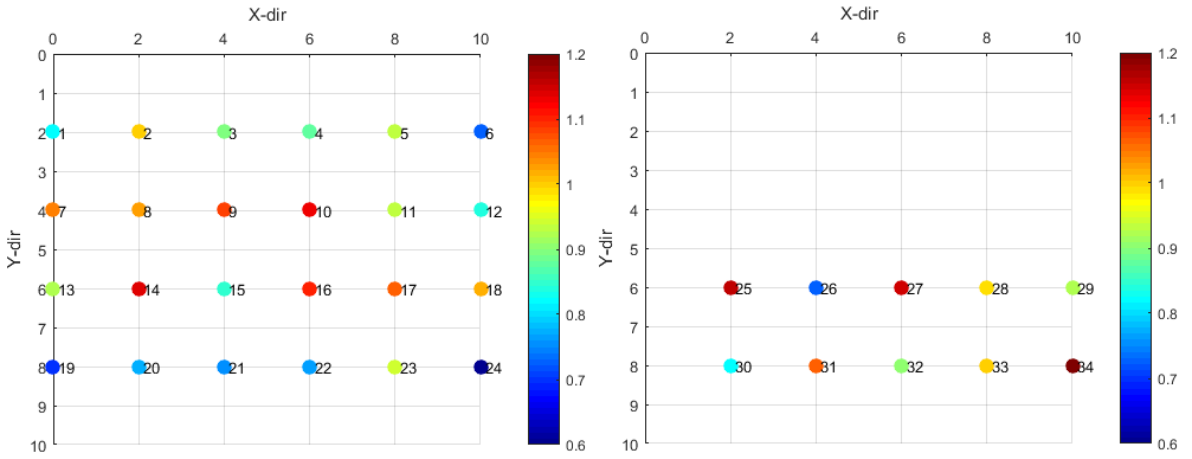

Figure 6.27: The estimated horizontal precision or HDOP by the BlooLoc IPS in [m]. at z=1 (left) and at the subfloor z=4 (right).

7

Interpretation and discussion

7.1. Validation of the modeled precision

7.1.1. Geometric experiment 1

The theoretical design computations can be validated by comparing precision results of the model and the measurements of the geometric experiments (section 6.4). To validate the model, the horizontal precision or HDOP obtained with the practical experiments is compared to the precision values of the theoretical design computations for $z = 1$. From Fig. 7.1 can be seen that the precision of the design computations ranges from 0.75-1 meter, whereas the estimated precision of the IPS ranges from 0.75-1.5 meter. However, the majority of the estimated precision lies between 0.75 and 1.1 meter corresponding with the precision range of the design computations. The best precision is found in the center of the area for both design computations as the results of the practical experiment. As expected, the precision values of the practical experiment differ slightly from the precision predicted by the design computations. Furthermore, at some places the precision values of the IPS shows a significant decrease in precision (nr. 15 - 18 and 34) as a consequence of systematic errors, e.g. due to signal reflections of the metal elevator shaft.

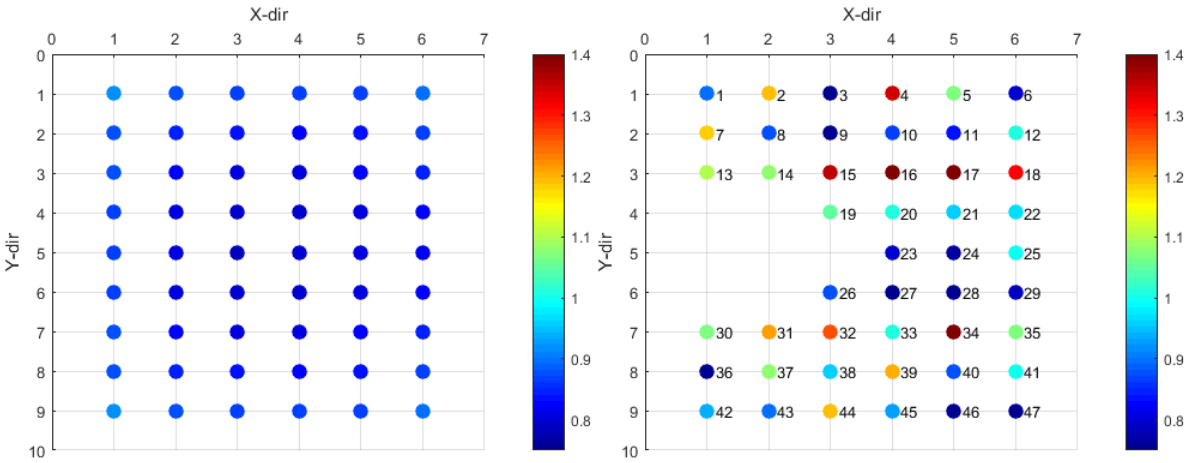

Figure 7.1: Left, precision of the design computations in [m]. Right, the estimated precision by the BlooLoc IPS in [m] both at *z=1*.

The design computations define the precision for a given geometric configuration in an ideal 3D space and do not take reflections, materialistic properties, signal attenuation etc. into account. Furthermore, the precision has only been validated at one height level $z = 1$. This height level has been chosen because most people wear mobile devices in their pockets at approximately $z = 1$ meter.

7.1.2. Geometric experiment 2

In addition to the validation of the first practical experiment, the precision results of the model were compared to the measurements of the second geometric experiment (section 6.4). From Fig. 7.2 can be seen that the precision of the design computations at $z = 1$ ranges from 0.85-1 meter, whereas the estimated precision of the IPS ranges from 0.55-1.15 meter. The majority of the estimates lies between 0.85 -1.15 meter which corresponds with range of the design computations. However, the precision pattern of the model shows a significant different pattern than obtained from the measurements. The only measurement locations that are slightly correlated, are the locations with nr. 19 - 24 at $y = 8$. Generally, the measured precision is lower than the modeled precision which is most likely due to NLOS and shadowing caused by the subfloor.

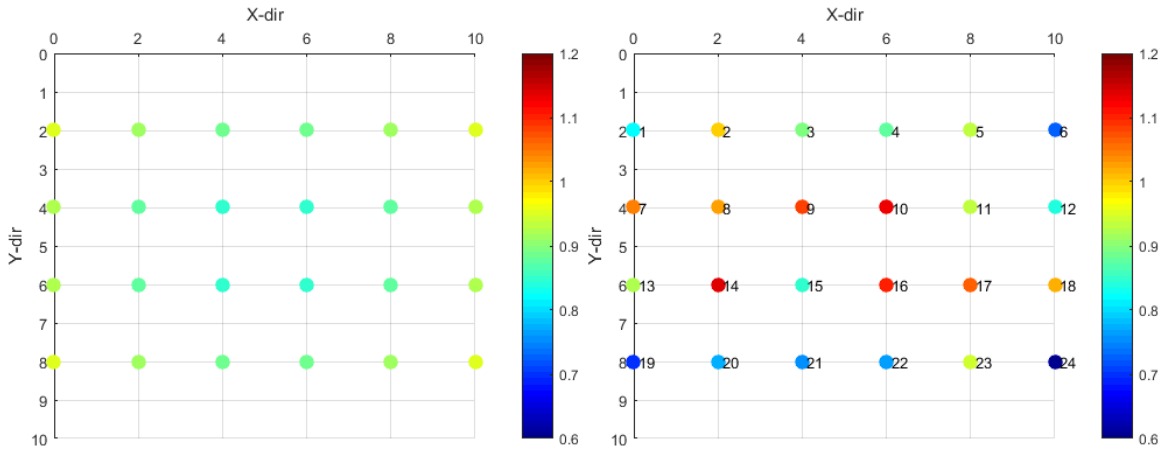

Figure 7.2: Left, precision of the design computations in [m]. Right, the estimated precision by the BlooLoc IPS in [m] both at *z=1*.

Additionally, a comparison of the modeled precision and the measured precision at $z = 4$ is illustrated in Figure 7.3. The modeled precision ranges from 0.85 - 1.1 meter and the majority of the measured precision at $z = 4$ ranges from 0.7 - 1.05 except for location nr. 34. The amplitudes and precision pattern are more correlated than at $z = 1$. Since the subfloor is an open space and is not separated by walls, the LOS improves which leads to an increase in precision with respect to the measured precision at $z = 1$.

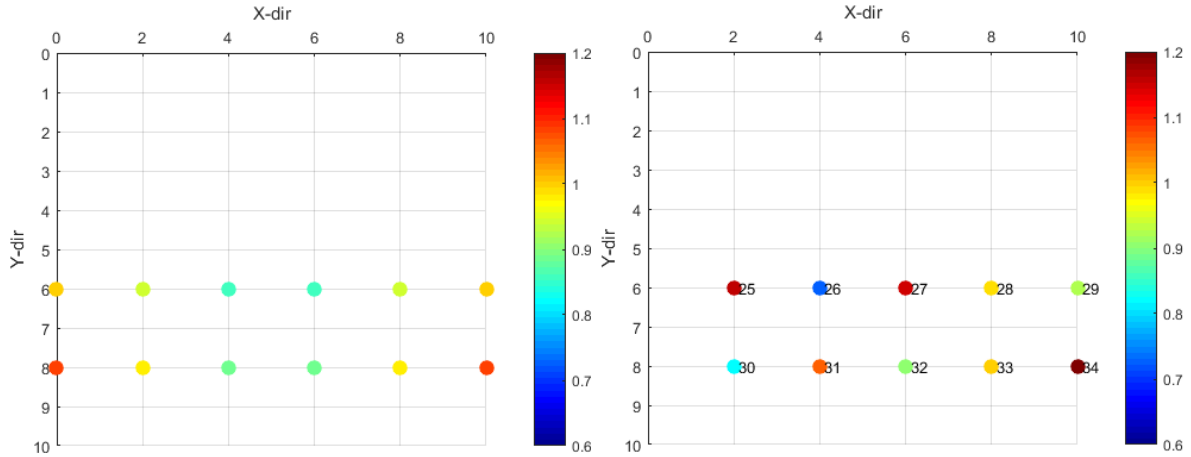

Figure 7.3: Left, precision of the design computations in [m]. Right, the estimated precision by the BlooLoc IPS in [m] both at *z=4*.

By examining the results of both practical experiments, it can be concluded that the design computations provide a good initial prediction model which is able to asses the quality of the data with multiple hypothetical geometries for any 3D space. For any given set of beacon and receiver locations, the precision, internal- and external reliability can be determined in advance, saving time and money of the customer in the process to find the geometric configuration that coincides with the best precision results. However, some signifi-

cant differences between the model results and the results of the practical experiments can only be explained physically. Therefore, the design computations will need to be elaborated further in order to account for reflections, materialistic properties, signal attenuation etc (see section 8.3). Furthermore, the design computations are not bound to a specific IPS and can be used for every IPS with transmitters and receivers for localization. In addition, it has to be mentioned that the positioning algorithm of BlooLoc (section 2.4.3) is more complicated than the positioning algorithm that is used in the theoretical design computations (chapter 5).

7.1.3. Geometric experiments: The accuracy

The accuracy results of both practical experiments (section 6.5) showed significant differences. In the first practical experiment, the majority of the measurements were located within a distance of $d < 1.5m$ off their true location. In contrast to the second practical experiment, where the majority of the measurements were located with a distance of $d > 1.5$ meter off their true locations. The accuracy decreased significantly by changing the indoor environment from a empty hallway to a open space with a subfloor and meeting room (section 6.4). The indoor environment of the first experiment, comprised an open hallway with a ceiling at 6 meter and almost no obstacles. The only obstacles were a metal elevator shaft and a plateau at $z = 2.5$. The indoor environment of the second experiment contained a subfloor with a closed meeting room underneath. Therefore, the amount of beacons within the LOS of the tag at the measurement locations was higher in the first experiment than in the second experiment. In case of NLOS the signal attenuates and influences the precision and accuracy, or in other words, the amount of visible beacons influence the precision and accuracy of the measurements. Note that the theoretical design computations does not take the LOS or NLOS of the beacons into account, since BlooLoc does not provide insights in the signal strengths per beacon at the tag locations. Therefore, the design computations assume LOS between every possible tag location and the beacons.

7.2. The optimal geometric configuration

The initial model requires a manual selection of beacon locations in order to compute the precision and reliability. However, the model can be transformed in a model selecting the optimal geometric configuration by assessing the precision results of millions of geometric configurations and a performance threshold (e.g. required precision) depending on the use case. In such a case, a customer could define several requirements or input parameters such as the dimensions of a 3D space, the number of available beacons, a performance threshold, and possible tag- and beacon locations. Subsequently, the model should be able to find the optimal geometric configuration based on the users requirements and input parameters.

7.2.1. Testing the optimal configuration

Instead of assigning the 15 positions of the beacons, an infinite amount of possible beacon positions can be given as input parameters. For this example, the beacons could be deployed on 27 possible locations within a 10x10x5 theoretical space, see Figure 7.4. From Fig. 7.4 can be seen that there are 8 possible beacon locations at $z = 1$ and another 8 possible beacon locations at $z = 3$. Additionally, 11 possible beacon positions are distributed over the ceiling at $z = 5$. For clarification, the 2D top-down views of the three different height levels ($z = 1$, $z = 3$ & $z = 5$) are depicted in Figure 7.5. Every geometry will consist of 15 beacons which is the maximum amount of available beacons in this case. The model will generate every possible combination for the 27 possible beacon locations with 15 beacon locations every run. Note that repetition of beacons is not allowed and that order of selection does not matter. In this case, the amount of possible combinations C can be derived by using the factorial as follows

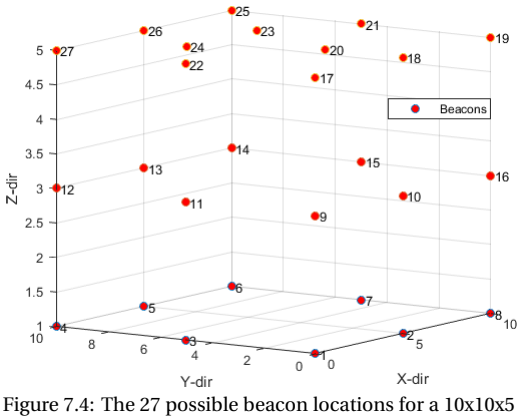

Figure 7.4: The 27 possible beacon locations for a 10x10x5 theoretical space.

$$C = \frac{n!}{r!(n-r)!} \tag{7.1}$$

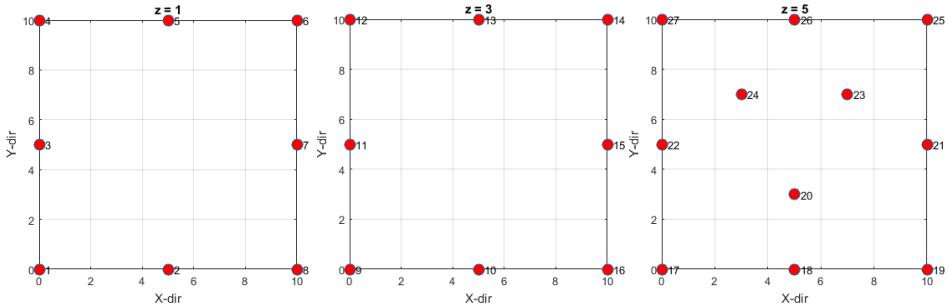

Figure 7.5: The 2D top-down views of possible beacon locations for z=1, z=3 & z=5.

where n represents the number of possible beacon locations and r represents the amount of selected beacons. Initially, $n = 27$ and $r = 15$ would result in $C = 17383860$ combinations or possible geometric configurations. However, the run time of the model is increases when C increases and for $C = 17383860$ the run time is too long for an efficient product. Therefore, the amount of combinations was reduced by distributing the 15 beacons over the three height levels $z = 1$, $z = 3$ and $z = 5$. The 8 possible beacon locations at $z = 1$ will take 4 of the 15 beacons into account, resulting in $C = 70$ combinations ($n = 8$, $r = 4$). Likewise, the 8 possible beacon locations at $z = 3$ take 4 of the 15 beacons into account, which also results in $C = 70$ combinations. The 11 possible positions at the ceiling ($z = 5$) use the resulting 7 of the 15 beacons, which gives $C = 330$ combinations ($n = 11$, $r = 7$). The total amount of combinations is then reduced to $C_{total} = 70 * 70 * 330 = 1617000$, which decreases the run time and makes the model more efficient and profitable.

In addition, a performance threshold (e.g. required precision) is used to filter the 1617000 possible geometries in order to find the optimal geometric configuration. The performance threshold is depending on the user requirements and thus on the use case. Furthermore, the performance threshold is used to filter all possible combinations of geometric configurations and to find the optimal solution. Assume a specific use case would require a precision (standard deviation) of 1 meter, the total precision at all possible user locations at $z = 1$ and $z = 4$ is examined against the threshold ($\sigma_T \leq 1.0$) for every single solution of the 1617000 possible geometries. Subsequently, the percentage satisfying the threshold was computed and compared to the previous percentage in an iterative model. Eventually, the optimal solution was obtained by finding the geometry that corresponds with the highest percentage of the possible user locations satisfying the threshold. The threshold of $\sigma_T \leq 1.0$ resulted in a single solution with a percentage of 94,4 % of the user locations at $z = 1$ and $z = 4$ satisfying the threshold. The geometric configuration and the precision results at $z = 1$ and $z = 4$ are depicted in Figure 7.6. A 2D top-down view of the optimal geometric configuration is given in Figure 7.7 and can be compared to the initial possible beacon locations (Fig. 7.5).

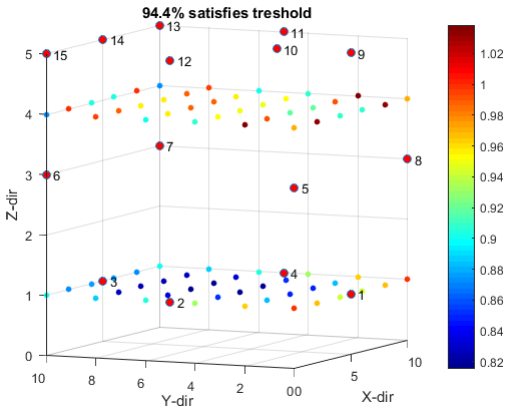

Figure 7.6: The optimal geometric configuration satisfying the threshold at 94.4% of the user locations.

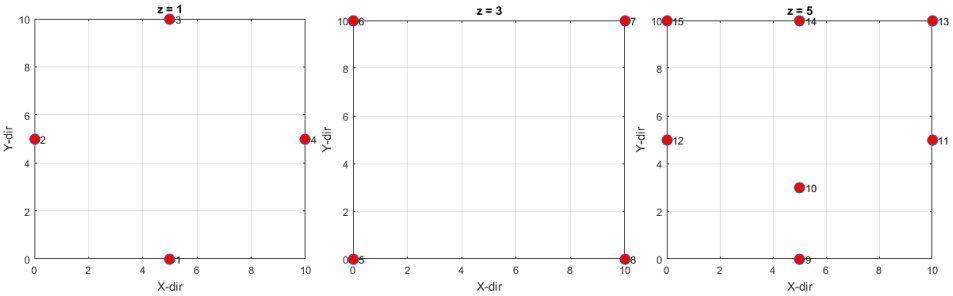

Figure 7.7: The 2D top-down views of the beacon locations for the optimal geometric configuration at z=1, z=3 & z=5.

7.2.2. Varying the threshold

The performance threshold is highly dependent on the use case and is therefore variable. Different thresholds result in different optimal geometric configurations. As mentioned earlier, the performance threshold is based on the user requirements and is used to filter all possible combinations of geometric configurations, which eventually leads to the optimal solution. Therefore, the model performed multiple runs to examine the differences in optimal geometric configurations for various thresholds. The threshold starts at $\sigma_T \leq 1.0m$ and decreases with intervals of 0.01 meter until the model has no possible solutions. For every given threshold, the model evaluates all 1617000 possible geometries based on the corresponding precision values and determines the best solution. Eventually, the best solution(s) corresponds with the highest percentage of the possible user locations that satisfies the threshold. The decreasing thresholds, corresponding percentage of the possible user locations that satisfies the threshold and the number of possible configurations are illustrated in Figure 7.8. From Fig. 7.8 can be seen that the model was not able to find any geometrical configurations satisfying the threshold of $\sigma_T \leq 0.77m$. Furthermore, decreasing the threshold leads to a decrease in the percentage of the precision that satisfies the threshold for most cases, however, the number of possible geometric configurations generally increases.

Threshold (m)	Percentage (%)	Nr. of solutions
1.00	94.4	1
0.99	87.5	2
0.98	86.1	1
0.97	86.1	1
0.96	73.6	4
0.95	70.8	3
0.94	66.6	16
0.93	63.8	8
0.92	61.1	8
0.91	54.1	26
0.90	48.6	12
0.89	44.4	16
0.88	40.2	12
0.87	33.3	24
0.86	27.7	12
0.85	22.2	35
0.84	19.4	13
0.83	15.2	109
0.82	12.5	54
0.81	11.1	1
0.80	6.94	64
0.79	4.16	556
0.78	1.38	1589
0.77	0	0

Figure 7.8: The threshold in [m], the percentage of the possible user locations that satisfies the threshold and the amount of possible configurations for 15 beacons

7.2.3. Number of beacons

In general, the model provides insight in the selection of the optimal configuration for various thresholds. During the first run, 15 beacons were distributed over 27 possible beacon locations at the three height levels $z = 1$, $z = 3$ and $z = 5$. The maximum amount of available beacons (15) was used for finding the first optimal geometric configuration. However, customers are not only interested in the optimal solution, but also in the optimal solution that reduces the costs while the solution still satisfies the performance threshold of the use case. If the optimal solution satisfies the performance threshold for less beacons, the total costs would reduce. Therefore, to investigate the optimal solution in terms of costs the amount of available beacons can be reduced.

Consequently, two additional runs have been performed by the model. The model generates every possible combination for the same 27 possible beacon locations of Fig. 7.4 and 7.5, however this time with 14 available beacons and another run with 13 available beacons. Similar to the run with 15 beacons, repetition of beacons is not allowed and that order of selection does not matter. The 8 possible beacon locations at $z = 1$ (Fig. 7.5) will take 4 of the 14 (13) beacons into account, resulting in $C = 70$ combinations ($n = 8$, $r = 4$), see equation 7.2. Likewise, the 8 possible beacon locations at $z = 3$ (Fig. 7.5) take 4 of the 14 (13) beacons into account, also resulting in $C = 70$ combinations. The reduced amount of beacons will effect the beacons at the ceiling. The 11 possible positions at the ceiling ($z = 5$, Fig. 7.5) use the resulting 6 (5) of the 14 (13) beacons, which gives $C = 462$ combinations for both $r = 6$ and $r = 5$ with n=11. Eventually, the total amount of combinations is $C_{total} = 70 * 70 * 462 = 2263800$ increasing the run time. After finding all possible geometric combinations, the model performed multiple runs to examine the differences in optimal geometric configurations for various thresholds. The threshold starts at $\sigma_T \leq 1.0m$ and decreases with intervals of 0.01 meter until the model has no possible solutions.

In case of 14 beacons, the model finds 6 optimal geometric configurations that satisfy the threshold of $\sigma_T \leq 1.0m$ at approximately 80% of the possible user tag locations at $z = 1$ and $z = 4$. One of the six optimal configurations has been by a 2D top-down view visualized in Figure 7.9 and can be compared to the initial possible beacon locations (Fig. 7.5). Depending on the use case, the customer can determine whether it is necessary

to use 15 beacons or 14 beacons in case the performance threshold is $\sigma_T \leq 1.0m$. If the user requirements would define $\sigma_T \leq 1.0m$ for 80% of the tag locations, the customer is able to use 14 beacons which reduces the costs. Note that the model provides the customer a 3D solution of the precision, such that the customer can check in which parts of the area the precision is expected to be lower than the threshold and if this solution still fits the user requirements.

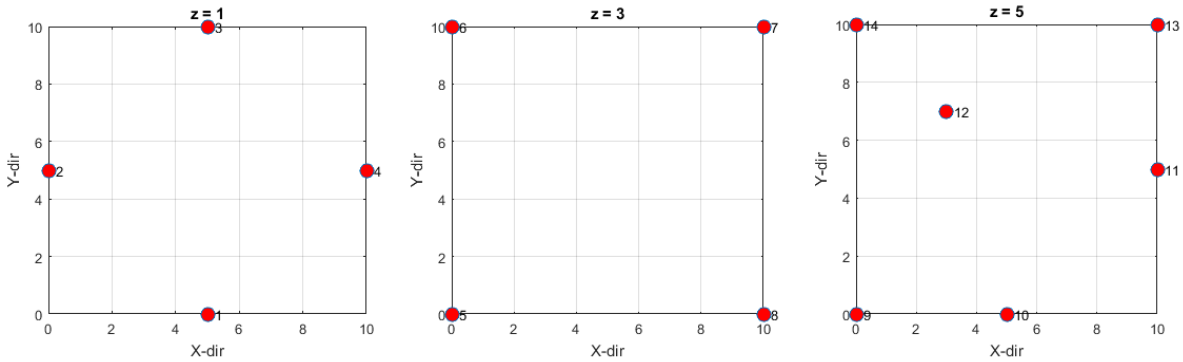

Figure 7.9: The 2D top-down views of the beacon locations for the optimal geometric configuration at z=1, z=3 & z=5.

The amount of optimal solutions satisfying the thresholds for the user locations at $z = 1$ and $z = 4$ for 14 and 13 beacons are depicted in Figure 7.10. Besides the amount of optimal solutions per threshold, the percentage of the possible user locations satisfying the threshold at $z = 1$ and $z = 4$ is also depicted in Fig. 7.10. In case of 14 beacons, a threshold of $\sigma_T \leq 1.0m$ corresponds with a percentage 79.2%, which is lower than the 94.4% obtained with 15 beacons. Whether this solution is sufficient depends on the use case and the user requirements. Additionally, in case of 13 beacons, a threshold of $\sigma_T \leq 1.0m$ corresponds with a percentage 62.5%, significantly lower the 94.4% obtained with 15 beacons. Furthermore, the model was not able to find any geometrical configurations satisfying the thresholds of $\sigma_T \leq 0.80m$ for 14 available beacons and $\sigma_T \leq 0.83m$ for 13 available beacons.

	14 Beacons		13 Beacons	
Threshold (m)	Percentage (%)	Nr. of solutions	Percentage (%)	Nr. of solutions
1.00	79.2	6	62.5	4
0.99	75	6	56.9	8
0.98	68	12	52.7	1
0.97	65.2	16	47.2	6
0.96	61.1	18	41.6	16
0.95	56.9	8	37.5	8
0.94	52.7	4	33.3	4
0.93	50	2	31.9	4
0.92	43	8	27.7	1
0.91	36.1	26	22.2	4
0.90	36.1	2	18.1	6
0.89	27.7	6	15.2	4
0.88	23.6	8	11.1	82
0.87	19.4	2	8.3	27
0.86	16.6	8	5.5	516
0.85	12.5	14	4.1	91
0.84	9.7	8	1.3	3014
0.83	6.9	20	0	0
0.82	5.5	2	0	0
0.81	1.3	8331	0	0
0.80	0	0	0	0

Figure 7.10: The threshold in [m], the percentage of the possible user locations that satisfies the threshold and the amount of possible configurations for 14 and 13 beacons.

To illustrate the effect of decreasing the amount of available beacons on the percentage of the user locations at $z = 1$ and $z = 4$ that satisfy the threshold, the results for 15, 14 and 13 beacons are visualized in Figure 7.11. By decreasing the threshold, the percentage of the user locations satisfying the threshold decreases and the three graphs almost show a linear pattern. The difference between the graphs of 15 and 14 beacons is on average 14.2 %, whereas the graphs of 14 and 13 beacons differ on average 15.0 %. The results can be used be used to determine how many beacons are needed for use cases with specific user requirements in terms of system performance. Therefore, the theoretical design computations help the customer in selecting the optimal geometry for a specified performance threshold and even show whether the same threshold is satisfied in case less beacons would be available. Eventually, the customer saves time and money in selecting the optimal configuration for his IPS and is able to get the required precision.

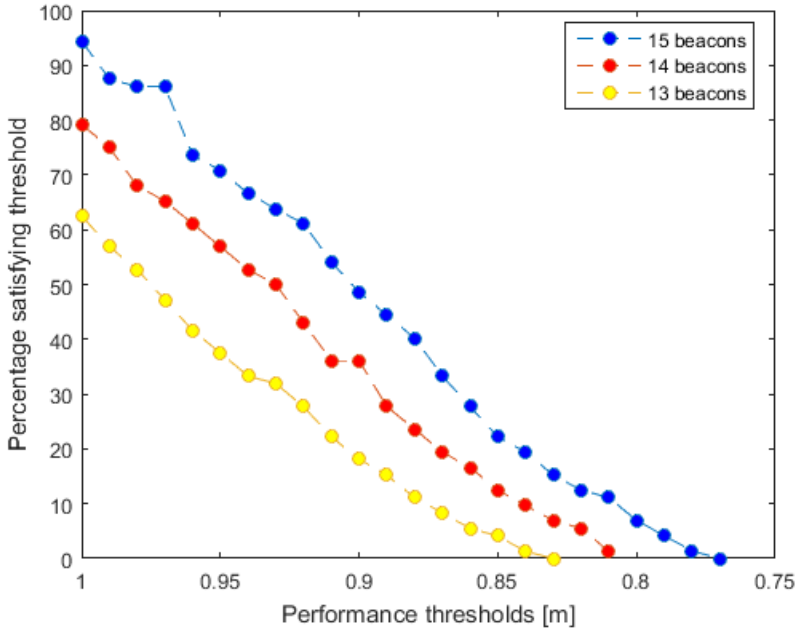

Figure 7.11: The percentage (%) of the user locations satisfying the thresholds versus the performance thresholds for 15, 14 and 13 available beacons.

7.3. Improving the model

7.3.1. Initial standard deviation

The initial uncertainty of the observations Δy_0 of the theoretical design computations is expressed by the Q_{yy} matrix. The Q_{yy} matrix is assumed to be diagonal and the observations come with initial standard deviation of 1 meter, since BlooLoc claims to achieve an accuracy of less than 1m for 80% of the measurements when the beacons are installed right and the system has self-calibrated properly [2]. Subsequently, the initial model assumes that the standard deviation is not distance related and is similar for every beacon. The results of the range experiments described in section 6.2 showed a the decay in signal strength over distance. The decay in signal strength with increasing distance differed slightly per beacon (Fig. 6.2). Furthermore, the standard deviation fluctuated over distance but did not clearly indicated an increase over distance. This is contrary to the expectations, since it is expected that the standard deviation would increase with increasing distance as a consequence of the signal attenuation of the BLE pulses. Therefore, for the enhancing of the model the standard deviation can be considered as a distance related variable which can be implemented in the model by using the relation between signal strength and distance (section 6.2.2). The empirical standard deviation related to the distance increased over distance (Fig. 6.9) and can therefore be used as a distance related variable in a future model. Furthermore, the range experiments provide insight into the characteristics of individual beacons. A general distance related standard deviation can replace the initial standard deviation, however, to optimize the model the distance related standard deviation can be determined for every beacon separately. Finally, these characteristics can be implemented in the initial model.

7.3.2. Properties of materials

To account for signal attenuation, reflections and multipath materialistic properties can be added as initial parameters of the model. Since the BLE signals are electromagnetic pulses propagating through space, the reflection and transmission coefficients are of interest for the model. When an electromagnetic wave is incident on a interface between two media, it can either be reflected back from the interface into the first medium, refracted into the second medium, or a combination of both things occurs [28]. Assume an electromagnetic wave is traveling trough medium 1 towards the interface with medium 2 (Figure 7.12). The incident wave is propagating through medium 1 towards the interface with medium 2 under an angle of θ_1 with respect to the normal to the interface. Generally, part of the incident wave is reflected back under the same angle θ_1 into medium 1, while some part is refracted into medium 2 with an angle of θ_2 with respect to the normal to the interface. The directions of the reflected and refracted waves are given by Snell's law, which relates the angles θ_1 and θ_2 through

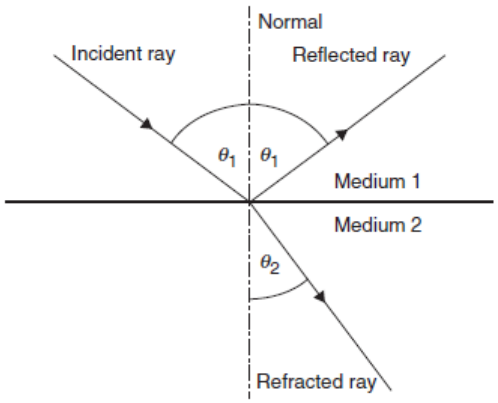

Figure 7.12: Reflection and refraction of an incident ray at an interface between two media. Source: Rees and Rees [28]

$$n_1 \sin\theta_1 = n_2 \sin\theta_2 \tag{7.1}$$

where n_1 and n_2 are the refractive indices of the two media [28]. Besides the directions, the amplitudes of the reflected and refracted waves are given by the Fresnel coefficients and are highly dependent on polarization. Furthermore, the Fresnel coefficients also take absorption coefficients into account. For the full derivation of the Fresnel coefficients study Chapter 3 "Interaction of electromagnetic radiation with matter" of Rees and Rees [28]. The combination of direction and amplitude of reflected and refracted waves could be used to account for reflections and multipath (reflected waves) and signal attenuation due to shadowing (refracted waves) in the theoretical design computations. Note that applying this principle is complicated and is highly dependent on the reflection characteristics. Therefore, it is recommended to apply this principle only when installing BlooLoc permanently.

7.3.3. LOS vs. NLOS

The initial model assumes LOS between every possible tag location and the beacons, since BlooLoc does not provide insights in the signal strengths per beacon at the tag locations. However, the model could be enhanced by accounting for NLOS between beacons and tag locations with a weighting system. For example, beacons that have LOS get assigned a higher weight than beacons that coincide with NLOS between the beacon and the tag location. The NLOS between the possible user locations and the beacons can be determined either by a visual inspection in situ or by using an indoor positioning system that gives more insight in whether beacon and tag are in direct LOS or not.

8

Conclusions and recommendations

To formulate well funded conclusions for this master thesis, firstly the sub-questions will be answered and subsequently an answer to the main research question will be formulated. The sub-questions (section 1.3) act as a foundation to create a well-structured answer on the main research question. The sub-questions will be answered on the basis of the performed literature study, the results of the experiments and the data analysis. After answering the sub-questions and the main research question, conclusions will be formed and the thesis will close up with a section elaborating some recommendations and future work.

8.1. Research questions

8.1.1. Sub-questions

1. **What is the current state of the system performances and what improvements are possible?**

   The state-of-the-art of the current Bluetooth systems is the Bluetooth Low Energy system. BLE was developed as a low-power solution for control and application monitoring. Due to its power-efficiency, BLE us suited for devices that run for longer periods on internal power sources, such as mobile phones. The BlooLoc IPS that is used for this research is a BLE positioning system and is still developing. Note that during this research the yooBee Software Development Kit (SDK) and Application Programming Interface (API) of BLooLoc had version 1.6, however, the functionality of the SDK and the API's are still evolving and thus subject to change. Currently, the BLE positioning system of BlooLoc has an update rate of 1 Hz and BlooLoc claims the positioning error is less than 1m for 80% of the measurements. However, the geometric experiments with BlooLoc showed that the positioning error often exceeded 1 meter, which is most likely a consequence of systematic errors, e.g. due to signal reflections of the metal elevator shaft (chapter 7). The geometric experiments also showed a significant decrease in accuracy and precision in case the area consisted of a subfloor and a meeting room, which is most likely caused by signal attenuation, reflections and NLOS. Furthermore, Bluetooth has a typical coverage of 5-10 meter and the RF signals are blocked by water, meaning that human beings cause signal attenuation, assuming an adolescent human body consists for 65% of water. The amount of applications for indoor positioning systems is increasing and the markets are growing rapidly. However, the major challenge still is to find in what kind of configuration the IPS needs to be deployed in order to satisfy a certain performance threshold (e.g. required precision).

2. **What are the pros and cons in terms of performance of the Bluetooth Low Energy system of BlooLoc?**

   The pros of an Bluetooth Low Energy systems are the costs, the power-efficiency and the flexibility of the deployment. A Bluetooth chip is less expensive than for instance the costs of Wi-Fi and the power consumption of BLE is much lower than Wi-Fi, Bluetooth uses approximately one fifth of the power of Wi-Fi. Furthermore, the beacons can be placed on user-specified locations causing good signal geometries in comparison with the Wi-Fi access points (AP) that often have fixed positions. On the other

hand, due to the fact that WLAN-based indoor positioning systems can operate via existing WLAN systems and have been implemented in almost all indoor environments, this IPS becomes relatively cheap and user-friendly and has access points almost everywhere. For more comparisons between positioning techniques such as Cameras, IR, ZigBee, Essensium and the Bluetooth technology, read chapter 2. The advantage in terms of performance of the IPS of BlooLoc (section 2.4.3) is that the positioning algorithm uses the state-of-the-art positioning principle of sensor fusion combined with a particle filter. The principle sensor fusion comprises the fusion of a RSSI (section 3.2.3) model of the environment, all gathered inertial sensor data and floorplan information. The RSSI model consists of all past RSSI values between each beacon and every tag or mobile device and is constantly improving and learning from historic data. Moreover, the floorplan information includes all obstacles and infrastructure of the indoor environment such as walls, corridors, doors, obstacles etc. Note that the floorplan has to be available and a floorplan can be dynamic in case of changing indoor environments, e.g. conferences. Sensor fusion leads to a self-learning auto-calibration system which over time leads to a more and more accurate positioning system by constantly updating and reanalyzing all gathered data. Cons of the BLE system of BlooLoc are that the users have no insight in which beacon is in direct Line-of-Sight (LOS) with respect to the tag. Direct LOS refers to a straight line along which a tag has unobstructed vision to the beacons. Furthermore, BlooLoc only operates in *x, y* direction and is therefore limited to a 2D solution.

3. **What are the most important factors that influence the system performance?**

   One of the most important factors that influences the system performance of a BLE positioning system is related to the geometry. The geometric configuration of a set of beacons within a certain 3D space has the largest impact on the precision and accuracy of the positioning. The DOP (section 4.2) represents a measure reflecting the geometric configuration of an IPS and is retrieved via the square root of the diagonal of the variance matrix $Q_{\hat{x}\hat{x}}$ (chapter 5), which contains the contribution to the position error of both the geometry and the random measurement error. The results in terms of precision or HDOP of the theoretical design computations were validated with the precision results derived during a practical experiment with BlooLoc. The first experiment in an empty hallway showed a similar precision pattern with some offsets. In contrast, the second experiment containing a subfloor showed significant differences between the modeled precision and the measured precision. Since some of the differences are not caused by the geometric configuration and can only be explained physically, the differences are most likely caused by factors as reflections (multipath), fading, shadowing and NLOS (section 4.2).

4. **What is the optimal (minimal) configuration to get the required precision?**

   The optimal (minimal) configuration is highly dependent on the use case, which on its turn determines the required accuracy/precision via the user requirements. The optimal configuration reflects on the optimal geometric configuration and does not include the effects caused by NLOS, signal attenuation, multipath etc. The model is able to select the optimal geometric configuration(s) for a given performance threshold (e.g. required precision) (section 7.2). Depending on the performance threshold, the optimal configurations can either be a single solution or consist of multiple solutions that satisfy the performance threshold of the customer. The performance threshold varies depending on the use case and the user requirements. Furthermore, an optimal configuration can satisfy the threshold for 15 beacons, however in some cases less beacons are needed for an optimal configuration that still satisfies the threshold. Several model runs were performed for selecting the optimal geometric configuration out of 27 possible beacon locations in case 15, 14 and 13 beacons are available. Eventually, the optimal configuration was selected by using an initial performance threshold of $\sigma_T \leq 1.0m$, decreasing with intervals of 0.01 meter until the model has no possible solutions (section 7.2). The model can be used for all kind of applications and the possibilities are limitless considering the amount of possible combinations in terms of 3D space, amount of available beacons, possible beacon locations, user tag locations and performance thresholds. Eventually, to find the optimal solution that minimizes the differences between the observed and measured data, the model has to be adapted in the future to account for multipath, signal attenuation, NLOS etc.

5. **What are different use cases and how should the system be adapted to fulfill these?**

   In our modern way of life indoor positioning has become a trending topic and is applicable in almost every branch. Moreover, considering the continuous improvement in technology and knowl-

edge, future indoor positioning systems will find even more applications, which makes it promising to enhance- and contribute to -indoor positioning systems. Several use cases have been elaborated in terms of their user requirements (section 4.1.1). The analysis on the values of the user requirements has been performed in consultation with Robert Voûte (CGI) and are based on both assumptions and previous applications (chapter 4). The elaborated use cases are *'Smart grocery shopping'*, *'Hospitals and Care Centers'*, *'Airports, Train/Subway Stations and Shopping Malls'* and *'Warehouses and Distribution Centers'* with the IPS of BlooLoc as example. The use cases and their corresponding user requirements define the adaptions that are necessary to apply to the system. For example, in case of the Distribution Centers both horizontal and vertical accuracy and precision for locating products have to be < 1 meter. The input for the threshold would thus be $\sigma_T \leq 1.0m$ and subsequently the model is able to select the optimal geometric configuration, if the 3D space, amount of available beacons, possible beacon locations, user tag locations are specified too. This principle can be applied for any use case meaning that the system adapts based on the thresholds that is provided by the user requirements.

6. **What are the maximum number of moving objects that can be seen for the use cases and monitored accurately by the system?**

   In contrast to the first five sub-questions, this sub-question has not been answered by practical experiments and is purely theoretically answered. The maximum number of moving objects that can be seen of a given use case is different for use cases that targeting the tracking of humans or the tracking of objects. Since the human body acts as a blockade for the Bluetooth signals, the maximum number of moving people that can be monitored is dependent on the distortion and signal attenuation that is caused by the human bodies. For example, locating somebody while at an crowded concert might lead to a decrease in the position accuracy due to the human blockade. However, for instance forklifts driving through warehouses do not have the issue of signal blockage but the accurate monitoring is dependent on the update rate. In order to prevent collisions between forklifts, the update rate has to be smaller than 0.5 seconds such that the drivers can be warned on time. Tracking more objects may also lead to an increase in signal interference, which on its way results in either constructive interference or destructive interference (chapter 4). However, to fully answer this sub-question some future work and experiments have to be done (see section 8.3).

8.1.2. Main research question

The answers to the sub-questions act as a foundation to formulate a well-structured answer on the main research question. The main research question is formulated in section 1.3.1 as

> **"What kind of geometric configuration of a BLE indoor positioning system is needed to enable the required system performance for given use cases in a 3D environment?"**

Based on the answers of the sub-research questions and the discussed results of this thesis, the main research question can be fully answered. Initially, the main research question was subdivided in two main parts, namely *'kind of geometric configuration of a BLE indoor positioning system ... in a 3D environment'* and *'to enable the required system performance ... for given use cases'*. First of all, the kind of geometric configuration is depending on the input parameters of the model, namely the dimensions of the 3D environment, the amount of available beacons, possible beacon locations, possible user tag locations and the performance threshold. The design computations provide a good initial prediction model which is able to assess the quality of data with multiple hypothetical geometries for any 3D space. For any given set of beacon and receiver locations, the precision, internal- and external reliability can be determined in advance, saving time and money of the customer in the process to find the configuration that coincides with the best precision results. Therefore, any geometric configuration can be tested to pre-assess the precision and evaluate if it satisfies the user requirements in terms of the performance threshold. As mentioned earlier, the performance threshold acts as a filter in the model for selecting the optimal geometric configurations. Thus, 'kind of geometric configuration' is selected by the model based on all possible geometric combinations of the available beacons and the performance threshold.

The performance threshold is the link between the two parts of the main research question. Since the performance threshold not only determines the optimal configuration, thus the kind of configuration, but also relates to the required system performance. Throughout this thesis, the performance threshold is synonym

for the required precision. On its turn, the required precision depends on the use cases and is defined in the user requirements. The use cases and their corresponding user requirements define adaptions to the model for selecting the optimal geometric configuration. The example of the use case 'Distribution Centers' required both horizontal and vertical a precision of < 1 meter. Therefore, the input for the threshold would thus be $\sigma_T \leq 1.0m$ and subsequently the model is able to select the optimal geometric configuration. Note that the dimensions of the 3D environment, amount of available beacons, possible beacon locations, user tag locations have to be specified as well. This principle can be applied for any use case meaning that the system adapts based on the thresholds that is provided by the user requirements. Therefore, the amount of possible combinations in terms of 3D space, amount of available beacons, possible beacon locations, user tag locations and performance thresholds are limitless and the model can thus be used for all kind of applications. Note that the geometry of the current model does not take reflections, NLOS, signal attenuation into account.

8.2. Conclusions

All in all, the design computations provide a good initial prediction model which is able to assess the quality of data with multiple hypothetical geometries for any 3D space. For any given set of beacon and receiver locations, the precision, internal- and external reliability can be determined in advance, saving time and money of the customer in the process to find the configuration that coincides with the best precision results.

Besides determining the precision based on a set of beacon and receiver locations, the model is able to select the optimal geometric configuration based on a performance threshold (e.g. required precision). Depending on the performance threshold, the optimal configurations can either be a single solution or consist of multiple solutions that satisfy the performance threshold of the customer. In case the optimal solution comprises multiple geometric configurations, the customer is free to select one of the configurations. The performance threshold varies depending on the use case and the user requirements. Therefore, the amount of possible combinations in terms of 3D space, amount of available beacons, possible beacon locations, user tag locations and performance thresholds are limitless and the model can thus be used for all kind of applications. In addition, the design computations are not bound to a specific IPS and can be used for every IPS using transmitters and receivers for localization, although the user has to think carefully about the characteristics of the RF signals of the IPS.

The validation of the model by the practical experiments showed several similarities in the precision pattern for the first experiment without obstacles. However, some significant differences between the model results and the results of the practical experiment can only be explained physically. Furthermore, the second practical experiment including a subfloor showed significant offsets between the modeled and the measured precision. To explain these differences, the design computations will need to be elaborated further such that corrections for reflections, materialistic properties, signal attenuation etc. can be applied. In addition, it has to be mentioned that the positioning algorithm of BlooLoc (section 2.4.3) is more complicated than the positioning algorithm that is used in the theoretical design computations (chapter 5).

To conclude, the initial model (design computations) can be used by IPS customers for all kind of applications. The model is able to select the optimal geometric configuration in terms of precision based on a performance threshold specified by the user. Furthermore, the model requires user specified input parameters and the amount of possible combinations are therefore unlimited. Although the initial model has to be adapted further to account for the differences in modeled and measured data, the initial model is a good initiative for the rising indoor positioning market and its customers.

8.3. Recommendations and future work

As discussed, the model can be adapted such that it can explain significant differences between the modeled and the measured data in by including factors that influence the system performance in real life, such as materialistic properties, signal attenuation, NLOS etc. Currently, the theoretical design computations do not account for reflections and interference. Furthermore, LOS between every user tag location and the beacons is assumed which makes the predictions suitable for an ideal 3D space with no objects or obstacles. However, the physical world is never perfect and the signals easily get disturbed. Even if a physical 3D space consists of a large open space and excludes obstacles, the walls will cause reflections and interference, where the magnitude of the reflected waves is depending on the materialistic properties, see section 7.3. To enhance the model, several factors have to be investigated and/or adapted:

1. **Characteristics of the beacons**

   The initial model assumes that the Q_{yy} matrix is diagonal and the observations have an initial standard deviation of 1 meter. However, the results of the range experiments described in section 6.2 showed a the decay in signal strength over distance. The results of the range experiments described in section 6.2 showed a the decay in signal strength over distance. The decay in signal strength with increasing distance differed slightly per beacon (Fig. 6.2). Furthermore, the standard deviation fluctuated over distance but did not clearly indicated an increase over distance. This is contrary to the expectations, since it is expected that the standard deviation would increase with increasing distance as a consequence of the signal attenuation of the BLE pulses. Therefore, for the enhancing of the model the standard deviation can be considered as a distance related variable which can be implemented in the model by using the relation between signal strength and distance (section 6.2.2). The empirical standard deviation related to the distance increased over distance (Fig. 6.9) and can therefore be used as a distance related variable in a future model. A general distance related standard deviation can replace the initial standard deviation, however, to optimize the model even further the distance related standard deviation can be determined for every beacon separately based on their characteristics.

2. **Limiting factors**

   To minimize the differences between the modeled precision and the measurements, the model has to be adapted for its limiting factors. The limiting factors comprise the effects caused by reflections (multipath), signal interference and shadowing. The model could account for reflected and refracted waves by implementing Snell's law and the Fresnel coefficients (section 7.3). The directions of the reflected and refracted waves are given by Snell's law, relating the angles and the refractive indices of two media. In addition, the amplitudes of the reflected and refracted waves are defined by the Fresnel coefficients. The combination of direction and amplitude of reflected and refracted waves could be used to account for reflections (reflected waves) and signal attenuation due to shadowing (refracted waves) in the theoretical design computations. Practical experiments could include the placement of a single beacon in a room and measuring signal strengths within the room and outside the room at the other side of a wall, such that the signal attenuation can be analyzed. Reflected waves are harder to distinguish and measure in a practical experiment, but if a Bluetooth transmitter can be limited in sending one pulse which is both theoretically and practically possible, the data received at another location in the room can be analyzed and a distinction between direct wave and multipath waves can be made. Note that applying this principle is complicated and is highly dependent on the reflection characteristics. Therefore, it is recommended to apply this principle only when installing BlooLoc permanently.

3. **Disclosure of information**

   The model can be enhanced further by adding information that is currently undisclosed by BlooLoc. For example, it would be useful to get insight in whether a beacon is in direct LOS with the tag or not. In such a case, if a beacon is in NLOS with respect to the tag on a certain location, the model could use this information for either a correction in the signal strength due to NLOS or the model could be enhanced with a weighing system. Moreover, it would be interesting if the beacons can be switched on and of by the user instead of constantly emitting BLE signals, which would be very useful when the IPS is used for experimental purposes. Furthermore, BlooLoc only operates in x, y direction and is therefore limited to a 2D solution.

4. **Moving objects and maximum objects**

   This research could be extended by examining the system performance of moving objects and investigate the effect of increasing the amount of objects to follow. In general, the position of an object becomes more accurate if it is static, however the effect on the system performance by mobile objects would be interesting to implement in the model. Moreover, most applications for indoor positioning are tracking mobile objects or persons. Furthermore, the effect of large crowds or an increased amount of objects/persons within a certain space has to be investigated in terms of system performance. The first test to perform is filling a room with persons while only one person carries a tag. Subsequently, the measurements can be compared to a situation in the same room without people. In the second test all the people in the room carry a tag and the effect on the system performance can be derived by comparing the measurements with the results of the first test.

5. **Analysis tool**

   Eventually, a finalized model can be used as analysis tool for property owners. The model is able to recommend the users where to place the beacons such that their performance threshold in terms of precision is satisfied. The model would be dependent on several parameters that have to be provided by the user/customer. The parameters of interest would be the size of the property/3D space, performance threshold in terms of precision, amount of available beacons, possible user within the 3D space and the materialistic properties of the walls and objects. Therefore, if a customer would provide these parameters, the model would be able to find the optimal solution and a recommendation for the customer could be made based on the results of the analysis tool.

Bibliography

[1] Pravin Bhagwat. Bluetooth: technology for short-range wireless apps. *IEEE Internet Computing*, 5(3): 96–103, 2001.

[2] BlooLoc. Blooloc products and technology, 2016. https://www.blooloc.com/ (15 Apr. 2017).

[3] SIG Bluetooth. Bluetooth core specification version 4.0. *Specification of the Bluetooth System*, 2010.

[4] Dirk Callaerts. Yoobee, a sensor fusion platform for accurate indoor positioning. *Guest lecture by BlooLoc at the course 'Positioning and Location Awareness (GEO3001)' at MSc track Geomatics, TU Delft*, 2016.

[5] Sudarshan S Chawathe. Beacon placement for indoor localization using bluetooth. In *2008 11th International IEEE Conference on Intelligent Transportation Systems*, pages 980–985. IEEE, 2008.

[6] M Depsey. Indoor positioning systems in healthcare. *Radianse Inc., White Paper*, 123, 2003.

[7] Dirk Devisch. Essensium - accurate realtime indoor position. *Guest lecture by Essensium at the course 'Positioning and Location Awareness (GEO3001)' at MSc track Geomatics, TU Delft*, 2016.

[8] Andrew Dursch, David C Yen, and Dong-Her Shih. Bluetooth technology: an exploratory study of the analysis and implementation frameworks. *Computer standards & interfaces*, 26(4):263–277, 2004.

[9] Naveen Erasala and David C Yen. Bluetooth technology: a strategic analysis of its role in global 3g wireless communication era. *Computer Standards & Interfaces*, 24(3):193–206, 2002.

[10] Ramsey Faragher and R Harle. An analysis of the accuracy of bluetooth low energy for indoor positioning applications. In *Proceedings of the 27th International Technical Meeting of The Satellite Division of the Institute of Navigation (ION GNSS+ 2014), Tampa, FL, USA*, volume 812, 2014.

[11] Carles Gomez, Joaquim Oller, and Josep Paradells. Overview and evaluation of bluetooth low energy: An emerging low-power wireless technology. *Sensors*, 12(9):11734–11753, 2012.

[12] Mohinder S Grewal, Lawrence R Weill, and Angus P Andrews. *Global positioning systems, inertial navigation, and integration*. John Wiley & Sons, 2007.

[13] Yanying Gu, Anthony Lo, and Ignas Niemegeers. A survey of indoor positioning systems for wireless personal networks. *IEEE Communications surveys & tutorials*, 11(1):13–32, 2009.

[14] Naresh Gupta. *Inside Bluetooth low energy*. Artech house, 2013.

[15] Daniel Hauschildt and Nicolaj Kirchhof. Advances in thermal infrared localization: Challenges and solutions. In *Indoor Positioning and Indoor Navigation (IPIN), 2010 International Conference on*, pages 1–8. IEEE, 2010.

[16] Michal Irani, Benny Rousso, and Shmuel Peleg. Recovery of ego-motion using image stabilization. In *Computer Vision and Pattern Recognition, 1994. Proceedings CVPR'94., 1994 IEEE Computer Society Conference on*, pages 454–460. IEEE, 1994.

[17] Jumbo. Jumbo, feiten en cijfers, 2016. https://www.jumbowerkt.nl/over-jumbo/feiten-en-cijfers/ (12 Jun. 2017).

[18] Yen-Liang Kuo and Kin-Lu Wong. Printed double-t monopole antenna for 2.4/5.2 ghz dual-band wlan operations. *IEEE Transactions on Antennas and Propagation*, 51(9):2187–2192, 2003.

[19] Axel Küpper. *Location-based services: fundamentals and operation*. John Wiley & Sons, 2005.

[20] Richard B Langley. Dilution of precision. *GPS world*, 10(5):52–59, 1999.

[21] Janire Larranaga, Leire Muguira, Juan-Manuel Lopez-Garde, and Juan-Ignacio Vazquez. An environment adaptive zigbee-based indoor positioning algorithm. In *Indoor Positioning and Indoor Navigation (IPIN), 2010 International Conference on*, pages 1–8. IEEE, 2010.

[22] Hui Liu, Houshang Darabi, Pat Banerjee, and Jing Liu. Survey of wireless indoor positioning techniques and systems. *IEEE Transactions on Systems, Man, and Cybernetics, Part C (Applications and Reviews)*, 37 (6):1067–1080, 2007.

[23] Rainer Mautz. Indoor positioning technologies, 2012. Habilitation thesis, ETH Zurich.

[24] Rainer Mautz and Sebastian Tilch. Survey of optical indoor positioning systems. In *IPIN*, pages 1–7, 2011.

[25] Redaction of NHD gezond, 2015. URL `http://www.noordhollandsdagblad.nl/gezond/nieuws/article27333152.ece/Wat-doet-de-technische-dienst-van-een-ziekenhuis-eigenlijk`. Consulted on 12 Dec. 2016.

[26] Alf Helge Omre and Steven Keeping. Bluetooth low energy: wireless connectivity for medical monitoring. *Journal of diabetes science and technology*, 4(2):457–463, 2010.

[27] Chuan-Chin Pu, Chuan-Hsian Pu, and Hoon-Jae Lee. *Indoor location tracking using received signal strength indicator*. INTECH Open Access Publisher, 2011.

[28] Gareth Rees and William Gareth Rees. *Physical principles of remote sensing*. Cambridge University Press, 2013.

[29] Chris Rizos, 1999. URL `https://web.archive.org/web/20141122153439/http://www.gmat.unsw.edu.au/snap/gps/gps_survey/chap1/149.htm`. Chapter 1, section 4.9 consulted on 8 May 2017.

[30] JJ Spilker. Satellite constellation and geometric dilution of precision. *Global Positioning System: Theory and applications.*, 1:177–208, 1996.

[31] Fazli Subhan, Halabi Hasbullah, Azat Rozyyev, and Sheikh Tahir Bakhsh. Indoor positioning in bluetooth networks using fingerprinting and lateration approach. In *2011 International Conference on Information Science and Applications*, pages 1–9. IEEE, 2011.

[32] Peter Teunissen, DJ Simons, and CCJM Tiberius. Probability and observation theory. 2004.

[33] M. F. S. van der Ham, S. Zlatanova, E. Verbree, and R. Voûte. Real time localization of assets in hospitals using quuppa indoor positioning technology. *ISPRS Annals of Photogrammetry, Remote Sensing and Spatial Information Sciences*, IV-4/W1:105–110, 2016. doi: 10.5194/isprs-annals-IV-4-W1-105-2016. URL `http://www.isprs-ann-photogramm-remote-sens-spatial-inf-sci.net/IV-4-W1/105/2016/`.

[34] Yapeng Wang, Xu Yang, Yutian Zhao, Yue Liu, and Laurie Cuthbert. Bluetooth positioning using rssi and triangulation methods. In *2013 IEEE 10th Consumer Communications and Networking Conference (CCNC)*, pages 837–842. IEEE, 2013.

[35] Roy Want, Andy Hopper, Veronica Falcao, and Jonathan Gibbons. The active badge location system. *ACM Transactions on Information Systems (TOIS)*, 10(1):91–102, 1992.

[36] Martin Werner. Indoor location-based services. *Prerequisites and foundations. Cham: Springer*, 2014.